INFORMATION TO USERS

This reproduction was made from a copy of a manuscript sent to us for publication and microfilming. While the most advanced technology has been used to photograph and reproduce this manuscript, the quality of the reproduction is heavily dependent upon the quality of the material submitted. Pages in any manuscript may have indistinct print. In all cases the best available copy has been filmed.

The following explanation of techniques is provided to help clarify notations which may appear on this reproduction.

1. Manuscripts may not always be complete. When it is not possible to obtain missing pages, a note appears to indicate this.

2. When copyrighted materials are removed from the manuscript, a note appears to indicate this.

3. Oversize materials (maps, drawings, and charts) are photographed by sectioning the original, beginning at the upper left hand corner and continuing from left to right in equal sections with small overlaps. Each oversize page is also filmed as one exposure and is available, for an additional charge, as a standard 35mm slide or in black and white paper format.*

4. Most photographs reproduce acceptably on positive microfilm or microfiche but lack clarity on xerographic copies made from the microfilm. For an additional charge, all photographs are available in black and white standard 35mm slide format.*

***For more information about black and white slides or enlarged paper reproductions, please contact the Dissertations Customer Services Department.**

Chang, David Lungpao

ALKYLDIMETHYLAMINE OXIDE/ALKYL SODIUM-SULFATE ACTION, INTERACTION AND SOLUBILISATION

City University of New York PH.D. 1985

PLEASE NOTE:

In all cases this material has been filmed in the best possible way from the available copy. Problems encountered with this document have been identified here with a check mark __√__.

1. Glossy photographs or pages _____
2. Colored illustrations, paper or print _____
3. Photographs with dark background _____
4. Illustrations are poor copy _____
5. Pages with black marks, not original copy _____
6. Print shows through as there is text on both sides of page _____
7. Indistinct, broken or small print on several pages __√__
8. Print exceeds margin requirements _____
9. Tightly bound copy with print lost in spine _____
10. Computer printout pages with indistinct print _____
11. Page(s) _____ lacking when material received, and not available from school or author.
12. Page(s) _____ seem to be missing in numbering only as text follows.
13. Two pages numbered _____. Text follows.
14. Curling and wrinkled pages _____
15. Dissertation contains pages with print at a slant, filmed as received _____
16. Other _____

_____

_____

ALKYLDIMETHYLAMINE OXIDE/ALKYL SODIUM SULFATE ACTION, INTERACTION AND SOLUBILISATION

by

DAVID LUNGPAO CHANG

A dissertation submitted to the Graduate Faculty in Chemistry in partial fulfillment of the requirements for the degree of Doctor of Philosophy, The City University of New York.

1985

This manuscript has been read and accepted for the Graduate Faculty in Chemistry in satisfaction of the dissertation requirement for the degree of Doctor of Philosophy.

07/29/85
date

Chairman of Examining Committee

7/29/85
date

Executive Officer

Supervisory Committee

The City University of New York

Abstract

ALKYLDIMETHYLAMINE OXIDE/ALKYL SODIUM SULFATE

ACTION, INTERACTION AND SOLUBILISATION

by

David L. Chang

Advisor: Professor Henri L. Rosano

Alkyldimethylamine oxide (C_xDAO) aqueous solutions alone and in combination with alkyl sodium sulfate have been investigated as model surfactant systems. At any pH the amine oxide is in equilibrium with its protonated form. The solution viscosity depends strongly on the degree of ionisation (β) with a maximum at β=0.5 due to formation of elongated structures. At at high and low pHs spherical micelles are present with low solution viscosity. C-13 nmr reveals downfield chemical shifts for all carbons upon micellisation, and is attributed to the rotational isomerisation about the C-C bonds (gauche to trans), reflecting a more extended conformation of the chains in the micelle which maximises paraffin-paraffin interactions. Ionisation of the head group causes upfield shift of the first 3 carbons in the chain due to increased water penetration into the micelle with increasing cationic character. Monolayers of the C_{18} homolog show that the nonionised amine oxide produces a more expanded film and that minimum film expansion and maximum surface potential are obtained for β=0.5, suggesting closer packing because of hydrogen bonding. Progressive addition of SDS to C_{12} or C_{14}DAO leads to pH and viscosity increases and the maximum is reached at $3C_x$DAO/SDS molar ratio, while lowest surface tension is observed in the equalmolar mixture. The C_{16} or C_{18}DAO/SDS mixtures are tur-

bid with filament formation when the amine oxide is in excess. Their difference in behaviour, which illustrates the importance of chain compatibility, is attributed to the adsorption of protons on the micelle surface in the former, and protonation of amine oxide leading to complex formation occurs in the latter. When the solution is sufficiently acidic, precipitation of a 1:1 complex takes place for the compatible chain mixtures. Mixed monolayers of the C_{18} homologs show marked contraction at all subsolution pHs, indicating strong interaction between these species. Addition of an oil to the 1:1 mixed monolayer causes film expansion, provided that the chain lengths match, such that optimum penetration by the oil into the film is achieved. In some cases an increase in the collapse pressure is also observed, indicating greater stability of the film. This phenomenon can be treated as a restriction in the duplex film model for the formation of microemulsion.

Acknowledgements

At times, either by chance or by destiny, we come to meet a certain person who may have such an impact that, life can never be the same again. Those who are fortunate get to meet someone and become enlightened and inspired. Those who are even more fortunate get to meet and work with Professor Henri L. Rosano. I am certainly amongst the more fortunate ones.

He is passionately addressed as the "Chief" in the laboratory. Indeed, not only is he our research advisor, he is a friend on a more personal level. For he truly understand that there are more to it than just a teacher-student relationship that is involved, if only because the amount of time and thoughts we shared together. "Keep going" says he with his characteristic French accent. And keep going we must. A seasoned teacher and chemist, Professor Rosano opened the door for me to the world of Surface Chemistry and more. It is to him I owe my deepest gratitude. A mentor he is. And always.

A few other individuals have played an integral part during my tenure as a graduate student. Professors D. Locke and C. Maldarelli, and Dr. E. D. Goddard. They took time out from their busy schedules to listen to what I had to say and to read what I have written, and to guide me along the way. Their support and guidance have been a major factor in the successful completion of this thesis. I would like to take this opportunity to express my most sincere appreciation to them. And to those who have kept me company all these years, in particular, Professor J. Rennert, thanks.

I am in deep debt to my parents, Mr. and Mrs. W. K. Chang, who literally gave me a new life some twelve years ago by sending me here to the States. And to everyone in my family. It is only with their love, understanding and unequivocal support, this work was made possible.

Table of Contents

List of Figures

Chapter 2

Chapter 3

Chapter 4

Chapter 5

Chapter 6

Appendix B

CHAPTER ONE

INTRODUCTORY REMARKS

1.1. SURFACTANT ACTION

Substances possessing both hydrophilic (water-attracting) and hydrophobic (water-repelling) parts are generally termed amphiphilic. One of the most well known properties of these substances is their ability to aggregate into colloidal particles as an alternative to minimise the unfavourable paraffin-water contact. McBain (1) introduced the term *micelle* (from Latin *micella* meaning small bit) to describe these aggregates. Hartley (2) at some forty years ago introduced the idea that micelles are roughly spherical in shape in solution, although the general acceptance was a much later occurence. Micelle formation is always accompanied by a peculiar concentration dependence, and this notion was established very early on. At low concentrations, an aqueous solution of an ionic amphiphile behaves essentially as any strong electrolyte. At high concentrations it is usually assumed that an increase in amphiphile concentration leads to a corresponding increase in the amount micellised while the monomer concentration remains unchanged. Many physico-chemical properties of the solution such as osmotic pressure, surface tension and conductivity, undergo drastic alterations upon micellisation. The changes in the concentration-dependence of a large number of properties in the region where micelle formation starts lead to the concept of critical micelle concentration ,CMC (4).

Practical applications of amphiphilic substances which trace back long in

history, are generally either directly or indirectly based on their lowering of surface or interfacial tension; thus the names surface-active-agent and surfactant. At an interface, the non-polar part tends to stretch into the gas phase or into an adjacent non-polar liquid, in order to minimise paraffin-water interfacial area. Soaps, the alkali salts of fatty acids, are classical examples.

1.2. SURFACTANT INTERACTION

Solutions containing more than one type of surfactant species can show marked alterations in solution properties when compared with the single component system, if their mutual influence takes place to a significant extent. In the bulk mixed micelles are formed, while mixed films are formed at the surface (interface). Generally, the surface activity of the mixed surfactant solutions is often greater than that of the single surfactant solution. This synergistic effect, defined as the lowering of CMC and surface tension reduction (5), is of obvious importance in a wide range of surface activity-based phenomena, such as foaming, emulsification, detergency, etc..

In general, mixtures of cationic/anionic surfactant solutions show the most pronounced synergistic effects, while ionic/nonionic mixtures show appreciable synergism, but the synergistic effects are negligible for nonionic mixtures. The enhanced surface activity can be best explained by ion-ion or ion-dipole interactions among the constituent species, in addition to the hydrophobic interaction among the non-polar hydrocarbon chains.

1.3. SURFACTANT SOLUBILISATION

One immediate consequence of micellisation by surfactant molecules is the ability of the micelle to solubilise an otherwise insoluble or only slight soluble compound in water (i.e. hydrocarbon in water) into the micellar core, and thereby increasing the apparent solubility of the compound in water. This

phenomenon is attributed to the accepted view that the interior of micelle resembles pure hydrocarbon, which provides energetically favourable sites for interaction with non-polar compounds. In detergency, solubilisation plays a vital role. The solubilising power of micelle has many other practical applications, such as in pharmaceutical preparations, in polymerisation procedures, and photographic processes. The pronounced catalytic effects of micellar solutions as reaction media are also under intense research (6).

One phenomenon closely related to the micelle solubilisation process is the formation of the so-called *microemulsion*. The term was first introduced by Hoar and Schulman (7) to describe transparent or transluscent systems formed *spontaneously* when oil and water(brine) are mixed with relatively large amounts of surfactant and a cosurfactant (usually a medium chain length alcohol). These systems are dispersions of very small drops of oil-in water (O/W) or water-in-oil (W/0) type with radii of the order of 5-50 nm. Microemulsions differ from ordinary emulsions (macroemulsions) in two main aspects, namely their lack of turbidity and their thermodynamic stability, although the latter point is still under discussion (8,9).

Since their discovery, microemulsions have attracted much interest. However, it was only after their likely use in enhanced oil recovery was demonstrated that a considerable research effort was undertaken in many countries. But inspite of the advances made in recent years in the theoretical bases of explaining the physics and chemistry of microemulsions (10), the science of their formation has not reached the point of their exact formulation. The mechanics of microemulsion formation differ somewhat from those used for macroemulsions. The most significant difference lies in the fact that putting (mechanical)work into a macroemulsion or increasing surfactant concentration usually improves their stability. This is not the case with microemulsions,

which appear to be dependent for their formation on specific interactions among the constituent molecules and the interface. If these interactions are not achieved, neither work input nor increased surfactant concentration will produce a microemulsion (11). On the other hand, once the conditions are right, spontaneous formation occurs and no mechanical work is required. Thus the crucial step in formulating the required microemulsion lies in the choice of emulsifiers. In other words, the nature (whether O/W or W/O) and structure of microemulsions depend to a large extent on the structure and chain length of the surfactant and cosurfactant used in their preparation (12).

1.4. THERMODYNAMICS OF SURFACTANT ASSOCIATION

The molecular organisation of micellar systems depends on the delicate interplay between hydrophobic and hydrophilic interactions. The balance between these forces is also related to a significant degree related to the structural organisation in living systems, such as biomembranes. A thermodynamic description of micellar solutions thus has much wider implications than just the understanding of micellar system itself.

The first quantitative attempt in the treatment of micellisation was made by Debye (13,14). Many refinements of different types have been made since, for example, Reich (15), Overbeek and Stigter (16), Hoeve and Benson (17), Poland and Scheraga (18) and more recently by Tanford (19), Ruckenstein and Nagarajan (20) and Israelachvili *et al* (21). Essentially four different approaches have been used: 1) the (pseudo)phase separation model; 2) the mass action model; 3) the small system model and 4) the multiple equilibrium model. The main features of these models are summarised below.

1.4.1. The Phase Separation Model

The onset micellisation process is considered as a transition into a two

phase region. The CMC is the concentration at which the system enters the two phase region. When the micelle is treated as a separate phase the chemical potential of the surfactant in the aqueous phase is

$$\mu_{aq} = \mu + kT \ln f_1 X_1 \qquad [1.1]$$

where μ is the standard chemical potential per molecule, f_1 is the activity coefficient and X_1 the monomer mole fraction. At a certain critical concentration, X_c, the chemical potential in the aqueous phase equals that of the micellar pseudophase

$$\mu_{aq} X_c = \mu_c \qquad [1.2]$$

and a phase separation occurs. The critical concentration is then the CMC. Below the CMC only the monomers and possibly non-micellar aggregates exist, while above the CMC the non-micellar surfactant concentration remains constant.

1.4.2. The Mass Action Model

The micelle is described by an aggregate M_m with an aggregation number m. The aggregation process in the solution is

$$mM \rightleftarrows M_m \qquad [1.3]$$

and the equilibrium constant is given by

$$K = \frac{f_m X_m}{m\ (f_1 X_1)^m} \qquad [1.4]$$

where f_m and X_m are the activity coefficient and mole fraction of the micelle, respectively. For large value of m ($m \geqslant 50$) this model is similar to the phase separation model. If it is assumed that the activity coefficients equal the

concentrations, *i.e.*, an ideal solution, the CMC can be expressed by

$$lnCMC \approx -\frac{\ln K}{m} \qquad [1.5]$$

1.4.3. The Micelle as a Small System

This method represents a refinement to the models discussed previously, which takes into account the changes in micelle size and shape. The model is based on a theory, the thermodynamics of small systems, developed by Hill (22). The micelle, treated as a small system, is considered to be surrounded by a bath which is defined by the environmental variables. Hill showed that the maximum number of independent variables is one more for the small system than for a corresponding macroscopic system. A dynamic equilibrium exists between micelles of different sizes. The intensive environmental variables include the temperature, pressure, and the chemical potential of the molecularly dispersed molecules. It is these variables that determine properties such as micelle size distribution. Hill adapted this formulism to micellar systems as an illustration to his theory. Hall and Pethica (23) further elaborated this model and derived a large number of formal thermodynamical relations. They were able to show for example that the mean aggregation number increases strictly with total surfactant concentration.

1.4.4. The Multiple Equilibrium Model

An extension of the mass action model is to introduce the equilibrium between aggregates of different sizes. The equilibrium is being considered as a stepwise growth of the micelle:

$$M_1 + M_{n-1} \rightleftarrows M_n \ , \quad n = 2,3,4..... \qquad [1.6]$$

with an equilibrium constant given by

$$K_n = (\frac{f_n X_n}{n}) / \frac{(f_1)(X_1)\, f_{n-1} X_{n-1}}{n-1} \qquad [1.7]$$

and the values of K_n determine the aggregation process.

The chemical potential of aggregate M_n is

$$\mu_n = n\,\mu_n + kT\,\ln(\frac{f_n X_n}{n}) \qquad [1.8]$$

where μ_n is the standard chemical potential per molecule in the micelle. The chemical potentials of the monomer in the micelle and in the solution are equal at equilibrium such that

$$\mu_n + \frac{kT}{n}\ln(\frac{f_n X_n}{n}) = \mu_{aq} + kT\,\ln f_1 X_1 \qquad [1.9]$$

for all n. The mole fraction of aggregate n is

$$\frac{X_n}{n} = \left\{ f_1 X_1 \exp[(\mu_{aq} - \mu_n) / kT] \right\}^n / f_n \qquad [1.10]$$

and the expression for the total surfactant concentration is

$$S = \sum_i X_i \qquad [1.11]$$

Equation [1.10] determines the size distribution of aggregates in solution. Eqs.[1.7] and [1.9] are related:

$$-kT \sum_{i=2}^{n} \ln K_i = n\,(\mu_n - \mu_{aq}) \qquad [1.12]$$

Application of these equations enables the description of the aggregation processes.

1.5. THE RESEARCH PROJECT

The goal of this thesis research is to provide a better understanding of the physico-chemical properties of surfactant systems. The aim is ambitious and the the topic is of enormous complexity. Therefore it is necessary to restrict the scope to certain aspects of these systems. Two classes of surfactants are used as model systems: alkyldimethylamine oxides and sodium alkyl sulfates. The former was chosen because it can be both cationic and nonionic, depending on the pH of the aqueous solution. The sulfates, which are an anionic surfactants, are used because of their popularity; it is almost the standard in surfactant research. These two compounds thus allow the study of the three general surfactant types, namely nonionic, cationic and anionic.

Owing to the nonionic-cationic duality of amine oxides, many papers have been published on its behaviours for various purposes set forth by different investigators. A general review of the characteristics of amine oxide would necessarily be long, hence it is omitted for the time being. Rather, relevant research on this substance is incorporated into this thesis as the latter develops. The lay-out of this thesis therefore follows the order: surfactant action (characterisation of alkyldimethylamine oxide, Chapters 2 and 3); surfactant interaction (amine oxide and alkyl sodium sulfate in combination, Chapters 4 and 5); and finally surfactant solubilisation (formation of microemulsion with amine oxide and the sulfate in combination based on the duplex film model, Chapter 6). Also included (Appendix C) is an alternative approach to the theoretical treatment of the energy of formation of a cylindrical micelles. Since most micelles are more or less spherical, the energy associated with the formation of cylindrical micelles has been largely ignored thus far. The same approach was first used by Hall and Mitchell (24) to formulate an expression for the free energy of formation of a spherical micelle.

1.6. REFERENCES

1. McBain, J. W., *Trans. Faraday Soc.* 9, 99 (1913).

2. Hartley, G. S., "*Aqueous Solution of Paraffin Chain Salts*", Hermann, Paris (1936).

3. Jones, E., and Bury, C., *Phil. Mag.* 4, 841 (1927).

4. Everett, D. H., *Pure Appl. Chem.* **31**, 579 (1972).

5. Rosen, M. J., and Hua, X. Y., *JAOCS*, 59, 168 (1982).

6. Fendler, J. H., and Fendler, E. J., "*Catalysis in Micellar and Macromolecular Systems*", Academic Press, New York (1975).

7. Hoar, T. P., and Schulman, J. H., *Nature (London)* **152**, 102 (1943).

8. Rosano, H. L., Lan, T., Weiss, A., Whittam, J. H., and Gerbacia, W. E. F., *J. Phys. Chem.* 85, 468 (1981).

9. Friberg, S. E., *Colloids and Surfaces* 4, 201 (1982).

10. Tadros, Th. T., in "*Solution Properties of Surfactants*", Mittal, K. L., Ed., Plenum Press, New York (1984).

11. Prince, L. M., "*Microemulsions, Theory and Practice*", Academic Press, New York (1977).

12. Tadros, Th. T., in "*Structure/Performance Relationships in Surfactants*", ACS Symposium Series 253, 153 (1984).

13. Debye, P., *J. Phys. Chem.* 53, 1 (1949).

14. Debye, P., *Ann. N. Y. Acad. Sci.* **51**, 573 (1949).

15. Reich, I., *J. Phys. Chem.* 60, 257 (1956).

16. Overbeek, J. Th. G., and Stigter, D., *Rec. Trav. Chim.* 75, 1263 (1956).

17. Hoeve, C. A. J. and Benson, G. C., *J. Phys. Chem.* **61**, 1149 (1957).

18. Poland, D. C., and Scheraga, H. A., *J. Colloid Interface Sci.* 21, 273 (1966).

19. Tanford, C., *J. Phys. Chem.* 78, 2469 (1974).

20. Nagarajan, R., and Ruckenstein, E., *J. Colloid Interface Sci.* 60, 221 (1977).

21. Israelachvili, J. N., Mitchell, D. J., and Ninham, B. N., *J. Chem. Soc., Faraday Trans. II* 72, 1525 (1976).

22. Hill, T. L., "*Thermodynamics of Small Systems*", Vols. 1 and 2, Benjamin, New York (1964).

23. Hall, D. G., and Pethica, B. A., in "*Nonionic Surfactants*", Schick, M. J. Ed., Marcel Dekker, New York (1967).

24. Hall, D. G., and Mitchell, D. J., *J. Chem. Soc. Faraday Trans. II* 79, 185 (1983).

CHAPTER TWO

CHARACTERISATION OF ALKYLDIMETHYLAMINE OXIDES

ACID-BASE TITRATION

2.1. INTRODUCTION

The solution behaviour of alkyldimethylamine oxide is considered in this chapter. The aggregation characteristic of long chain amine oxides (LDAO), especially the C_{12} homolog, in aqueous solution has been a subject of considerable interest to many researchers (1-6), owing to the nonionic-cationic nature of this class of compounds. Goddard and Kung (7) have investigated the monolayer properties of docosyldimethylamine oxide.

Thermodynamic properties including the freezing points, enthalpies of dilution, volumetric heat capacities, densities and sound velocities of butyl, hexyl, octyl and decyl dimethylamine oxides have been measured, and the osmotic coefficients and the apparent as well as the partial relative molar enthalpies, heat capacities, volumes, compressibilities, and expansibilities were calculated by Benjamin (3,8) and Desnoyers *et al* (9). Desnoyers *et al* further derived the isochoric heat capacities and isothermal compressibilities from the data obtained. They found a gradual change in trends of these functions when going from the lower homolog, which behaves like a medium size alcohol, to the higher one, which is typical nonionic surfactant. They also tested the applicability of the mass action model of micellisation and concluded that in the case of amine

oxide, the concentration dependence of various functions can be accounted for with this approach.

LDAO, a weak base having about the same basicity as the acetate anion (10), can exist in both the nonionic and cationic forms depending upon the pH of the solution. At any particular pH, an equilibrium is established between the cationic and nonionic forms,viz.,

$$LDAOH^+ \rightleftharpoons LDAO + H^+ \qquad [2.1]$$

According to Kolp *et al* (11), K_a, the molecular equilibrium constant as determined by potentiometric titration is

$$K_a = \frac{[H^+][LDAO]}{[LDAOH^+]} = 10^{-4.9} \qquad [2.2]$$

where the quantities in brackets are the activities of the indicated species relative to a standard state such that, at infinite dilution, the activities equal the molar concentrations.

Tokiwa and Ohki (4) have shown that 1) the K_a value of the micellised LDAO is different from the molecular form, viz., $10^{-5.9}$ and 2) while the value of K_a is independent of the degree of protonation (β) below the critical micelle concentration (CMC), it is dependent on β at concentrations above the CMC. These authours did not explain why the micellar pK_a(=5.9) at β=0 is different from the molecular value (pK_a=4.9).

2.2. EXPERIMENTAL

2.2.1. Material

Dimethyldodecylamine oxide was prepared from dimethyldodecylamine (Eastman-Kodak). The long chain amine was first fractionated under reduced

pressure. The fraction taken had a boiling point of 88°C at 1 torr. To a solution of dimethyldodecylamine in ethanol kept at 65°C in a constant temperature bath, 1.2 equivalents of 35% H_2O_2 were added slowly over a period of one hour, while constant stirring was maintained with the aid of a mechanical stirrer. As the mixture thickened, more ethanol was added. The temperature was then raised to 80°C, and an equal volume of distilled water was added. After approximately 4 hours at that temperature, the solution gelled. A large amount of ethanol was added to dissolve the gel. Excess peroxide was destroyed with MnO_2 in catalytic amount. MnO_2 was used instead of the usual choice of sodium sulfate as the reducing agent because it was reported (9) that the latter is more difficult to eliminate during recrystallisation; thus traces of it are present in the final product as contaminant. After filtration, the solvent was evaporated under reduced pressure in a rotary evaporator. The resulting solid was recrystallised several times from acetone and once from ethyl ether. The hygroscopic final product was dried and stored over P_2O_5 *in vacuo*. The surface tension versus concentration plot did not show a minimum.

Dimethyltetradecylamine oxide was a commercial sample (Onyx Chemical Company, Jersey City, N. J.). After evaporation of the solvent in a rotary evaporator under reduced pressure, the solid was purified by repeated recrystallisation from acetone. The final product was dried and stored in the same manner as the C_{12} homolog.

2.2.2. Surface Tension Measurements

Surface tension of amine oxide solutions was measured with a Rosano Tensiometer (Arenberg-Sage), equipped with a sandblasted platinum blade. The surface tension was determined at both pH 11 and pH 2, by preparing stock solutions at these pHs with the addition of concentrated NaOH and HCl, respectively. Subsequent dilutions were made by adding $1x10^{-3}$M NaOH solution

or HCl solution at $1x10^{-2}$M. All glassware was cleaned with freshly prepared potassium dichromate/sulfuric acid solution. Freshly deionised-distilled water was used in all preparations.

2.2.3. Viscosity Measurements

A Brookfield Viscometer (model LVT, Brookfield Engineering Lab.) was employed for the measurement of relative viscosity.

2.2.4. Acid-Base Titration

For the titration of amine oxide, solutions were made up with their pH adjusted to about 11 with NaOH and titrated with standardised HCl solution with a microburet. The pH was monitored continously during the titration with an Orion Research Ionalyzer (model 801A). Titration of dimethyldodecylamine oxide was done by first purging the solution with N_2 gas for 15 minutes, and then titrated under N_2 atmosphere. Titration of dimethyltetradecylamine oxide was done in open atmosphere. Constant stirring was maintained with a magnetic stirrer. The temperature of the solution was maintained at 25°C.

2.3. RESULTS

2.3.1. Surface Tension

Figure 2.1 shows the surface tension variation as a function of surfactant concentration at pH 11.3 and pH 2. The higher pH corresponds to the nonionic form of dimethyldodecylamine oxide (C_{12}DAO), while the lower corresponds to cationic amine oxide ($C_{12}DAOH^+$). Surface tension decreases rapidly with increasing surfactant concentration and reaches a break, above which no further change results. The break corresponds to the critical micelle concentration (CMC). In the case of C_{12}DAO, the CMC is $1.58x10^{-3}$M, and the ionised

Figure 2.1 Surface tension vs. concentration plots of dodecyldimethylamine oxide (C_{12}DAO) at pH 11.3 (nonionic) and pH 2 (cationic).

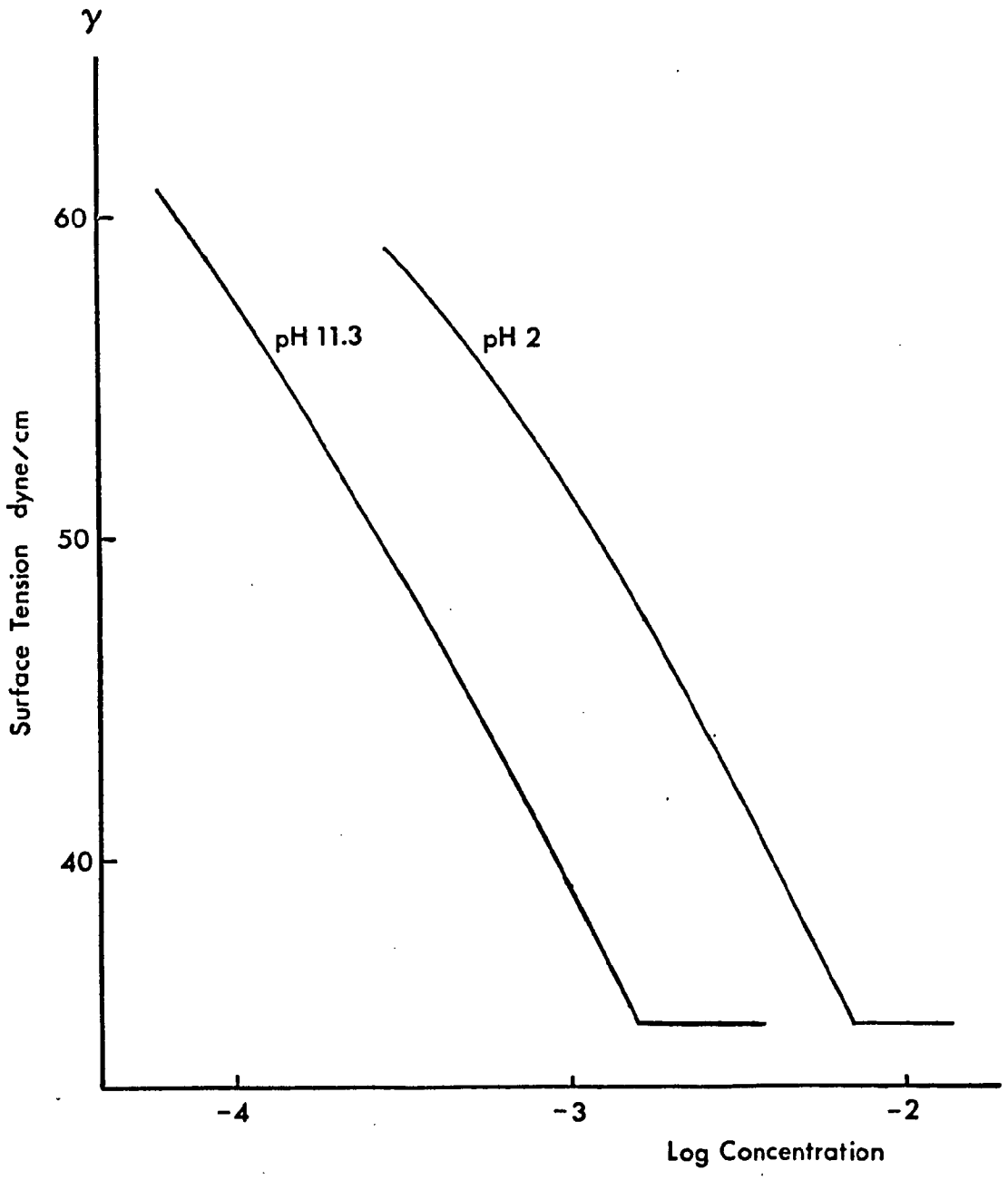

$C_{12}DAOH^+$ has a value of 6.92×10^{-3}M. The difference is probably due to higher solubility of the cationic species. From the slope of the curve, the apparent surface excess of the surfactant can be calculated, viz.,

$$\Gamma = - \frac{1}{2.303\, RT} \frac{d\gamma}{d\ logC} \qquad [2.3]$$

where Γ is the surface excess, γ is the surface tension, R and T have their usual meanings, and

$$\frac{1}{\Gamma} = area\ per\ molecule = \sigma \qquad [2.4]$$

At the CMC, the value of σ of the nonionic form is $\sim 43.1 \text{å}^2$, and that of the cationic species is $\sim 40.7 \text{å}^2$. It is of interest that the limiting surface tension of the two forms is equal (35 dyne/cm).

2.3.2. Acid-Base Titration and Viscosity

Figure 2.2 represents the titration curves of $C_{12}DAO$ at various concentrations at 25°C. For comparison these curves are plotted in pH against the degree of protonation (β). Below the CMC (5×10^{-4}M) a typical buffering action region is observed. Above the CMC the titration curves are slanted toward lower pH with increasing degree of protonation, 0.1M having a steeper slope than 5×10^{-3}M.

The titration curves of $C_{14}DAO$ are shown in Fig.2.3, plotted as pH against equivalent HCl scale. These curves have the same appearence as those of the $C_{12}DAO$ in general. The CMC of $C_{14}DAO$ is about 1×10^{-3}M at 25°C. Below the CMC, again a typical buffering action region is observed, and above the CMC the curves are more slanted with increasing concentration. However, when compared with the titration behaviour of the C_{12} homolog, it is clear that the value of pH at any particular value of β is somewhat higher in the case of

Figure 2.2 Acid-base titration curves of C_{12}DAO at 25 °C and under N_2 atmosphere, plotted as pH vs. degree of protonation (β). Amine oxide concentrations: 1-5×10^{-4}M, 2-5×10^{-3}M, 3-1×10^{-2}M, 4-0.1M.

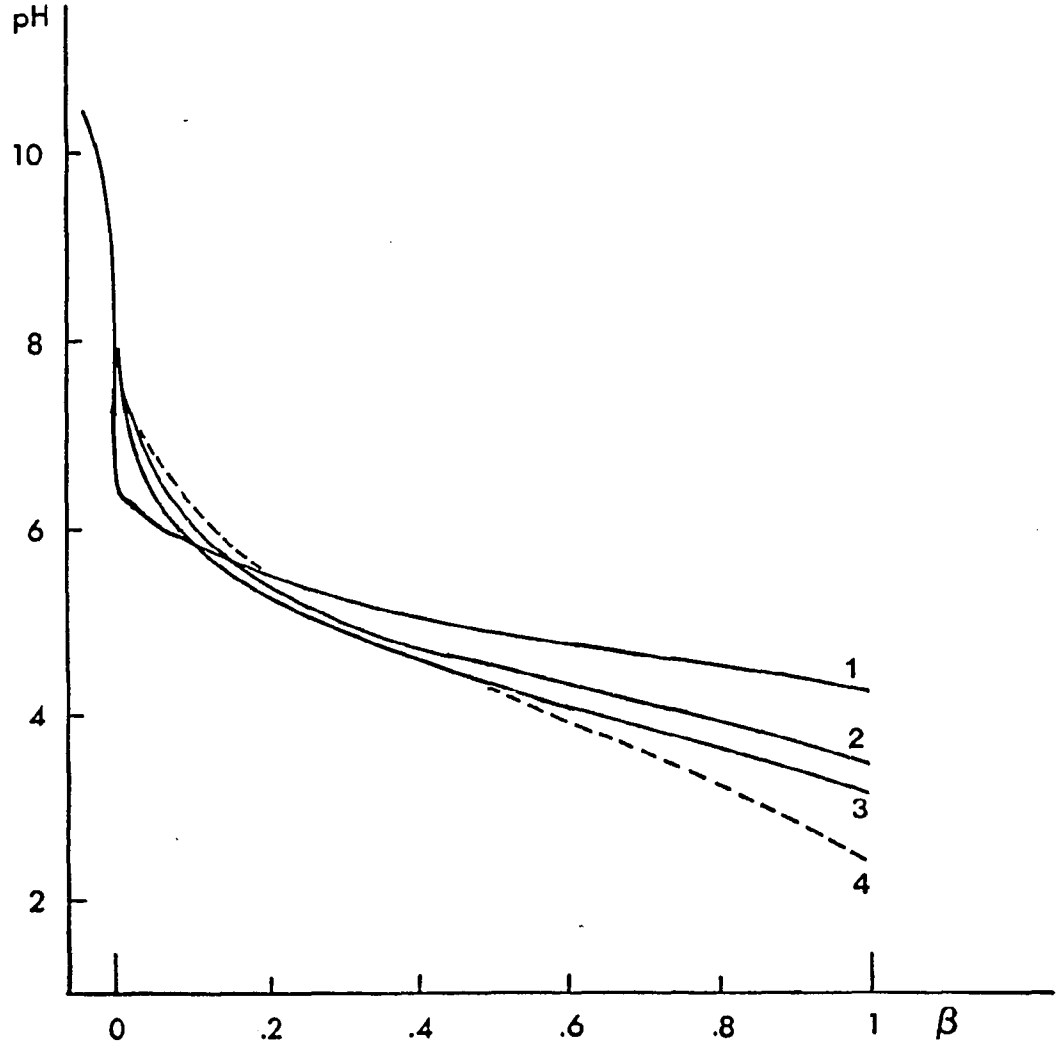

Figure 2.3 Acid-base titration curves of C_{14}DAO at 25 °C and in open atmosphere, plotted as pH vs. HCl equivalent added. Amine oxide concentrations: 1-4×10^{-5}M, 2-8×10^{-4}M, 3-0.2M. Curve 4 is the viscosity (η) variation of the 0.2M C_{14}DAO solution as a function of acidity.

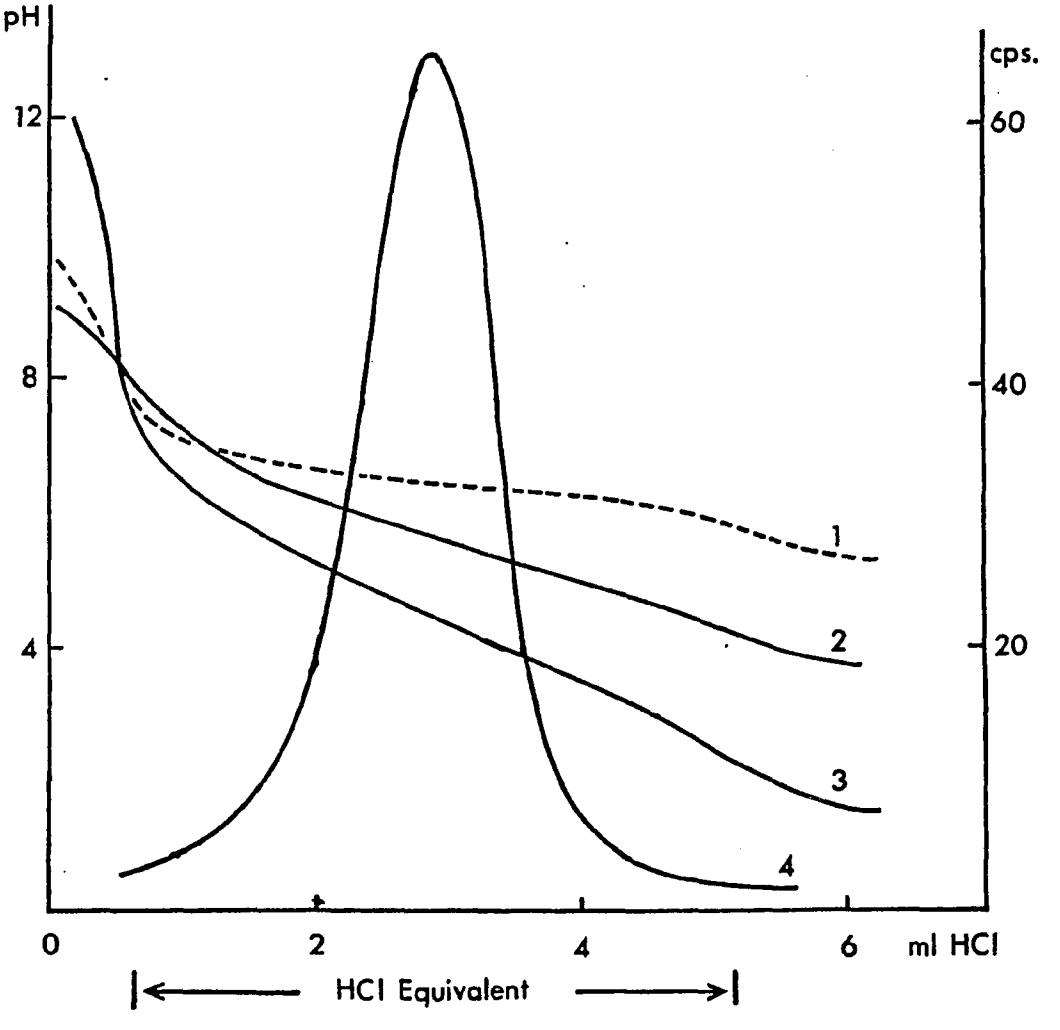

C_{14}DAO; this is probably due to the presence of bicarbonate ions and/or dissolved CO_2 in the solution of C_{14}DAO, since the titrations were carried out in open atmosphere in this case. It is well known that the presence of CO_2 in alkaline solution can cause a shift in the apparent pH value of the solution.

Also plotted on Fig.2.3 is the viscosity variation with HCl added for 0.2M C_{14}DAO. Maximum viscosity is observed when half of the amine oxide molecules are in the cationic form. However, in the absence of initially added NaOH, the change in viscosity with HCl added is less pronounced (by about an order of magnitude). C_{12}DAO shows the same behaviour but to a lesser extent. The increase in viscosity of the solution at a one-to-one cationic/nonionic mole ratio of the amine oxide molecules suggests possible complex formation between the two species, and may be similar to that observed in an acid-soap (12,13).

2.4. DISCUSSION

2.4.1. Molecular Area

An unusual feature of long chain amine oxides is that the ionised molecule occupies a slightly smaller surface area than the nonionised species. With a formal positive charge on the nitrogen, a substantial repulsive interaction among the head groups is expected, which results in a larger area occupied per molecule. Goddard and Kung (7) have investigated the monolayer properties of C_{22}DAO, and found that C_{22}DAO yields a less expanded film in the ionised form than in the nonionised form. They suggested the cause of this might be a diminished repulsive force in the ionised case; the quaternary ammonium group in the ionised amine oxide is unusual in possessing a hydroxy group, and the strongly electron-attracting, positively charged nitrogen substantially augments the polarisation of this OH group. With increased proton character, the H has an

increased tendency to hydrogen bond. Even though direct H bonding to neighbouring head groups would be difficult, augmented H bonding through surrounding water molecules is certainly likely. This may explain the slightly smaller area occupied by the ionic species as observed in the surface tension study.

2.4.2. Acid-Base Equilibrium and Viscosity

The amine oxide (LDAO) micelle surface can develop a surface charge as a result of protonation of the head groups. We can write a local equilibrium reaction and equilibrium constant for this ionisation process of surface sites, i.e.,

$$LDAOH^+ \rightleftarrows LDAO + H_s^+ \qquad [2.5]$$

where the subscript s indicates the surface and the equilibrium constant is given by

$$K_0 = \frac{[\,LDAO\,][H_s^+]}{[\,LDAOH^+]} \qquad [2.6]$$

The concentration of protons at the surface is related to the bulk proton concentration by the Boltzmann distribution,

$$[\,H_s^+] = [\,H^+]\,exp(\,-e\,\Psi_0/\,kT\,) \qquad [2.7]$$

where Ψ_0 is the electrostatic potential at the surface. Hence

$$K_0 = \frac{[\,LDAO\,][\,H^+]\,exp(\,-e\,\Psi_0/\,kT)}{[\,LDAOH^+]} \qquad [2.8]$$

Since the total oxide concentration remains constant during the ionisation process, Eq.[2.8] can be written as

$$K_0 = (\frac{1-\beta}{\beta})\,[H^+]\,exp(-e\Psi_0/kT) \qquad [2.9]$$

where β is the fraction ionised of the surface sites (degree of protonation), and is determined experimentally from the titration curve. Rearranging and expressing in negative logarithmic form,

$$pH = pK_0 - \log(\frac{\beta}{1-\beta}) - \frac{e\Psi_0}{2.3\,kT} \qquad [2.10]$$

where pK_o is the intrinsic dissociation constant of the cationic acid conjugate. The value of pK_o can be obtained by plotting pH + log(β/1-β) as a function of β. Extrapolation to zero degree of protonation (zero surface charge and potential), yields the intrinsic dissociation constant pK_o. Ideally, the plot should yield a straight line for sufficient low surface potential. Eq.[2.10] is identical to the one obtained in the theoretical treatment of the potentiometric titration of polyelectrolytes having a uniform distribution of ionisable groups of one kind (14,15).

Figure 2.4 is a plot of pH + log(β/1-β) vs. β at different C_{12}DAO concentrations. The extrapolated pK_o value varies with concentration; the monomeric species has a pK_o value of 4.95 while the micelles have pK_o values greater than the pK_o of the monomer, up to a final value of 5.95. Both of these values are in good agreement with the reported data (4). In the micellar region, the apparent pK values decreases from 5.95 to about 4 with increasing degree of protonation. This implies that the micelle is less favoured as a proton acceptor with diminishing nonionic character. The difference in pK_o values between micellar and molecular forms may then due to the surface charge effect. Protonation of the micelle is favoured for small values of β, and only when β exceeds a certain value, depending on the total concentration, does protonation of the monomer become predominant. As can be seen in the

Figure 2.4 pH + log (β/1-β) vs. β plot for C_{12}DAO. Amine oxide concentrations: 1-5x10^{-4}M, 2-5x10^{-3}M, 3-1x10^{-2}M, 4-0.1M. Extrapolation to β=0 yields pK_0, the intrinsic acid dissociation constant.

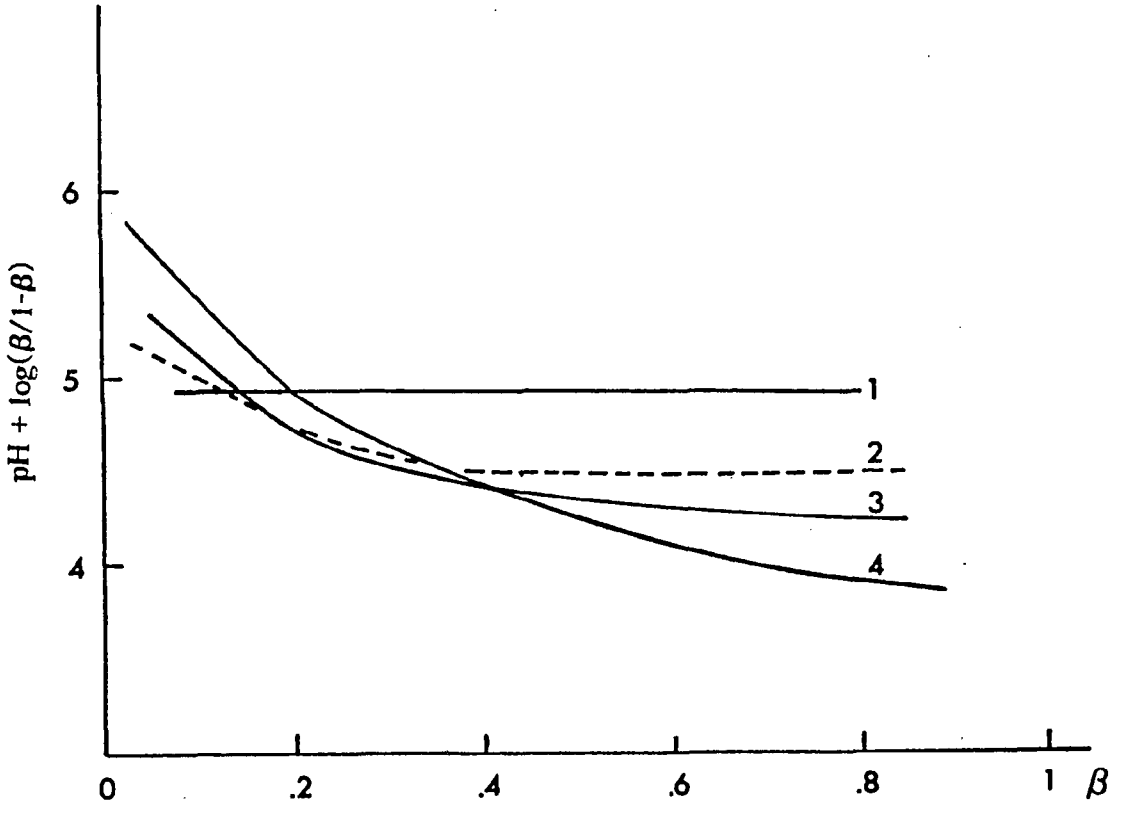

titration curves, the buffering region of the monomeric solution occurs for the most part, at a higher pH value than for concentrations above the CMC.

Difference in micellar and molecular pK_o values have been reported for other systems (16,17). However, no explanations were provided. In the case of C_{12}DAO, Mille (18) concluded on a theoretical ground that a smeared surface charge model alone, or a model which calculates ΔpK using only the electrostatic potential at a given charge due to the electrostatic potential of all other charges, is insufficient to explain the difference observed in the pK values at a (micelle)surface, and an analogous nonaggregating molecule in bulk solution. It was suggested that additional attractive interaction must be included, such as hydrogen bonding formation, in the interpretation of the data.

Another feature revealed in Fig.2.4 is the occurrence of nonlinearity in the plot, except for concentration below the CMC, because the last term in Eq.[2.10] is zero; therefore no electrical work is required to protonate the amine oxide. Above the CMC, a change in the micelle shape with increasing charge can cause the nonlinearity, as in the case of a protein (19). For amine oxides, the change in shape is accompanied by an increase in the viscosity of the solution, indicative of the formation of elongated structures. The light-scattering data obtained by Ikeda *et al* (20) suggest the formation of large rod-like micelle of C_{12}DAO at β=0.5 in the presence of NaCl, while at high and low pH values, the micelles are small and are probably spherical. There is a transition in shapes going from spherical→ elongated→ spherical of the amine oxide micelles as β is varied from 0 to 0.5 and then to 1. As was pointed out by Nagarajan and Ruckenstein (21), transition from spherical to cylindrical micelle is favoured by factors which contribute to an increase in the attractive component or a decrease in the repulsive component of the free energy of micellisation. In the case of ionised amine oxide, the ionisable proton is capable of hydrogen bonding to the neigh-

bouring oxygen, the average distance between adjacent head groups decreases effectively. As a result, the tail groups have to readjust spatially, thus leading to a breakage of the spheroid. Protonation of the monomer can also lead to the breakage of the spheroid if the assumption is made that the concentration of the monomer remains constant above the CMC (22). Both mechanisms contribute to the production of elongated structures.

2.4.3. Micelle Aggregation Number

Long chain dimethylamine oxide micellar solutions are viscous between pH 7 and pH 2. The number of amphiphiles per aggregate reaches a maximum value when half of the constituent molecules in the micelle are protonated. That leads to the formation of elongated or nonspherical structures due to an effective decrease in the area occupied by the head group, caused by the diminished repulsion between the polar heads and hydrogen bonding between adjacent molecules. We adapted to amine oxides a theory developed by Persoz and Rosano (23) which relates the surface area per molecule to optimum aggregation numbers.

This theory assumes a bileaflet disc-like micelle shape whose thickness is therefore equal to twice the length of the surfactant molecule. The disc faces are occupied by the amine oxide groups while the paraffinic tails constitute the interior of this bilayer.

Let us consider first the energy liberated by the addition of one molecule from the bulk solution to the micelle. This energy has two origins: [1] chain-chain interaction energy (positive), and [2] head groups interaction energy (negative). The first is constant and independent of the number (2N) of molecules already in the micelle. The second energy term increases with increasing 2N. Therefore, for a certain value, N_m, of N, the free energy becomes zero. Beyond that value, energy would need to be provided to add one molecule to the

micelle.

The formulation for the calculation of chain interaction energy for a half micelle (containing N molecules) can be found in Appendix A. Accordingly, the addition of one molecule liberates the energy

$$W_0 = [\, N - \alpha\,(\, 3.3\sqrt{N} - 2.7\,)]\,\omega_0 \qquad [2.11]$$

Head group interaction energy for a half micelle (Appendix B) represents the total electrostatic energy needed in order to add one dipole to the half micelle and is given by

$$W_e = \beta\left[\frac{\pi}{4} + \frac{3.75}{2\sqrt{2\pi}}\left(\frac{25}{8} + \frac{1}{\sqrt{3}}\right) - \frac{\ln N}{2\sqrt{N}} - \frac{4}{2\sqrt{N}} + \frac{2}{3\pi N}\right] \qquad [2.12]$$

The total energy liberated when adding one molecule is therefore

$$\frac{d\,(W_0 - W_e)}{dN} = \omega_0 - 2.469\beta + 0.5\beta\frac{\ln N}{\sqrt{N}} + \frac{1.333\beta - 1.65\alpha\omega_0}{\sqrt{N}} - \frac{0.2122\beta}{N} \qquad [2.13]$$

Consider an adsorbed monolayer as being formed by bringing in one molecule at a time (similar to the addition of one molecule to the half micelle). The formation of that monolayer allows one therefore to determine the energy that was just formulated, except that in this case N is very large.. Under this condition, Eq.[2.13] reduces to

$$\frac{d\,(W_0 - W_e)}{dN} = \omega_o - 2.469\beta \qquad [2.14]$$

Traube (24) has determined the value of ω_0 to be 4.4×10^{-14} ergs per CH_2 group in the hydrocarbon chain of a fatty acid for the free energy of adsorption.

Rosano (25) has shown that the free energy of adsorption at a water-paraffin interface is generally larger than at a water-air interface of the order of 10%. In the present model calculation, the Traube value is used.

If $\Delta\gamma$ is the surface tention reduction due to the surface pressure exerted by the monolayer, the same energy given by Eq.[2.14] can be expressed by $-\sigma\Delta\gamma$:

$$-\sigma\Delta\gamma = \omega_0 - 2.469\beta \qquad [2.15]$$

σ being the cross sectional area per molecule. This allows substitution in Eq.[2.13] of

$$\beta = \frac{\omega_0 + \sigma\Delta\gamma}{2.469} \qquad [2.16]$$

At equilibrium, the energy required to add one molecule is zero; and therefore

$$\Psi + 0.2025\,\frac{lnN}{\sqrt{N}} + \frac{0.54 - 1.65\alpha\Psi}{\sqrt{N}} - \frac{0.086}{N} = 1 \qquad [2.17]$$

where

$$\Psi = \frac{\omega_0}{\omega_0 + \sigma\Delta\gamma} \qquad [2.18]$$

Knowing Ψ and α, the number $2N_m$ of molecules in one micelle can be calculated from Eq.[2.14]. Fig.2.5 is a plot of the micelle aggregation number (2N) as a function of α at different values of $\sigma(\Psi)$ for C_{14}DAO. Assuming the CH_2 adjacent to the head group lies within the hydration sphere and does not enter into the formation of the hydrophobic core, the number of carbon atoms (N_c) that determines the maximum radius (R) is therefore one less than the total number. Using Tanford's relationship (26), the maximun radius is

Figure 2.5 The calculated micelle aggregation number (2N) as a function of area/molecule of C_{14}DAO for a given value of α, the fraction of molecules remained in contact with the aqueous phase. α values: 1-0.00, 2-0.05, 3-0.10, 4-0.15, 5-0.20.

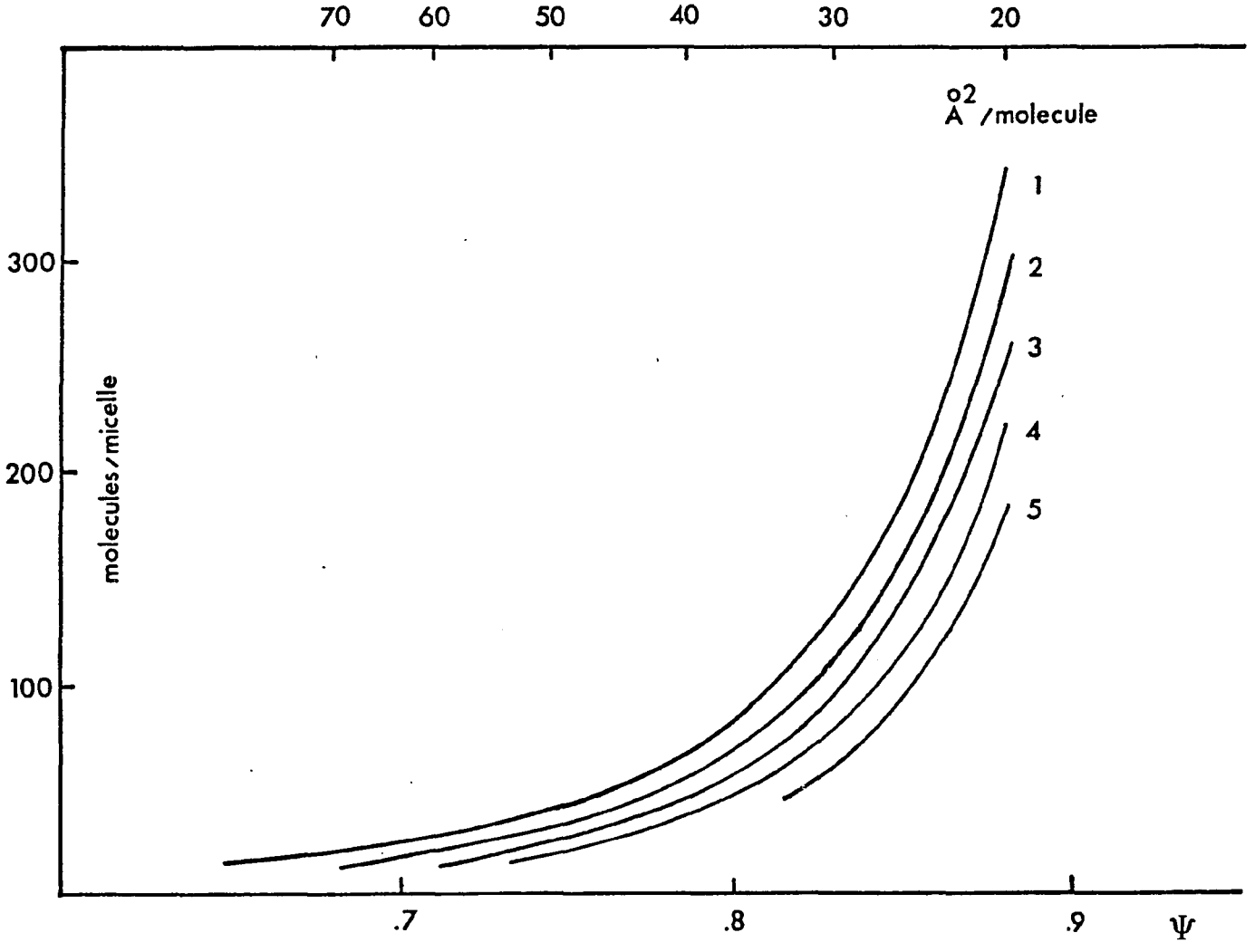

given by

$$R = (1.5 + 1.265N_c)a^{\circ} \qquad [2.19]$$

and for a C_{14} alkyl chain, R_{max}= 17.945å. It is generally accepted (27) that the radius (r) of a spherical micelle is about 80-90% of the maximum extended length, which sets an upper limit in the micelle aggregation number for any particular value of surface area per molecule. From the present theory, if the possibility of water penetration into the core is ignored (28) such that α=0.0, the calculated aggregation number will not exceed the limiting value for $\sigma > 40\text{å}^2$, if r=0.85R. Reduction in surface area below 40å^2 will not only increase the aggregation number, but will have to be accompanied by a change in the shape of the micelle.

2.5. REFERENCES

1. Herrmann, K. W., *J. Phys. Chem.* 66, 295 (1962).
2. *Ibid.*, 68, 1540 (1964).
3. Benjamin, L., *J. Phys. Chem.* 68, 3575 (1964).
4. Tokiwa, K., and Ohki, K., *J. Phys. Chem.* 70, 3437 (1966).
5. Ikeda, S., Tsunoda, M. A., and Maeda, H., *J. Colloid Interface Sci.* 67, 336 (1978).
6. *Ibid.*, 70, 448 (1979).
7. Goddard, E. D., and Kung, H. C., *J. Colloid Interface Sci.* 43, 511 (1973).
8. Benjamin, L., *J. Phys. Chem.* 70, 3790 (1966).
9. Desnoyers, J. E., Caron, G., DeLisi, R., Roberts, D., Roux, A., and Perron, G., *J. Phys. Chem.* 87, 1397 (1983).
10. Nylen, P., *Z. Anor. Allgem. Chem.* 246, 227 (1941).
11. Kolp, D. G., Laughlin, R. G., Krause, R. P,. and Zimmerer, R. E., *J. Phys. Chem.* 67, 51 (1963).
12. Rosano, H. L., Briendel, K., Schulman, J. H., and Eydt, A. J., *J. Colloid Interface Sci.* 22, 58 (1966).
13. Eagland, D., and Franks, F., *Trans. Faraday Soc.* 61, 2468 (1965).
14. Katchalsky, A., and Gillis, J., *Rec. Trav. Chim.* 68, 879 (1949).
15. Arnold, A., and Overbeek, J. Th. G., *Rec. Trav. Chim.* 69, 192 (1950).
16. Tokiwa, F., and Ohki, K., *J. Phys. Chem.* 71, 1824 (1967).
17. Corkill, J. M., Gemmel, K. W., Goodman, J. F., and Walker, T., *Trans. Faraday Soc. I* 66, 1817 (1981).
18. Mille, M., *J. Colloid Interface Sci.* 81, 169 (1981).
19. Tanford, C., Swanson, S. A., and Shore, W. A., *J. Am. Chem. Soc.* 77, 6414 (1955).
20. Ikeda, S., Tsunoda, M. A., and Maeda, H., *J. Colloid Interface Sci.* 70, 448 (1979).
21. Nagarajan, R., and Ruckenstein, E., *J. Colloid Interface Sci.* 71, 580 (1979).

22. Huchinson, E., Sheaffer, V. E., and Tokiwa, F., *J. Phys. Chem.* **68**, 2818 (1964).

23. Persoz, B., and Rosano, H. L., *J. Chim. Phys.* **51**, 534 (1954).

24. Adam, N. K., "*The Physical Chemistry of Surface Films*", 3 ed.,Oxford University Press (1941).

25. Rosano, H. L., *Mem. Serv. Etat.* **36**, 335 (1951).

26. Tanford, C., *J. Phys. Chem.* **76**, 3020 (1972).

27. Israelachvili, J. N., Mitchell, D. J., and Ninham, B. W., *J. Chem. Soc. Faraday Trans. II* **72**, 1525 (1976).

28. Tanford, C., *Proc. Nat. Acad. Sci.* **71**, 1811 (1974).

CHAPTER THREE

CHARACTERISATION
OF
ALKYLDIMETHYLAMINE OXIDES
C-13 NUCLEAR MAGNETIC RESONANCE

3.1. INTRODUCTION

It has been demonstrated in recent years that C-13 nmr studies of surfactant solutions can provide a wealth of information on the conformations of surfactant molecules (1-6). The advantages that C-13 nmr offers are [1] no labeling of the surfactant is required, [2] the resolution of C-13 nmr is considerably better than that of proton nmr because of the large chemical shift range; making it possible to differentiate the carbon atoms in an associating colloid, [3] the smaller magnetic moment of the carbon atom makes C-13 nmr less susceptible to line broadening due to magnetic dipole interactions which may be important at high surfactant concentrations, and [4] with the use of Fourier transform technique the low natural abundance (1.1%) of C-13 does not present a severe restriction. For example, detailed studies of the concentration dependence of the chemical shifts of the carbons in an alkyl chain can be used to deduce quantitative information on the micelle aggregation number, and the shift change on passage from the intermicellar solution to a micelle gives qualitative information on any accompanying conformational change of the alkyl chain.

The interpretation of the C-13 nmr data on surfactant self-assembly may be achieved without prior knowledge of the cause of the shift changes.

Nevertheless, such knowledge is of obvious interest since it may shed light on the micelle structure. Two principal mechanisms are mainly responsible for the origin of chemical shift changes on micelle formation. The first of these is the medium effect, i.e., the direct effect of the environment, and the second mechanism may be termed a conformation effect, i.e., the chemical shift may change as a result of a change in the conformation of the alkyl chain. Several different observations seem to rule out a sizable contribution from medium effects to the chemical shift values of methylene and methyl groups. The variation of chemical shift along the alkyl chain does not seem to correspond to the variation in the bulk environment to a large extent. Therefore conformational effects must play a dominant role in determining the chemical shift of carbon atoms in a chain. In this chapter, the average conformation of the aliphatic chain, as well as the effect of charging the head group on the chemical shifts of dodecyldimethylamine oxide (C_{12}DAO), are investigated with this technique.

3.2. EXPERIMENTAL

3.2.1. Chemicals

The synthesis and purification of C_{12}DAO have been described in Chapter 2. Solutions of C_{12}DAO were made in D_2O. Deuterium oxide and deuterium chloride were supplied by Stohler Isotope Chemicals (Waltham, Mass.), the former was 99.8% enriched and the latter was a 38% DCl solution in D_2O.

3.2.2. C-13 Measurement

C-13 nmr spectra were obtained using an IBM WP-200 SY Fourier Transform spectrometer at 50.33 MHz. Complete proton decoupling was used and the deuterium signal from D_2O was employed as the internal lock signal. The external reference was tetramethylsilane (TMS) contained in a

coaxial capillary inside a 10-mm tube with the sample solution. The carbons in TMS are all equivalent and are highly shielded as the protons, therefore it makes an ideal reference for carbon spectra, being shifted to the extreme upfield end of the spectrum for most compounds. Typical nmr parameters were : spectral width 5 KHz, pulse width 14 microsec (90 degree), relaxation delay 30 sec., and number of transients 1500 to 5000. The core memory was 32K resulting in the resolution of 0.305 Hz for a 5 KHz spectral width.

3.3. RESULTS

3.3.1. Assignment of Chemical Shift

Figure 3.1 shows the complete C-13 nmr spectra of dodecyldimethylamine oxide (C_{12}DAO) in the nonionic form (β=0, where β is the degree of ionisation) at two concentrations, 0.1 M (top) and $1x10^{-3}$ M (bottom). Since the CMC of nonionic amine oxide was found to be $1.6x10^{-3}$ M (Chapter 2), these spectra correspond to concentrations above and below the CMC. The poor signal to noise ratio in the dilute solution is purely a concentration factor. Tentative assignments of the 14 carbon atoms are made by comparison with similar compounds (1, 5, 6, 7), and are listed in Table 3.1. Consider the micellar solution first. The chemical shift of the two equivalent N-methyl carbons, C1', is considerably more downfield than the corresponding carbons in dodecyldimethylammonium chloride (DDAC), at 44ppm(5), and n-alkyltrimethylammonium ions, at 52-53ppm(1). The chemical shift of the C1 carbon of C_{12}DAO is about 70.6ppm, which is again more downfield than DDAC (59ppm) and the n-alkyltrimethylammonium ions. However, it is closer to the corresponding carbon in octylphosphate ion (6). The C2 carbon has a shift value of 26.6ppm, which is about 1ppm more upfield than the carbon in DDAC. The C3 carbon is also upfield shifted, by about 2ppm. The carbon atoms near the

Figure 3.1 50.33 MHz C-13 nmr spectra of C_{12}DAO in D_2O at 0.1M (top) and $1x10^{-3}$M (bottom). The assignment is made relative to external TMS without any susceptibility correction. C1': N-methyl carbons, C1: methylene carbon adjacent to nitrogen, C12: methyl carbon at chain end.

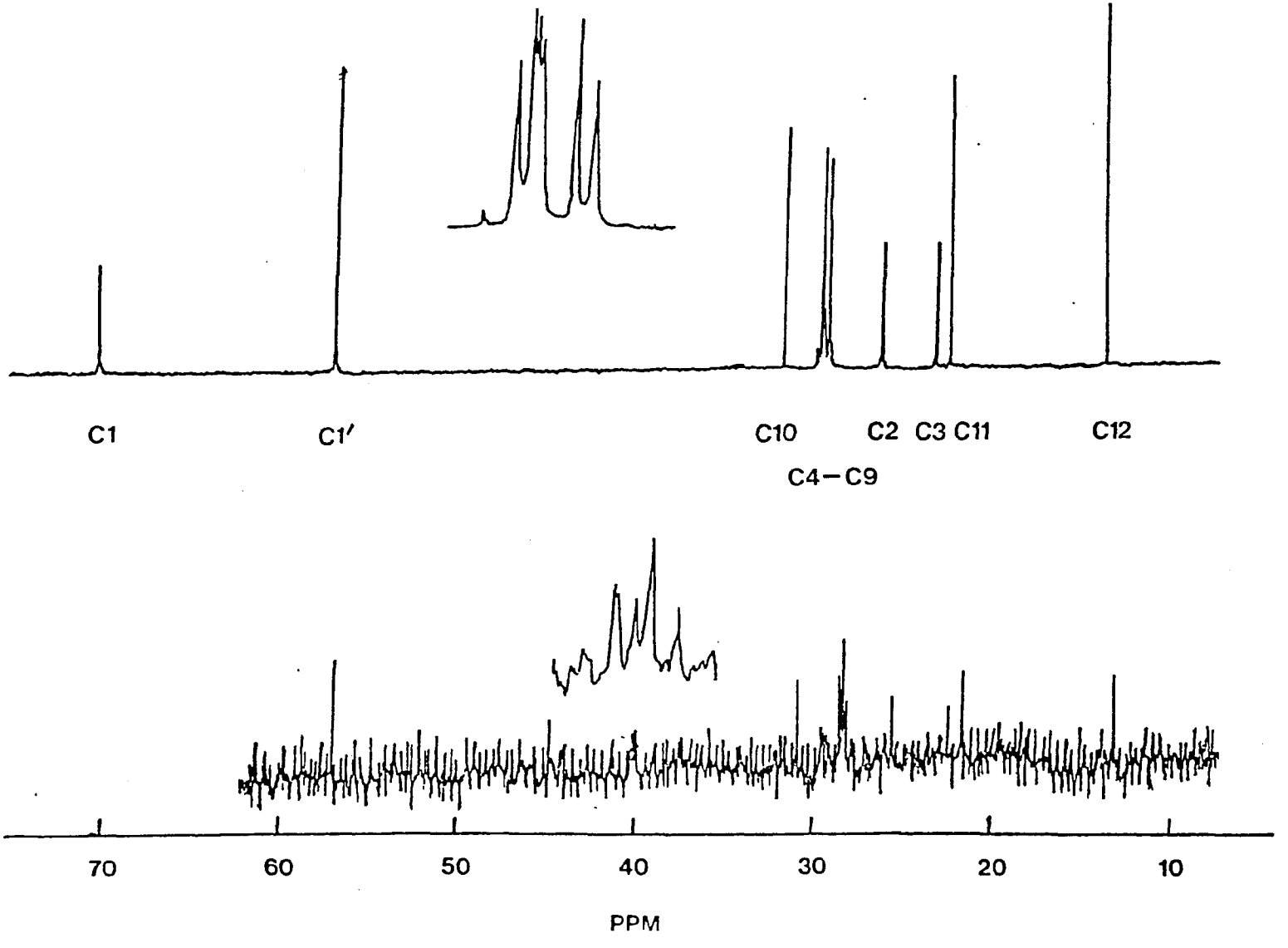

Table 3.1 — Chemical shift and chemical shift changes for various forms of dodecyldimethylamine oxide (C_{12}DAO).

Carbon atom number	Grant & Paul Hydro-carbon chain	Chemical Shift (δ) β=0 Micellar (δ_m) 0.1M	Chemical Shift (δ) β=0 Monomer (δ_1) 1×10^{-3}M	β=1 Monomer charging effect	Micelle charging effect — β — 0→0.5 , 0 →1
1'	—	57.24	57.11	−1.63	−0.71 −1.19
1	—	70.62	—	—	−1.12 −1.52
2	—	26.60	25.66	−0.45	−0.39 −0.57
3	—	23.48	22.91	−0.56	−0.64 −0.76
4	29.9	29.48	28.32	−0.20	−0.01 −0.02
5	"	29.86	28.51	−0.15	−0.14 −0.14
6	"	29.93	28.74	−0.03	+0.05 +0.06
7	"	29.89	28.62	−0.07	+0.09 +0.11
8	"	30.03	28.76	−0.02	−0.02 +0.00
9	"	29.61	28.51	−0.02	+0.02 +0.04
10	32.4	32.05	31.21	−0.01	+0.04 +0.06
11	23.0	22.70	22.07	−0.01	+0.01 +0.02
12	13.9	13.84	13.43	−0.01	+0.03 +0.04

*β= degree of protonation.

chain end, C10-C12, have shift values of 32.0, 22.7, and 13.8ppm, respectively, while the corresponding carbons in DDAC have values of 33.2, 23.8, and 15.1ppm. The assignments of carbon atoms in the middle of the chain, namely C4-C9, are made by comparing them with the respective carbons in sodium dodecyl sulfate (9). Setting the chemical shift of the C12 carbon as the reference, the agreement in frequencies from the C4 carbon to the C12 carbon is excellent.

Since the effects of various substituents on a particular carbon are always nearly additive in C-13 nmr, the chemical shifts can be predicted. Grant and Paul (10) have proposed an empirical formula for normal alkanes,

$$\delta_c = -2.1 + \Sigma\, n_{ik}\, A_i$$

where δ_c is the chemical shift of the k^{th} carbon, and A_i is the amount to add for each substituent in the i^{th} position relative to carbon k. The values of A_i were obtained from a linear regression analysis of some 30 chemical shift observations in normal alkanes (11). Aliphatic carbons are generally observed in the region of 2-50ppm from TMS. The more substituted the carbon, the further downfield is its chemical shift, this is called the α-effect, and it amounts to +9.1ppm for each carbon added. Additional carbons substituted β to a given carbon also cause downfield shift by +9.4ppm each and is called the β-effect. Another effect is observed on the chemical shift of the carbon once removed from that successively substituted and is referred to as the γ-effect, but it causes an upfield shift by -2.5ppm. The calculated values are listed in Table 3.1. It can be seen that they agree with the experimental values for the monomer within 1.6ppm and for the micelle within 0.4ppm. This is a direct evidence that the interior of micelles resemble bulk hydrocarbons (12).

Comparing the chemical shifts of the equivalent carbons in the micelle and

in the monomer, it is seen that downfield shifts occurred for all carbon atoms upon micellisation, with the largest change being observed in the central part of the alkyl chain, C4-C9. This phenomenon has been explained in terms of a steric effect (3,13). Downfield shifts indicate an increase in the population of *trans* conformer upon micellisation, while upfield shifts are indicative of an increase in the *gauche* conformer for the corresponding carbons. The former corresponds to a more extended configuration of the chain in the micellar core, maximising the hydrophobic interaction between the chains. The latter results in a more contracted chain configuration of the molecularly dispersed species, thereby minimising the unfavourable paraffin-water interfacial area.

3.3.2. Effect of Ionisation

The ionic form of amine oxide, $C_{12}DAOH^+$, was obtained by acidifying the solution. C-13 nmr spectra were obtained at a concentration of 0.1 M for β=0.5 and β=1, as well as $1x10^{-3}$M at β=1.. The difference in the chemical shift for respective carbon atoms in micellar $C_{12}DAOH^+$ vs. micellar $C_{12}DAO$ is given in the last column of Table 3.1. Protonation of the head group results in a formal positive charge on the nitrogen. It is expected that this positive charge can polarise(deshield) the electron density on neighbouring carbon atoms substantially, and the expected charging effect is then a downfield chemical shift. From Table 3.1, it is seen that only the carbons near the head group region, C1' and C1-C3, experience significant effects due to the charging process. However, the observed shift is in the opposite direction to what was expected, viz., an upfield shift, which seems to suggest that these carbon atoms are even more shielded in cationic amine oxide molecules. It is also seen that the change in chemical shift for the respective carbons is not linear; larger shift changes are observed when going from β=0 to β=0.5, while further protonation to β=1 produces changes that are smaller in magnitude. Table 3.1 also lists

the chemical shift change of carbon atoms in ionised amine oxide monomer as compared to the noninised species. It appears that protonation only affects carbon atoms near the head group, and the largest upfield shift is observed for the two equivalent C1' carbons.

3.4. DISCUSSION

3.4.1. Conformation Analysis

C-13 chemical shifts of resonances arising from carbons in a hydrocarbon microenvironment, such as that for most of the carbons in the interior of a micelle, are appreciably different from the values obtained for the molecularly dispersed surfactant species in an aqueous environment. Batchelor *et al* (14) have shown that in the case of bilayers, the only sizable factor affecting the shifts is linked to rotational isomerisation about the carbon-carbon bonds, while the solvent effects on methylenes are negligible, and that the shift variations due to temperature dependent solvation or electric field effects for most methylenes in the sheltered microenvironment are also insignificant. For C-C bonds in liquid hydrocarbon solutions and in the hydrocarbon portion of a fully saturated lipid bilayer, the trans conformer is usually the low energy form. Thus a downfield shift is expected when the trans state is more populated, as is observed when surfactant molecules undergo self-assembly. Another way of explaining the observed shift is to consider the chain/water interface. The energy of cohesion of water molecules, 144 ergs/cm^2, is larger than the energy of adhesion of paraffin/water, 45 ergs/cm^2,(15). Therefore the chain will take a conformation to minimise the paraffin/water interfacial area when it is molecularly dispersed. However, when the hydrocarbon chains are in the core of the micelle, the paraffin/paraffin cohesion energy is maximised ($\sim$56 ergs/cm^2), favouring a more extended conformation. Basically, these considerations can

account for the downfield C-13 chemical shifts of the carbons upon micellisation.

One of the most significant features of the C-13 chemical shift is the so-called γ effect observed in alkanes (16,17). An upfield shift is produced by steric compression of hydrogens in alkanes when the 1,4 carbons (γ carbons) are in the gauche conformation. Using the semiempirical formula which has both angle and distance dependence, proposed by Grant and Cheney (13) to describe the magnitude of the γ-effect, a 4.8ppm shift is predicted for a 100% gauche rotamer, while the γ shift for a trans rotamer is negligible. Based on this shift, the percent change of these rotamers upon micellisation (gauche to trans) of amine oxide is calculated to be in the order of 25% for the central carbon atoms in the chain (C4-C9), for an averaged value of 1.2ppm for the upfield chemical shift changes of these carbons. From the statistical calculations of Flory (18), the equilibrium rotamer population about the C-C bond of a polyethylene chain is 46% gauche. Using this percentage for the amine oxide monomer, it can be seen that the amount of gauche rotamers in the amine oxide micelle is about 34%.

3.4.2. Effect of Surface Ionisation

The direction of chemical shifts of carbon atoms near the head group region upon charging is probably caused primarily by a change in the solubility of the surfactant in the solution. It is well known that the CMC of surfactant decreases with increasing salt concentration (salting-out). In the case of amine oxide, increasing degree of protonation increases the solubility of the surfactant in water; the CMC of the cationic micelle is 6.92×10^{-3}M, slightly higher than that of the nonionic species. With increasing affinity for water, higher degree of water penetration into the micelle is achieved; the carbon atoms near the head group region become more hydrated as the micelle becomes more cationic in

character. With increasing water penetration, the unfavourable paraffin-water interaction is increased, resulting in an upfield C-13 nmr chemical shift of these carbons. It is interesting to note that in the present case, water molecules can penetrate up to three carbons in depth of a fully ionised micelle.

Modifications in the packing of molecules in the micelle upon charging may also influence the chemical shifts of carbons near the head group. From the study of the monolayer properties of docosyldimethylamine oxide (19) and octadecyldimethylamine oxide (Chapter 5), it is shown that long chain amine oxides characteristically undergo film condensation upon ionisation; the cationic species exhibits a more condensed film than the nonionic species. However, Davies (20) has demonstrated that the presence of an assembly of ionised head groups in a monolayer results in a substantial repulsive electrical contribution to the surface pressure of the film, and is usually readily evident from the expanded nature of the compression isotherms of ionised films. The unusual behaviour of amine oxide has been attributed to the ability of the hydroxy group in the ionised amine oxide to hydrogen bond, thus leading to a reduction in repulsive forces among the head groups, thereby decreasing the average distance between them. The condensing effect is therefore a reflexion of a closer packing in the molecular assembly. As a result, the carbon atoms near the head group become more shielded due to surface crowding, giving rise to the observed shifts upon ionisation. The possibility of hydrogen bonding is confirmed by the C-13 nmr data as well. Batchelor *et al* (21) have demonstrated in their study of fatty acids that solvent effects can make large contributions to the C-13 chemical shifts. When the solvent molecules donate hydrogen bonds, hence directly changing the head group dipole, downfield shift may be observed. Since the ionised amine oxide molecules are capable of donating hydrogen bonds to the solvent, chemical shift in the reversed direction,

i.e., upfield shift, is expected. The present results clearly support the earlier interpretation. Packing effects on C-13 nmr chemical shift have been shown in hexadecyldimethylammonium micelles in the presence of 1-methyl naphthalene (4), and in the phytol-lecithin bilayer structure (22). Schilling *et al* (23) have also reported upfield shift for the olefinic carbons in the 1,4-trans-polybutadiene lamella, and suggested that the observed shift may be attributed to the crystalline packing effects.

The monolayer results also showed that the most condensed film correspond to β=0.5, and exhibits the highest surface potential as well. In Chapter 2, it was shown that the solution viscosity approaches its maximum as β goes to 0.5, due to the formation of elongated structures. Furthermore, Ikeda *et al* (24) have shown that in the case of amine oxides, the largest micelle is obtained at half ionisation, and the shape of which is rod-like, while at β=1, the micelle assumes a spherical shape. This geometrical factor may affect the chemical shift of the carbon atoms near the head group region as well. In addition to affecting the CMC value of the surfactant, inorganic salt also induces micelle shape changes in surfactant solutions. Maeda *et al* (5) have measured the chemical shift of dodecyldimethylammonium chloride at fixed concentration but various concentrations of sodium chloride. They found that at high salt concentration (>0.8M), downfield chemical shifts were observed. Their results can be correlated with the light scattering data of this compound which showed a change of the micelle structure at the same salt concentration. The change was interpretated as a transition from spherical to rod-like micelle. Therefore it was concluded that a downfield chemical shift corresponds to a change of micelle structure from sphere to rod-like, and a upfield shift signifies the reverse. In the case of amine oxide, such a trend is observed in the chemical shift in going from β=0.5 to β=1, although the structural change is brought

about by acidifying the solution. Also, a direct hydrogen bonding between amine oxide molecule and the N-hydroxyammonium ion is possible as well. This direct bonding between neighbouring head groups would not only reduces the average distance between them, but also deshield the electron density effectively, thus alleviating the shielding effect brought about by the packing constraint. This type of complex formation is known for other half ionised molecules such as fatty acid soap (25-27). At β=1, hydrogen bonding is only possible through solvent molecules, and the effect of which in terms of electron density deshielding, is probably less significant than in the half ionised amine oxide.

In the case of nonionic amine oxide (β=0), the micelle is also spherical, upfield shifts are then expected for the respective carbons when compared to the half ionised micelle. However, the present results show that large downfield shifts are observed. In addition to the decrease in solubility of the nonionic species, this observation may also be caused by the strong dipole which has been shown to exist in the nonionic molecule (14), and is the primary cause of the expanded nature of the film. The presence of a strong dipole in the molecule thus favours the adsorption of counterions on the surface of the molecular assembly. From the study of the interactions between amine oxide and eletrolytes using Na-23 and H-2 nmr measurements, Rendall *et al* (28) have shown that significant concentrations of ions can penetrate between the head groups, leading to a reduction in micelle size and shape, because the ions occupy space between the head groups. Thus a decrease in the shielding of carbon atoms near the head group is likely, resulting in a downfield chemical shift of these carbon atoms when compared to the half ionised species.

From the C-13 nmr results the extent of water penetration near the head

group at the micelle surface may be determined quite accurately (3 carbons in the case of cationic amine oxides). These results when coupled with informations obtained from monolayer studies, can provide a better understanding as to the way the surfactant molecules are associated in a micelle.

3.5. REFERENCES

1. Williams, E., Sears, B., Allerhand, A., and Cordes, E. H., *J. Amer. Chem. Soc.* 95, 4871 (1973).

2. Drakenberg, T., and Lindman, B., *J. Colloid Interface Sci.* 44, 184 (1973).

3. Persson, B. O., Drakenberg, T., and Lindman, B., *J. Phys. Chem.* 80, 2124 (1976).

4. Ulmus, J., Lindman, B., Lindblom, G., and Drakenberg, T., *J. Colloid Interface Sci.* 65, 88 (1978).

5. Maeda, H., Ozeki, S., Ikeda, S., Okabayashi, H., and Matsushita, K., *J. Colloid Interface Sci.* 76, 532 (1980).

6. Chevalier, Y., and Chachaty, C., *Colloid and Polymer Sci.* 262, 489 (1982).

7. Kolp, D. G., Laughlin, R. G., Krauss, R. P., and Zimmerer, R. E., *J. Phys. Chem.* 67, 51 (1963).

8. Tokiwa, F., and Ohki, K., *J. Phys. Chem.* 70, 3437 (1966).

9. Cabane, B., *J. de Physique* 42, 847 (1981).

10. Grant, D. M., and Paul, E. G., *J. Amer. Chem. Soc.* 86, 2984 (1964).

11. Cooper, J. W., "*Spectroscopic Techniques For Organic Chemists*", Wiley, New York (1980).

12. Gerbacia, W. E., and Rosano, H. L., and Zajac, M., *JAOCS* 53, 101 (1976).

13. Grant, D. M., and Cheney, B., *J. Amer. Chem. Soc.* 89, 5315 (1967).

14. Batchelor, J. G., Prestegard, J. H., Cushley, R. J., and Lipsky, S. R., *Biochem. Biophys. Res. Comm.* 48, 70 (1972).

15. Adam, N. K., "*The Physics and Chemistry of Surfaces*", Oxford University Press, 3rd edition (1941).

16. Dalling, D. K., and Grant, D. M., *J. Am. Chem. Soc.* 89, 6612 (1967).

17. *Ibid.*, 94, 5318 (1972).

18. Flory, P. J., "*Statistical Mechanics of Chain Molecules*", Wiley, New York, (1969).

19. Goddard, E. D., and Kung, H. C., *J. Colloid Interface Sci.* 27, 247 (1968).

20. Davies, J. T., *J. Colloid Sci.* 11, 377 (1956).

21. Batchelor, J. G., Cushley, R. J., and Pretigard, J. H., *J. Org. Chem.* 39, 1698 (1974).

22. Cushley, R. J., and Forrest, B. J., *Can. J. Chem.* 54, 2059 (1976).

23. Schilling, F. C., Bovey, F. A., Tonelli, A. E., Tseng, S., and Woodward, A. E., *Macromolecules* 17, 728 (1984).

24. Ikeda, S., Tsunoda, M., and Maeda, H., *J. Colloid Interface Sci.* 70, 448 (1979).

25. Rosano, H. L., Breindel, K., Schulman, J. H., and Eydt, A. J., *J. Colloid Interface Sci.* 22, 58 (1966).

26. Feinstein, M. E., and Rosano, H. L., *J. Phys. Chem.* 73, 601 (1969).

27. Stigter, D., *J. Phys. Chem.* 64, 842 (1960).

28. Rendall, K., Tiddy, G. J. T., and Trevethan, M. A., *J. Colloid Interface Sci.* 98, 565 (1984).

CHAPTER FOUR

INTERACTION OF ALKYLDIMETHYLAMINE OXIDE WITH SODIUM DODECYL SULFATE

4.1. INTRODUCTION

Considerable attention has been given to the study of mixed surfactant solutions (1-4). Aqueous solutions of these systems may exhibit striking changes in their physical properties, owing to their ability to form mixed micelles in the bulk and mixed films at the (air-solution) interface. In this respect, study of these systems is of obvious importance, both for practical and theoretical reasons (5-7).

The surface activities of mixed surfactant solutions is often greater than would be expected in the absence of any mutual influence between the surfactants. Generally, such synergistic effects seen to be negligible for mixtures of nonionic surfactants (8,9). Ionic/nonionic mixtures can show appreciable synergism (10). The largest however, are the synergistic effects in cationic/anionic mixtures. In this chapter, the interaction between alkyldimethylamine oxide (LDAO) and sodium dodecyl sulfate (SDS) is investigated. The former has been well characterised in previous chapters; the latter compound, an anionic surfactant, is almost the "standard" of surface chemical investigations (11).

SDS has been shown to interact with a variety of compounds of either cationic or nonionic nature. For example, Lucassen-Reynders *et al* (4) have shown that upon mixing dilute solutions of SDS and dodecyltrimethylammonium bromide, the surface pressure can increase by more than 40 dyne/cm, resulting from an additional adsorption of the double long chain salt consequent of mixing. At the solubility limit of the mixed system, micelles or crystals of equimolar composition are formed. When the overall bulk composition is not equimolar, the formation of an equimolar second phase shifts the solution composition in favour of the surfactant in excess. At high concentration the phase of equimolar composition is solubilised in the micelles of the surfactant in excess. Kung and Goddard (12) as well as Abe and Ogino (13) studied the interaction between SDS and long chain primary alcohols. They reported the formation of a complex and/or a liquid crystal of molar ratio of 2:1 of SDS to alcohol, while Jones (14) investigated the interaction of SDS with polyethylene oxide and found an enhancement in solution viscosity. Since amine oxide shows the cationic-nonionic duality, and judging from the studies done with SDS, it seems that SDS is a well suited candidate with which large interaction between the two classes of compounds is possible.

4.2. EXPERIMENTAL

4.2.1. Material

Alkyldimethylamine oxides with the long chain containing 12, 14, 16, and 18 carbon atoms (Onyx Chemical Co. Jersey City, N.J.) and laboratory grade sodium dodecyl sulfate (Fisher Scientific Co. Fairlawn, N.J.) were used without further purification. Another sample of SDS of 99% purity (Sigma Chemical Co. St.Louis, MO.) together with dodecyldimethylamine oxide prepared in this laboratory (see Chapter 2) were also used in some experiments. The results

with different samples did not show large discrepencies in their values. The impurities in the commercial samples did not seem to pose any difficulties. Since fairly concentrated solutions were used in most cases, the impurities probably were solubilised in the micelles. This impurity solubilisation by micelles has been shown to be the cause of elimination of the minimum in surface tension-concentration plot at high surfactant concentration (15).

4.2.2. Solution Preparation and Measurements

Binary mixtures of amine oxide (LDAO) and SDS solutions were prepared by mixing different volumes of the surfactant solutions at equal molar concentration. In one experiment, the amount of LDAO was held constant while an increasing amount of solid SDS was dissolved into several beakers containing the amine oxide solution for the purpose of comparison.

For the acidometric titration of surfactant mixtures, pH was monitored with an Orion Research Ionalyser (model 801A, Orion Res. Inc. Cambridge, Mass.). The mixture were initially adjusted in pH to about 12 with concentrated NaOH and then titrated with standardised HCl solution. All other pH measurements were made with a Photovolt pH meter (Photovolt Corp. New York, N. Y.) The instruments used for the determination of surface tension and viscosity have been described in Chapter 2. The percent light transmission was monitored for each of the mixture at 490nm utilising a Spectronic 20 spectrophotometer (Bausch & Lomb Co. Rochester, N. Y.). In some cases, especially for viscous mixtures, it was necessary to centrifuge the solution before the percent light transmission was taken.

4.2.3. Wettability Test of Glass Surface

A glass surface in water is negatively charged. When the corner of a cleaned and water covered microscope cover slide touches the surface of a solu-

tion containing cationic surfactant just below its CMC, *instantaneous* dewetting occurs; the positive charge of the surfactant interacts electrostatically with the negative charge of the glass surface. The solid surface is then covered by a thin layer of the surfactant molecules with their hydrophobic tails pointing outward, thus the surface is no longer wettable. This effect is not observed with anionic and nonionic surfactant solutions, although exception can occur in the latter case (16). This method provides a rapid test as part of surface characterisation.

4.2.4. Viscoelasticity

Viscoelasticity of solution was determined visually by the simple method of swirling a vial containing the solution and observe the recoiling of air bubbles entraped in the solution (17). Although this method of detecting viscoelasticity seems primitive, it is a highly sensitive method nonetheless.

4.3. RESULTS

4.3.1. Surface Tension, Viscosity and pH

Mixtures of C_{12} or C_{14}-DAO with SDS show surface tension reduction upon mixing, and a minimum is observed at a 1:1 molar ratio, as shown in Fig. 4.1 for C_{14}DAO at a total surfactant concentration of 0.15M. Also shown is the variation in pH for different mixing ratios. The increase in pH of the mixed solution seems to indicate that the addition of SDS to an amine oxide solution favours the protonation of amine oxide, water molecules being the proton donor, thus producing an excess of hydroxide ions in the bulk solution, giving rise to the observed increase in pH. The change in viscosity of the mixture at different compositions is plotted in Fig.4.1 as well, the maximum of which corresponds to a $3C_{14}$DAO/SDS association. These sizable increases in viscosity suggest a change in micellar structure. Similar behaviour is observed for

Figure 4.1 Relative viscosity (η:◊), surface tension (γ: ○) and pH (□) variations at different C_{14}DAO/SDS mixing ratios. Total surfactant concentration equals 0.15M.

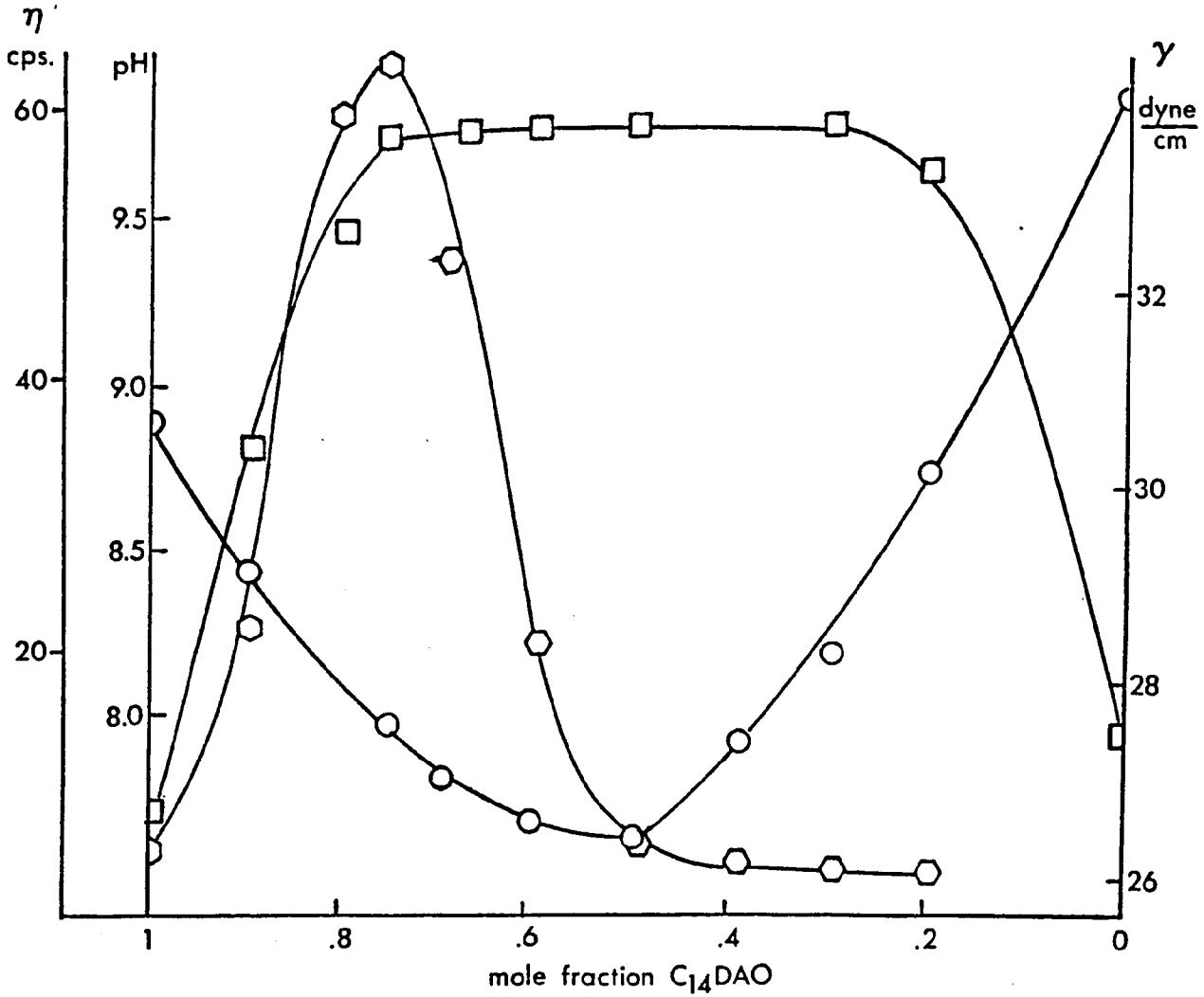

the C_{12}DAO/SDS mixtures.

Minimum surface tension at a 1:1 cationic/anionic surfactant mixing ratio has been reported in the system containing SDS and dodecyltrimethylammonium bromide (3). In addition, 1:1 association has been observed for C_{12}DAO with sodium dodecyl benzene sulfonate and with potassium dodecane sulfonate (1,2), both in dilute solutions. In these two cases, hydrogen bonding between the protonated amine oxide and the anionic sulfonate was shown to exist in the solid state. Double dodecyl salt may separate out in crystalline form, as reported in (1,2,18), but no precipitation was observed in this work when the pH of the solution was kept above 9. It is probable that the crystalline solid is readily solubilised by the surfactant in excess in the solution.

The 3:1 C_{12} and C_{14}-DAO/SDS mixtures exhibit non-Newtonian fluid characteristics. Fig.4.2 shows the viscosity at different shear rates as a function of time of shearing for a 3:1 C_{14}DAO/SDS mixture. A decrease in viscosity with increased shear rate is observed. At high pH (~12), adjusted by adding NaOH, the mixture is still non-Newtonian and its viscosity is enhanced by about an order of magnitude (at high shear rate) to two orders of magnitude (at low shear rate), when compared to the values at its natural pH (~10). The solution also exhibits birefringence when shaken. Upon cooling, the solution become milky, indicating possible crystal formation; this behaviour is reversible when the temperature is raised. These observations suggest that the mixed solution can probably be categorised as a liquid crystal.

Figure 4.3 is a plot of viscosity vs. concentration for a C_{14}DAO/SDS mixture. The viscosity varies strongly with concentration, and the shape of the curve indicates that the micelles are not spherical, but they may be rod-like, as in the case of concentrated cetyltrimethylammonium bromide solutions (19), or disc-like. The 3:1 mixture becomes viscoelastic and rheopectic when a small

Figure 4.2 Relative viscosity (η) vs. time of shearing plot of the $3C_{14}$DAO/SDS mixture at a total surfactant concentration of 0.2M. Shearing rate: 1-6rpm, 2-12rpm, 3-30rpm, 4-60rpm.

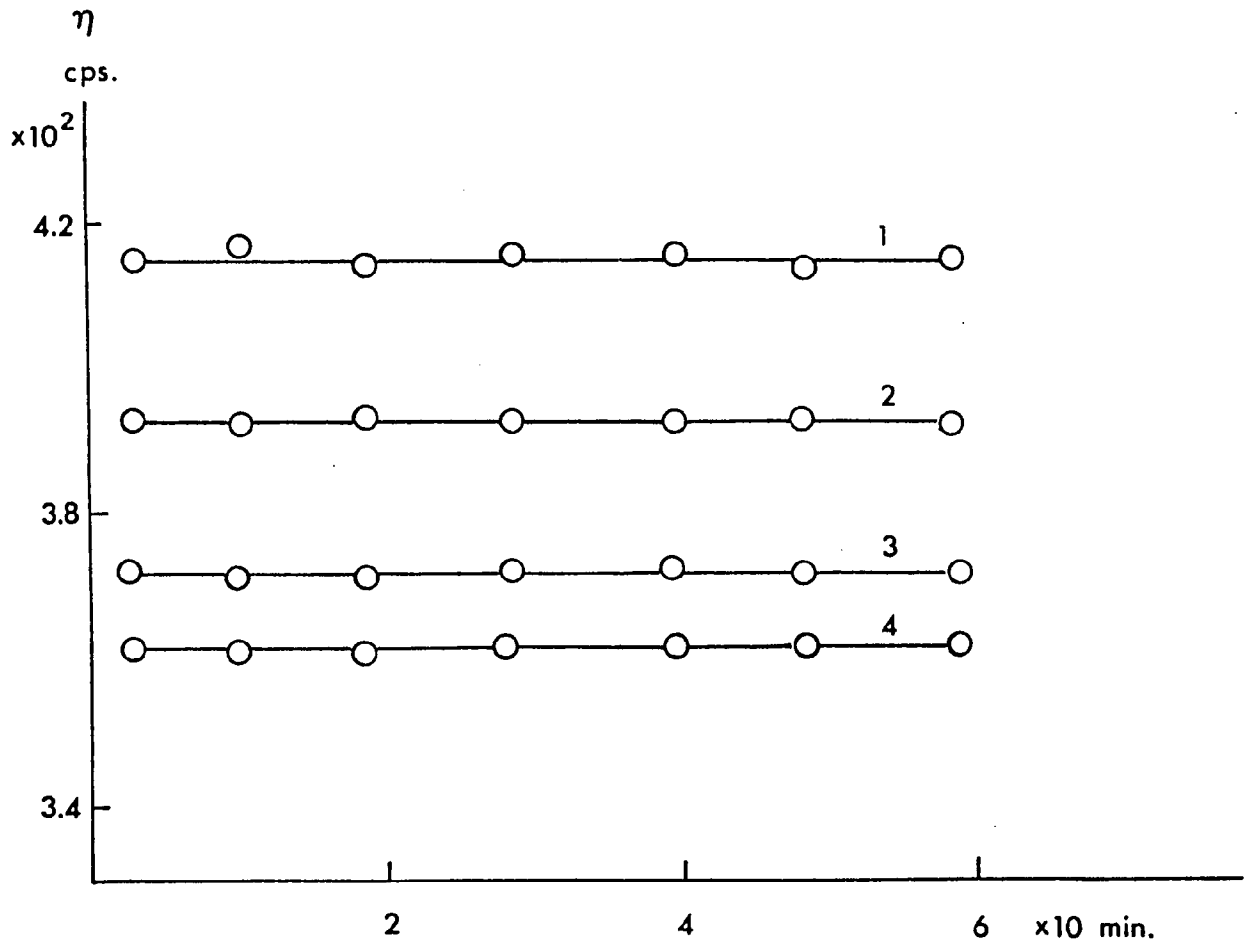

Figure 4.3 Relative viscosity/concentration (η/C) vs. concentration plot of the $3C_{14}$DAO/SDS mixed solutions at 25 °C and constant shearing rate.

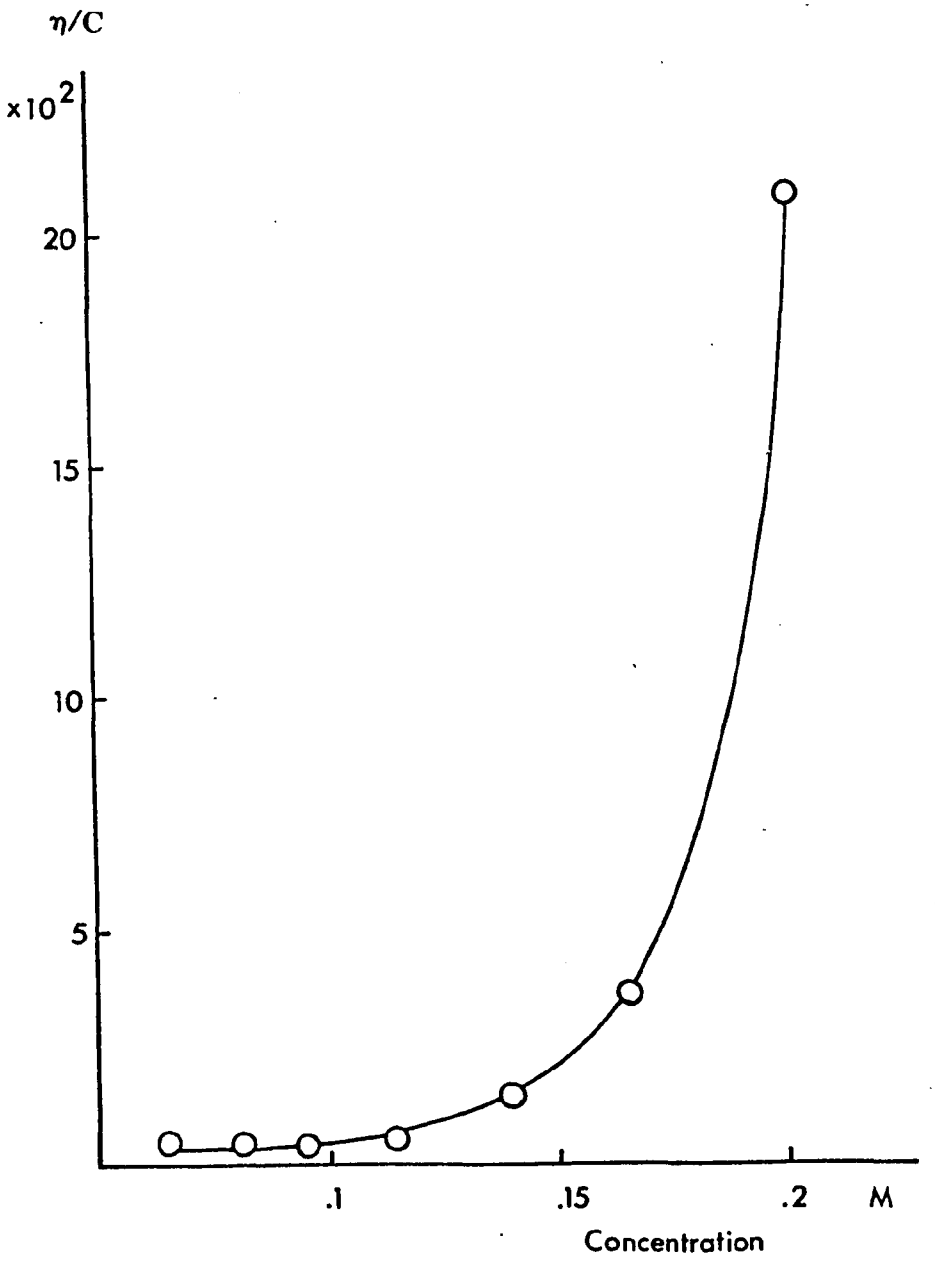

amount of NaCl is added. Rheopectic solutions are defined as solutions exhibiting a reversible increase in shear stress with time at a constant shear rate under isothermal conditions. It has been correlated with the onset of micellar growth (17). The rheopectic behaviour is probably due to long thread-like micelles that are aligned parallel to the flow in weakly bound clusters, as in the case of cetyltrimethylammonium bromide and mono-substituted phenol mixed solutions (20).

Figures 4.4 and 4.5 show the interactions between C_{16}DAO and C_{18}DAO with SDS at a total surfactant concentration of 0.05M and 0.005M, respectively. For amine oxide/SDS ratio greater than 1, these mixed solutions are turbid and birefringent. The birefringency is determined visually by placing the samples between two cross-polarised plates. Addition of SDS results in production of filament-like structures. When the molar amount of SDS is equal to or greater than that of the amine oxide, the solutions then become clear and isotropic.

At 3:1 C_{16}DAO or C_{18}DAO/SDS molar composition, the change in pH reaches its maximum and levels thereafter until the amount of SDS is in excess, and then decreases, reaching the pH of pure SDS solution. Minimum surface tension is reached when the LDAO content is still in excess, unlike the cases of C_{12} and C_{14}-DAO. This observation indicates that the surface of the solution has already been saturated with a mixed species, formed between C_{16} or C_{18}-DAO with SDS, although the bulk concentration of the individual species are different, and that the composition of this mixed species may be the same throughout the low surface tension region. If indeed a new species is formed, then surface tension lowering will be expected, since the double chain surfactant is less water soluble and therefore more surface active. Enhancement in viscosity is still observed with C_{16}DAO. However, C_{18}DAO shows a rapid

Figure 4.4 Relative viscosity (η:◇), surface tension (γ: ○) and pH (□) variations at different C_{16}DAO/SDS mixing ratios. Total surfactant concentration equals 0.05M.

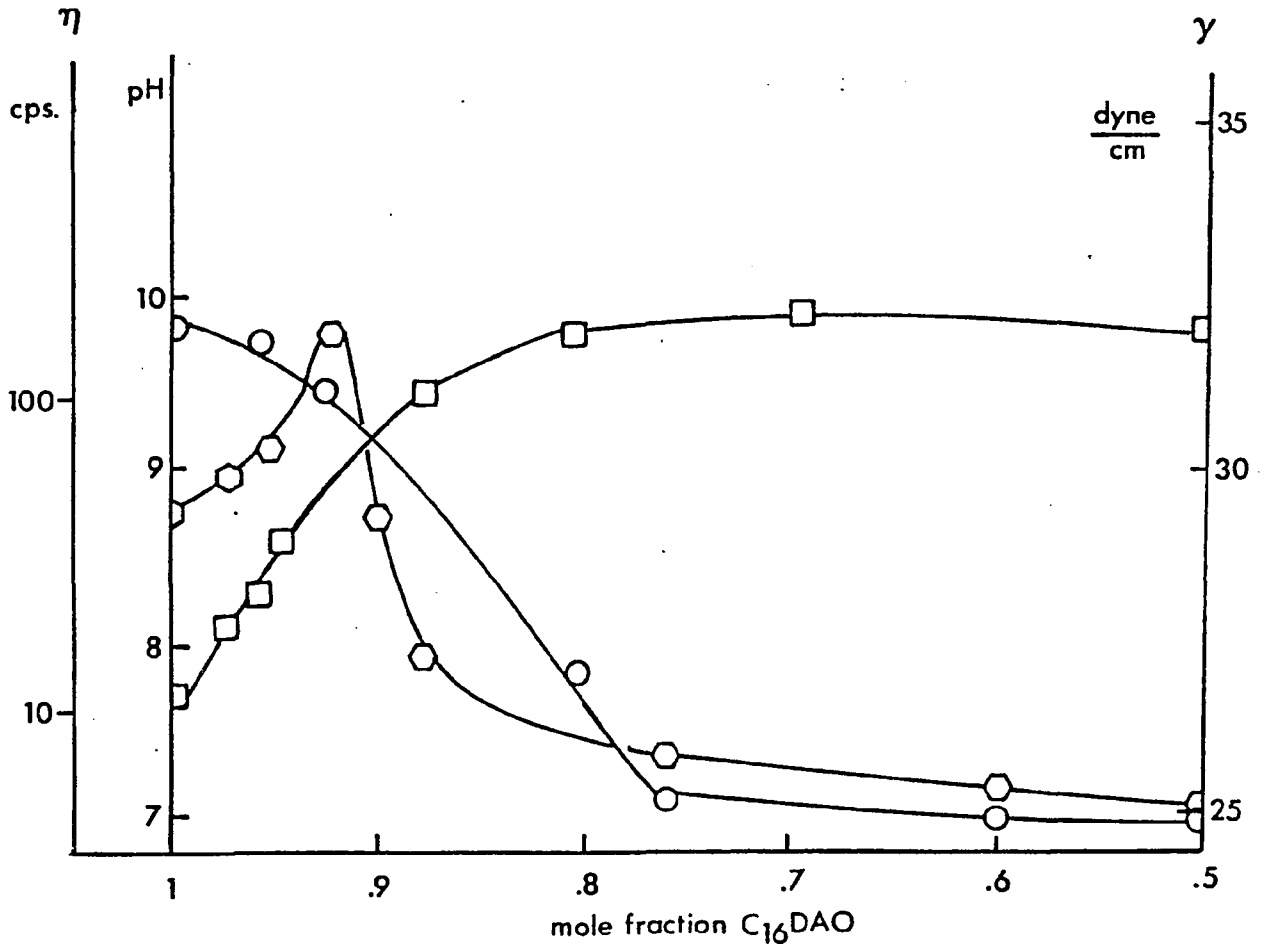

Figure 4.5 Relative viscosity (η:○), surface tension (γ: ○) and pH (□) variations at different C_{18}DAO/SDS mixing ratios. Total surfactant concentration equals 0.005M.

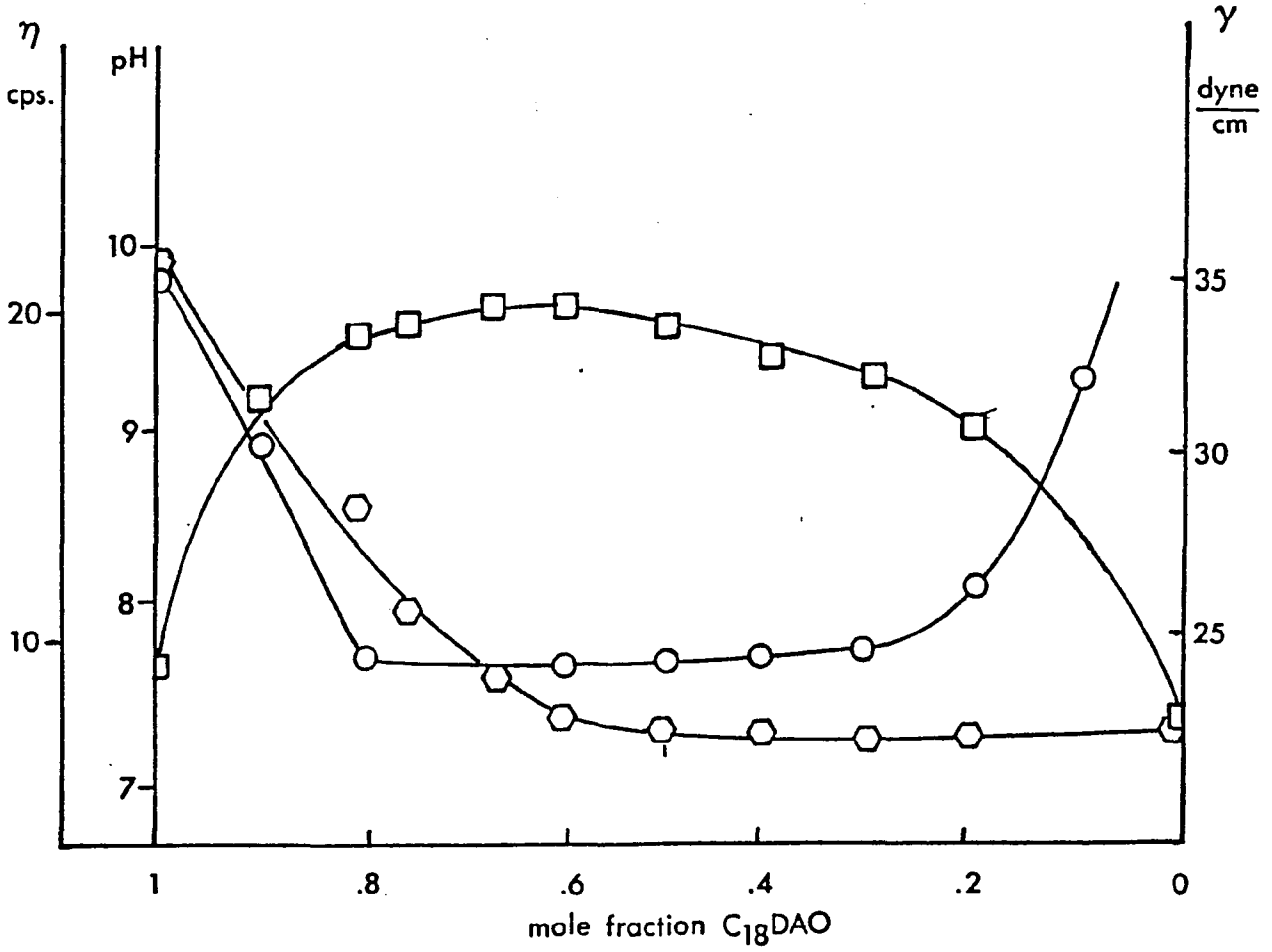

decrease in viscosity upon mixing SDS, the value of which reaches that of the SDS solution at equal molar composition.

4.3.2. Titration of LDAO/SDS Mixtures

Figure 4.6 shows the titration curves of a 0.2M C_{14}DAO solution and a 3:1 C_{14}DAO/SDS mixture, at a total concentration of 0.2M. A large shift in the titration curve from the pure C_{14}DAO curve is observed for the mixture. At pH 9, a small but significant plateau is observed, and crystal formation takes place thereafter. After filtration and recrystallisation from ethanol, the precipitate was analyzed for its composition using spectroscopic techniques. The ir, (proton)nmr and mass spectra of the precipitate reveal that its structure is $CH_3(CH_2)_{13}N(CH_3)_2{}^+OH^-O_3SO(CH_2)_{11}CH_3$, with the proton of the cationic amine oxide involved in hydrogen bonding with the sulfate anion. Similar structural features were also detected in the double long chain salts formed between dodecyldimethylamine oxide and dodecyl benzene sulfonate or dodecane sulfonate anions (1,2).

4.4. DISCUSSION

4.4.1. LDAO/SDS Interaction

Mixing of cationic and anionic surfactant solutions results in the formation of a mixed species that is more surface active than the individual component. The enhanced synergistic effect has been explained (2,3) by showing that the adsorption of a close-packed electroneutral R^+R^- complex takes place to a very significant extent (R^+ and R^- represent the long chain cation and anion, respectively). In the case of C_{12}- and C_{14}DAO, a 1:1 LDAO/SDS molar ratio produces a minimum in surface tension and is accompanied by an increase in the pH of the bulk solution; the association seems to be of the type R^+R^-, in which the protonated amine oxide plays the role of the cation, and the absence of visible

Figure 4.6 Titration curves of the $3C_{14}$DAO/SDS mixture at 0.2M (curve 1) and C_{14}DAO at 0.2M (curve 2). Titrations performed at 25 °C and in the presence of atmospheric CO_2.

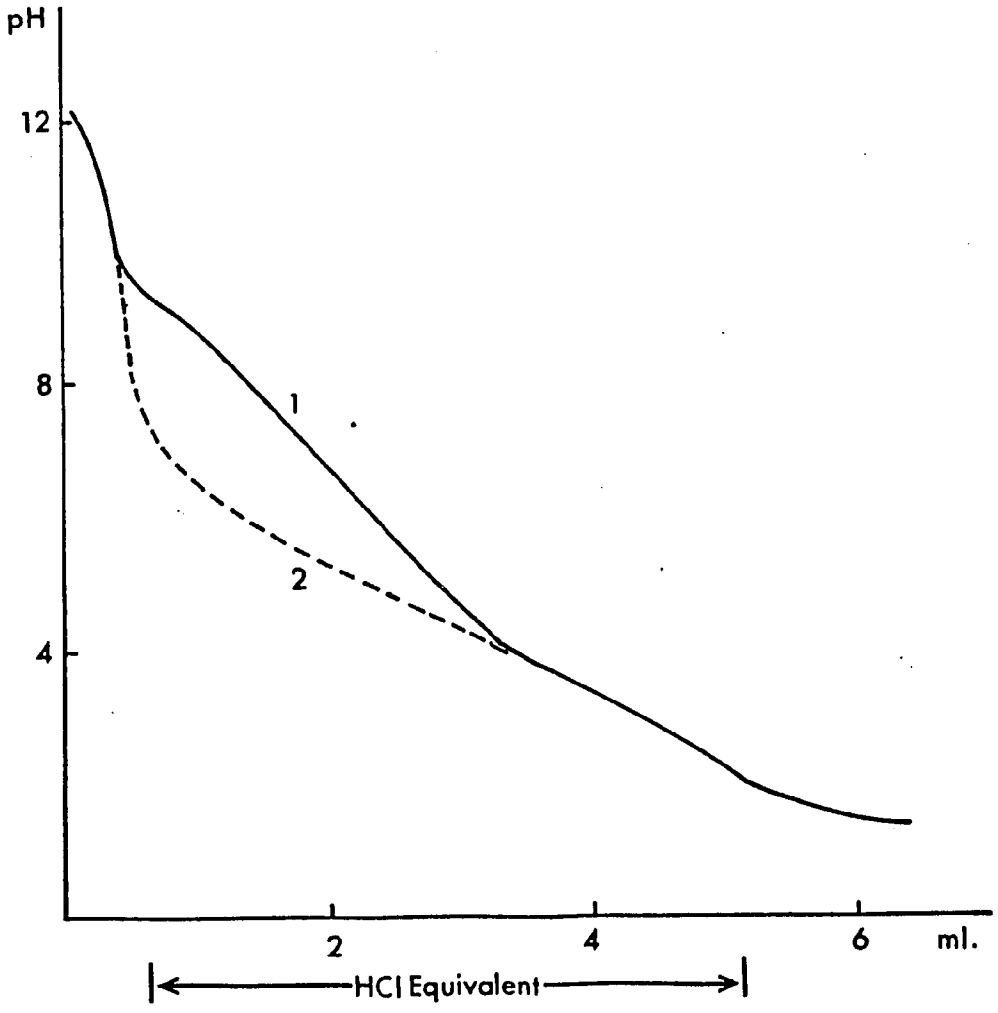

precipitate may be attributed to the solubilisation of the R^+R^- complex in the solution. In Chapter 2, it was shown the amine oxide molecules are protonated in acidic medium, and that above pH 7, all the molecules are practically in the nonionic form. However, an acid-base equilibrium shift may be induced by the addition of long chain sulfate (21). From the Gouy-Chapman theory of the electric double layer (22,23), a diffuse layer of counter ions builds up near a charged surface. When the surface is negatively charged, one well known consequence is the adsorption of protons at the surface, leading to a lower surface pH value than the bulk. The acid-base equilibrium state of amine oxide can be significantly modified due to the presence of long chain sulfate in the molecular assembly; the equilibrium is shifted toward the cationic side even when the bulk pH is higher than 7. In the region where LDAO is in excess, the association is probably [cationic ($LDAOH^+$) anionic SDS] nonionic (LDAO), while [cationic ($LDAOH^+$) anionic (SDS)] anionic (SDS) is formed when SDS is in excess. Equal molar concentration results in [cationic ($LDAOH^+$) anionic (SDS)] complex, and since there is no excess surfactant present, precipitation should be observed. However, there is no indication of precipitation even when the total solution concentration is as high as 0.35M. Only when the pH is adjusted to below 9 does precipitation take place. Therefore alternative explanations must be considered.

The second possibility is that the interaction occurs between neutral amine oxide and SDS, with adsorption of H_3O^+ ions on the aggregate surface. This type of association not only explains the increase in the pH but also the absence of visible precipitation for any given mixing ratio in the concentration range studied. This interpretation is supported by the titration behaviour of, for example, the 3:1 LDAO/SDS mixture (see Fig.4.6): above pH 12, addition of HCl neutralises the excess OH^- ions in the bulk. When more H^+ ions are

added, the concentration of H^+ ions increases in the bulk until surface neutralisation occurs below pH 10, and around pH 9 precipitation of the 1:1 $LDAOH^+$/SDS complex takes place. Since the amine oxide is in excess, below pH 7 when all the long chain sulfate molecules have been consumed in the production of the complex, protonation of amine oxide occurs, reminiscent of the titration of pure LDAO solution.

Although it may be argued that the choice of the words *protonation* and *adsorption* in the present context is probably somewhat semantic, in the sense of the distance of the proton from the micelle surface, nevertheless they are different. For amine oxide the former implies an actual covalent bond formation between the oxygen and hydrogen atoms, while adsorption only indicates the presence of hydrogen ions near the vicinity of the head groups without the covalent bond being formed. It is by necessity that the difference between them be realised in the present case in order to achieve a satisfactory interpertation of the results.

4.4.2. Liquid Crystalline Phase

Another feature of surfactant-water systems in addition to their ability to form micellar solutions, is that they can also aggregate into lyotropic liquid crystalline phases when intermicellar interactions are significant. Typically, non-Newtonian and highly viscous behaviours are usually found for these liquid crystalline solutions. There is a multitude of such liquid crystalline structures (24), and preference of one structure over another is usually determined by the characteristics of the surfactants forming the system. For the 3 C_{12} or C_{14}-DAO/SDS mixed system, all evidence including X-ray diffraction patterns (not published data) suggests that they do form liquid crystal phases. It is also interesting to note that increasing basicity of the solution results in a corresponding increase in the relative vicosity, which suggests that the

association between nonionic amine oxide and the sulfate favours an enhanced solution viscosity. Therefore, it seems that in the absence of added base, the nonionic form of amine oxide is also responsible for producing viscous mixture, with adsorption of protons at the surface, leading to an increase in the bulk pH value.

4.4.3. Chain Compatibility

The difference in properties when the aliphatic chain of amine oxide contains more than 14 carbons is attributed, in part, to the mismatch of the hydrophobic chain with that of the SDS. The extra terminal segment results in a disruptive effect on the packing of the surface active molecules. The observed association behaviour in the case of C_{12} or C_{14}DAO with SDS is then also due to the maximum cohesive interaction between hydrocarbon chains, in addition to the reduced electrostatic repulsion in the head groups. Chain length compatibility effects in different systems have been discussed by other investigators (25-27). Solubilisation of the 1:1 amine oxide/SDS complex is also determined by this chain length compatibility effect which may contribute to the absence of visible precipitation in C_{12}/C_{12} and C_{14}/C_{12} mixtures; however, a closer look at the results of the C_{16} or C_{18}-DAO/SDS mixtures seems to rule out this possibility. For example, consider the C_{18}DAO/SDS systems in the region where SDS is in excess. Since the total surfactant concentration is $5x10^{-3}$M, the amount of excess SDS is much less than its CMC, $\sim 8x10^{-3}$M (28); therefore there is no micelle available to solubilise the complex formed between the protonated amine oxide molecule and the sulfate anion, if it is indeed formed. Furthermore, incompatible double long chain salts are usually less soluble in the component in excess; hence visible precipitation should be observed in the region under discussion, but experimentally the mixtures are clear and isotropic. This simple reasoning seems to suggest again that

adsorption of protons on the mixed micelle surface is responsible for the increase in bulk pH value, a possibility raised previously.

4.5. REFERENCES

1. Kolp, D. G., Laughlin, R. G., Krause, R. P., and Zimmerer, R. E., *J. Phys. Chem.* 67, 51 (1963).

2. Rosen, M. J., Friedman, D., and Gross, M., *J. Phys. Chem.* 68, 3219 (1964).

3. Lucassen-Reynders, E. H., Lucassen, J., and Giles, D., *J. Colloid Interface Sci.* 81, 150 (1982).

4. Al-Saden, A. A., Florence, A. T., Whateley, T. L., Puisieux, F., and Vaution, C., *J. Colloid Interface Sci.* 86, 51 (1982).

5. Hua, X. Y., and Rosen, M. J., *J. Colloid Interface Sci.* 90, 212 (1982).

6. Holland, P. M., and Rubingh, D. N., *J. Phys. Chem.* 87, 1984 (1983).

7. Rosano, H. L., *U. S. Patent Application*, #473078, 07 March 1983.

8. Lange, H., and Beck, K. H., *Kolloid Z. Z. Polym.* 251, 424 (1973).

9. Garrett, P. R., *J. Chem. Soc. Faraday Trans. I* 72, 2174 (1976).

10. Ingram, B. T., *Colloid Polym. Sci.* 258, 191 (1980).

11. Rosen, M. J., *J. Colloid Interface Sci.* 79, 587 (1981).

12. Kung, H. C., and Goddard, E. D., *J. Am. Chem. Soc.* 67, 1965 (1963).

13. Abe, M., and Ogino, K., *J. Colloid Interface Sci.* 80, 146 (1981).

14. Jones, M. N., *J. Colloid Interface Sci.* 23, 36 (1967).

15. Clint, C. H., *J. Chem. Soc. Faraday Trans.I* 71, 1327 (1975).

16. Aronson, M. P., and Princen, H. M., *J. Colloid Interface Sci.* 52, 345 (1975).

17. Gravsholt, S., *J. Colloid Interface Sci.* 57, 575 (1976).

18. Rosano, H. L., Breindel, K., Schulman, J. H., and Eydt, A. J., *J. Colloid Interface Sci.* 22, 58 (1966).

19. Ekwell, P., Mandell, L., and Solyom, P., *J. Colloid Interface Sci.* 35, 519 (1971).

20. Hyde, A. J., Maguire, D. J., and Stevenson, . D. M., *Proc. VIth Intern. Congr. Surface Active Substances (Zurich)* II, 2 (1972).

21. Dorion, F., Charbit, G., and Gaboriaud, R., *J. Colloid Interface Sci.* **101**, 27 (1984).

22. Verwey, E. J. W., and Overbeek, J. Th. G., "*Theory of the Stability of Lyotropic Colloids*", Elsevier, Amsterdam (1948).

23. Davis, J. T., and Rideal, E. K., "*Interfacial Phenomena*", Academic Press, New York (1961).

24. Brown, G. H., and Crooker, P. P., *Chemical and Engineering News*, **Jan. 31**, 24 (1984).

25. Schick, M. J., and Fowkes, F. M., *J. Phys. Chem.* 66, 1136 (1962).

26. Fort, T. Jr., *J. Phys. Chem.* 66, 1136 (1962).

27. Cameron, A., and Crouch, R. F., *Nature (London)* 198, 475 (1936).

28. Baxter-Hammond, J., Powley, C. R., Cook, K. D., and Nieman, T. A., *J. Colloid Interface Sci.* 76, 434 (1980).

CHAPTER FIVE

MONOLAYER PROPERTIES OF OCTADECYLDIMETHYLAMINE OXIDE AND SODIUM ALKYL SULFATE

5.1. INTRODUCTION

In the previous chapter, results were presented on the micellar properties of binary mixtures of surfactant solutions consisting of alkyldimethylamine oxide (C_{12} to C_{18} alkyl chains) and sodium dodecyl sulfate. It was reported that upon mixing, striking alteration in physical properties was observed, most notably in the viscosity, surface tension, and bulk pH values. These changes were attributed to 1) formation of elongated structures, 2) protonation of amine oxide molecules, and 3) adsorption of hydronium ions on the mixed micelle surface. In addition, possible solubilisation of a less soluble 1:1 complex, form between the protonated amine oxide and the long chain sulfate was also considered.

In this study, the monolayer technique is used to investigate the surface properties of octadecyldimethylamine oxide and sodium octadecyl sulfate, as single component films and in combination. The interpretation of the results provides a direct understanding of the mechanism of interaction between these two surface active agents.

Goddard and Kung (1) studied the surface characteristics of docosyldi-

methylamine oxide alone and in mixed films with nonadecylbenzene sulfonate. The amine oxide single component film showed large variations with the pH of the substrate, but the mixed films did not reveal evidence of pronounced interaction. However, these autuours indicated that a differential thermal analysis study of the shorter chain homologs, dodecyldimethylamine oxide and sodium dodecylbenzene sulfonate, did show interaction between these components, in accord with results obtained from studies of aqueous solution containing similar materials (2). They suggested that the choice of more suitable spreading solvents, to effect more complete mixing of the components would enable the detection of interaction between these two species. As will be shown in this work, mismatch of the long chains may account for their results.

5.2. EXPERIMENTAL

5.2.1. Chemicals

Octadecyldimethylamine oxide (C_{18}DAO) was a commercial solution sample from Onyx Chemical Company, Jersey City, N. J. (25% active). After evaporating the solvent in a rotary evaporator under reduced pressure, the crude product was recrystallised several times from ethyl acetate. The final product was dried and store *in vacuo* over P_2O_5. Sodium octadecyl sulfate (SODS) was a sample prepared in this laboratory previously, and was recrytallised from ethanol before use. Sodium dodecyl sulfate (SDS) was obtained from Aldrich Chemical Company, and was of 98% purity. It was further purified by repeated crystallisation from ethanol followed by ether extraction. Benzene and methanol were gold-label reagent grade, purchased from Aldrich Chemical Company (Metuchen, N. J.).

5.2.2. Solution Preparation

The spreading solutions were prepared as follows: C_{18}DAO was dissolved in 45/5, the SODS in 25/25, the SDS in 40/10, benzene/methanol mixture. The concentrations of these solutions were 1.157×10^{-3}M. For mixed monolayers, mixtures at different volume ratio were made from stock solutions prior to spreading. The aqueous substrates used were unbuffered, and the experiments were performed in the presence of atmospheric CO_2. Deionised-distilled water was used to prepare the substrate.

5.2.3. Apparatus

The experimental apparatus employed was described elsewhere (3). Briefly, surface pressures were determined continuously from surface tension measurements using a sand blasted platinum blade, suspended from a transducer-amplifier (Sandborn, model 311A). The transducer signal was fed to a X-Y recorder. Surface potential was measured with an electrometer (Keithley, model 610B) using an air electrode coated with ^{226}Ra and an Ag/AgCl electrode in the subsolution.

The surface of the subsolution was cleaned by first dusting it with Talc powder and then sweeping the surface with a Teflon slide from one side of the trough to the other. The Talc powder along with the impurities (if any) were then removed using suction from an aspirator. This was done several times to make sure no impurities remained on the surface. The monolayers were spread evenly on the surface using an Agla microsyringe. A time interval of three minutes was allowed for spreading solvent to evaporate from the monolayers. Three to five monolayers of each solution were made, and the results reported are average values.

5.3. RESULTS

5.3.1. Single Component Systems

Surface pressure-area (π-A) and surface potential-area (ΔV-A) isotherms of C_{18}DAO on 0.01M NaCl subsolution at various pH values are shown in Fig.5.1. At the highest pH investigated, pH 10.9, the amine oxide is in the nonionic form and gives rise to the most expanded curve as well as a lower collapse pressure. Reduction in bulk pH results in contraction of the film. At pH 2.2, protonated amine oxide predominates and resulted in a less expanded curve. However, the least expanded film is obtained at an intermediate bulk pH value,viz., pH 5.5. The film is expected to be composed of both nonionic and cationic forms of the amine oxide molecules at approximately a 1:1 mole ratio, as suggested by the acid-base titration behaviour of its C_{14} homolog (Chapter 2). These results are in agreement with the monolayer properties of docosyldimethylamine oxide reported by Goddard and Kung (1); however in their case the amine oxide also shows a phase transition from expanded to the condensed states, and that the film condensation upon ionisation is more pronounced than in the case of C_{18}DAO. The surface potentials of amine oxide films vary strongly with the bulk pH of the substrate, and hence the cationic/nonionic ratio of the constituent molecules in the film. With a formal positive charge on the nitrogen in the cationic species, it is expected that the cationic film has the highest potential. However, the mixed film of cationic and nonionic amine oxides exhibits an even higher potential than the completely ionised film, while the nonionic species (pH 10.9) shows the lowest potential. This behaviour is also seen with the C_{22} homolog which shows a maximum in surface potential in the vicinity of pH 5.6 under identical experimental conditions.

In Fig.5.2 the π-A and ΔV-A plots for SODS on 0.01M NaCl subsolutions having different pH values are shown. In all cases, phase transitions from

Figure 5.1 Effect of pH on π-A and ΔV-A isotherms of octadecyldimethylamine oxide ($C_{18}DAO$) at 25°C, 0.01M NaCl subsolutions (NaOH or HCl/NaCl). Substrate pH: 1-10.9, 2-5.5, 3-2.2.

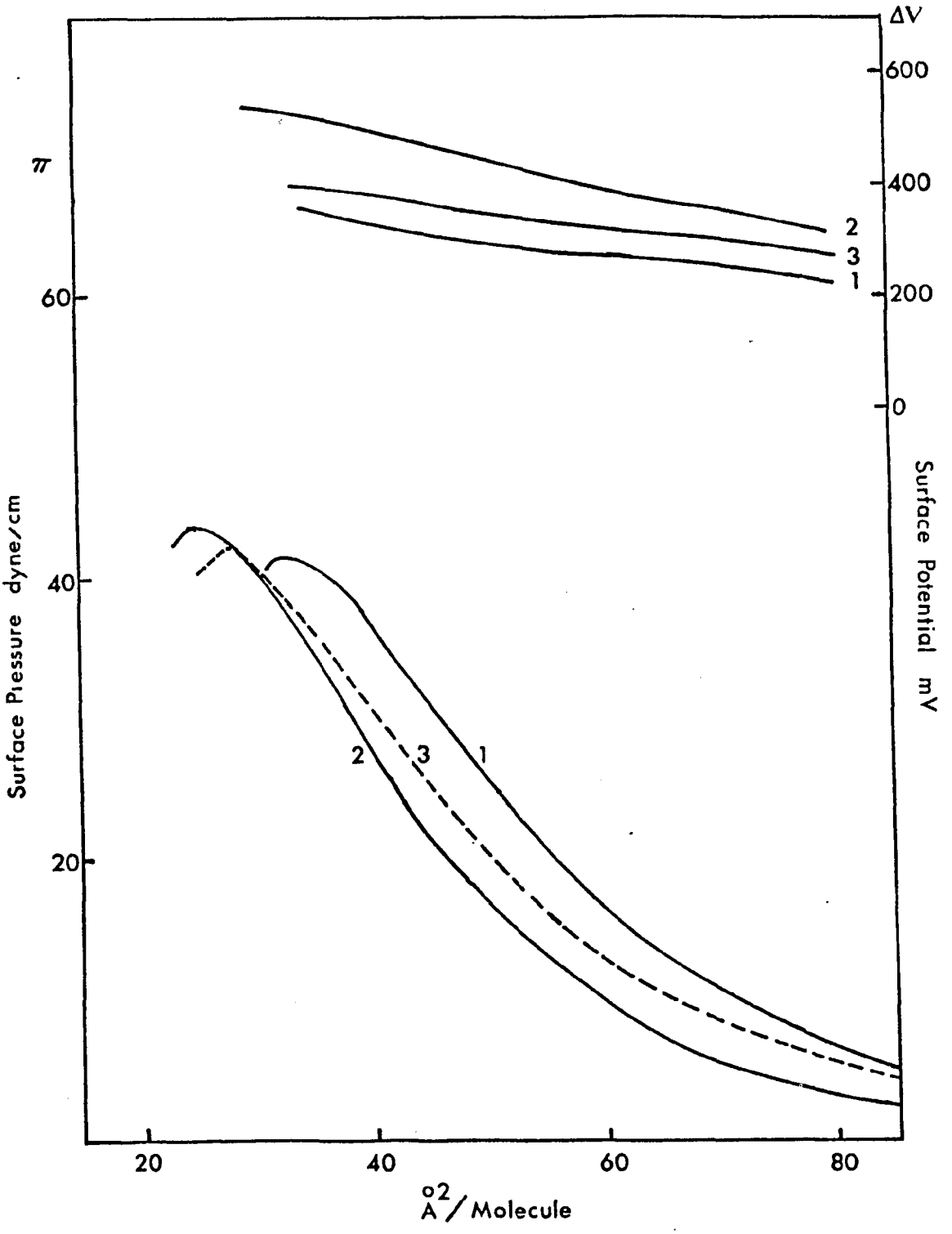

Figure 5.2 Effect of pH on π-A and ΔV-A isotherms of sodium octadecyl sulfate (SODS) at 25°C, 0.01M NaCl subsolutions (NaOH or HCl/NaCl). Substrate pH: 1-10.9, 2-5.5, 3-2.2.

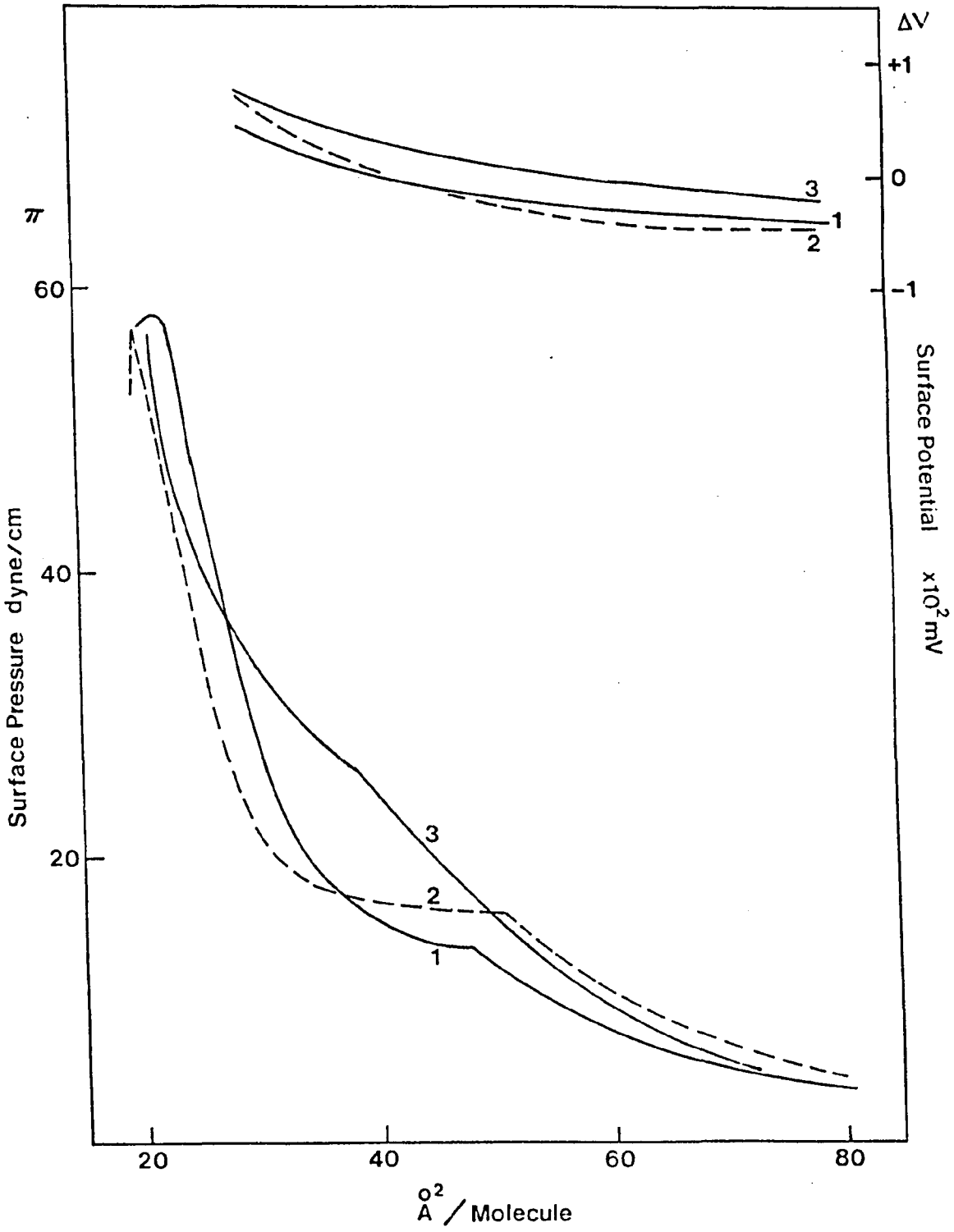

liquid-expanded to liquid-condensed state are evident (4). Acidification of the subsolution increases the transition pressure but the transition is less pronounced at the lowest pH studied. This is also accompanied by an expansion of the condensed part of the the curve. Small negative surface potentials are observed over most areas. The highest potential is obtained for film spread on the pH 2.2 subsolution. For small areas, the surface potential attains a positive value. This may be related to reorientation of the dipole moments of the molecules which occur once a threshold surface concentration is exceeded (5). Mingins and Pethica (7) studied the monolayer properties of SODS on various sodium chloride solutions (0.1, 0.01 and 0.001M) at 9.5°C, and they showed that the monolayer is only stable on the more concentrated salt solutions (0.1 and 0.01M). In the present study, no noticeable difference in both the π and ΔV results were observed from the different experimental runs.

5.3.2. Mixed Component Systems

C_{18}DAO/SODS

These systems were examined at three subsolution pH values, namely 10.9, 5.5, and 2.2 (0.01M NaCl), and various compositions. The compression isotherms are shown in Figs.5.3, 5.4, and 5.5, respectively, and for comparison, isotherm of C_{18}DAO is also plotted. At high pH values, interaction between the two components is quite noticeable. Addition of SODS produces a condensing effect on the film (with respect to C_{18}DAO film in all cases, and in most cases with respect to SODS film). The phase transition which is characteristic of the SODS curve, is still evident at all mixing ratios. Reduction in transition pressure is observed for the mixed films with increasing SODS content up to the equimolar mixture, which shows the lowest transition pressure. Thereafter the value increases when the amount of SODS in the film becomes excess. In

Figure 5.3 π-A and ΔV-A isotherms of mixed films of $C_{18}DAO$ and SODS on pH 10.9 (NaOH), 0.01M NaCl subsolution at 25°C. $C_{18}DAO$/SODS ratio: 1-4:1, 2-3:1, 3-2:1, 4-1:1, 5-1:2, 6-1:3, 7-1:4.

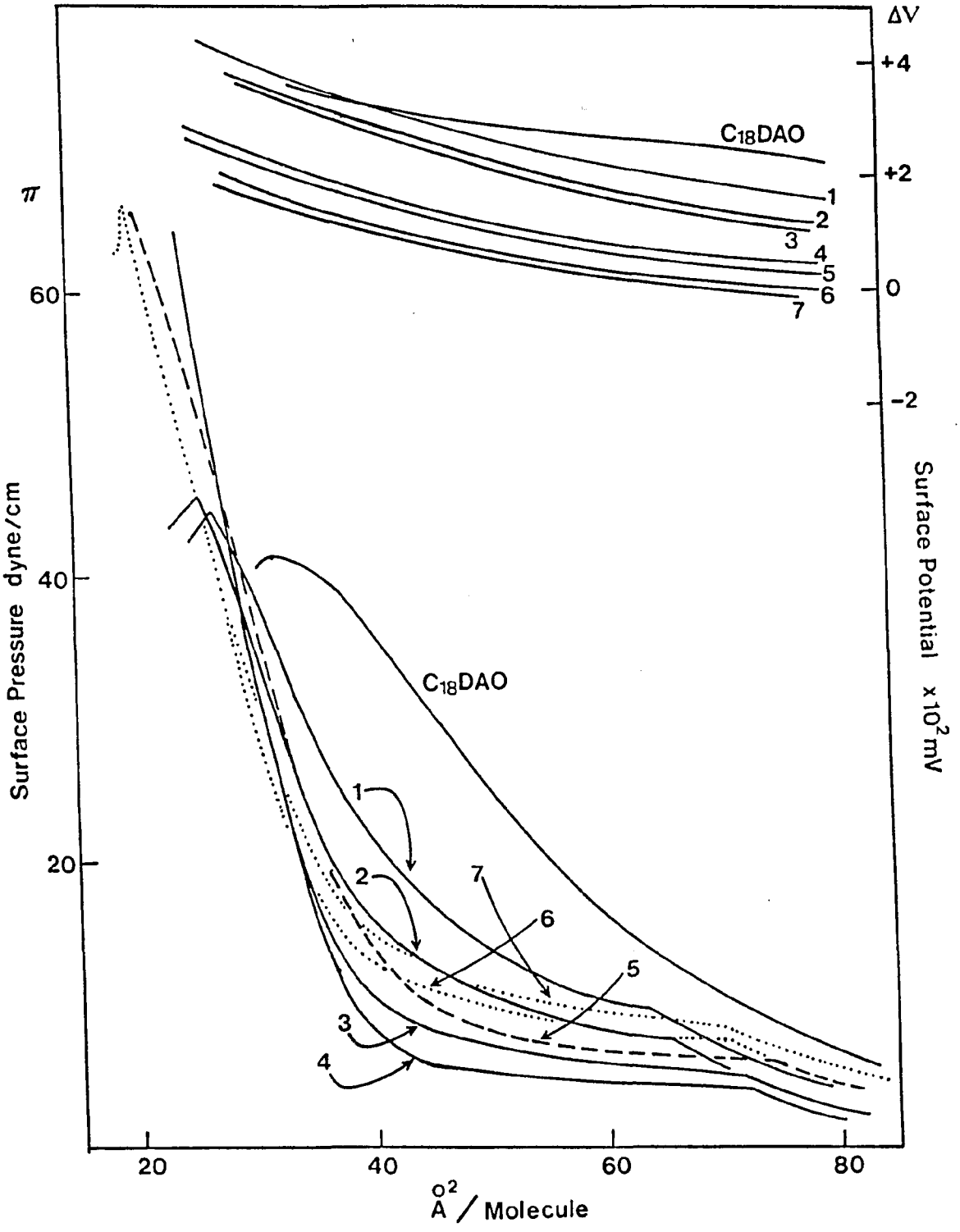

Figure 5.4 π-A and ΔV-A isotherms of mixed films of $C_{18}DAO$ and SODS on pH 5.5 (HCl), 0.01M NaCl subsolution at 25°C. $C_{18}DAO$/SODS ratio: 1-4:1, 2-3:1, 3-2:1. 4-1:1, 5-1:2, 6-1:3, 7-1:4.

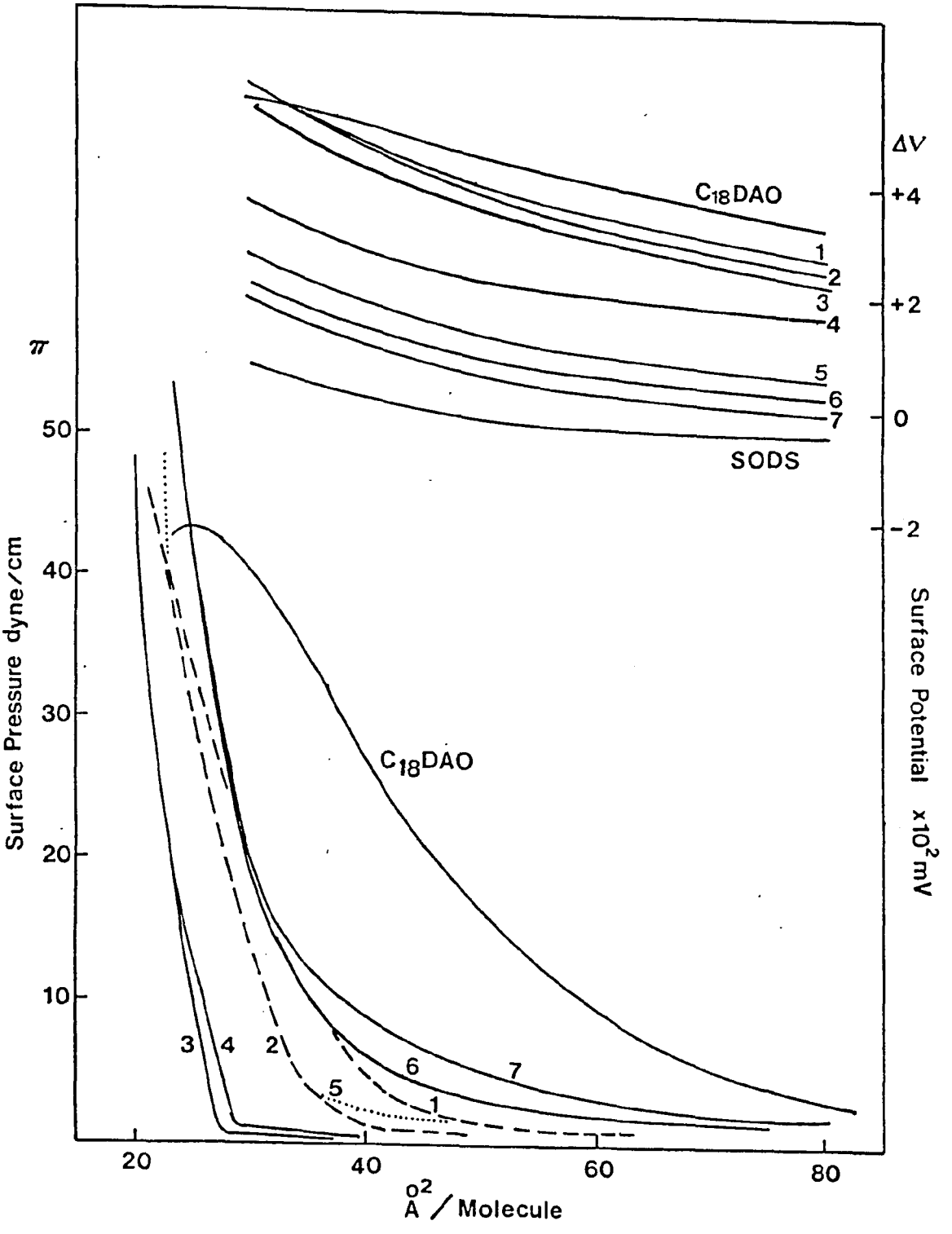

Figure 5.5 π-A and ΔV-A isotherms of mixed films of $C_{18}DAO$ and SODS on pH 2.2 (HCl), 0.01M NaCl subsolution at 25°C. $C_{18}DAO$/SODS ratio: 1-4:1, 2-3:1, 3-2:1, 4-1:1, 5-1:2, 6-1:3, 7-1:4.

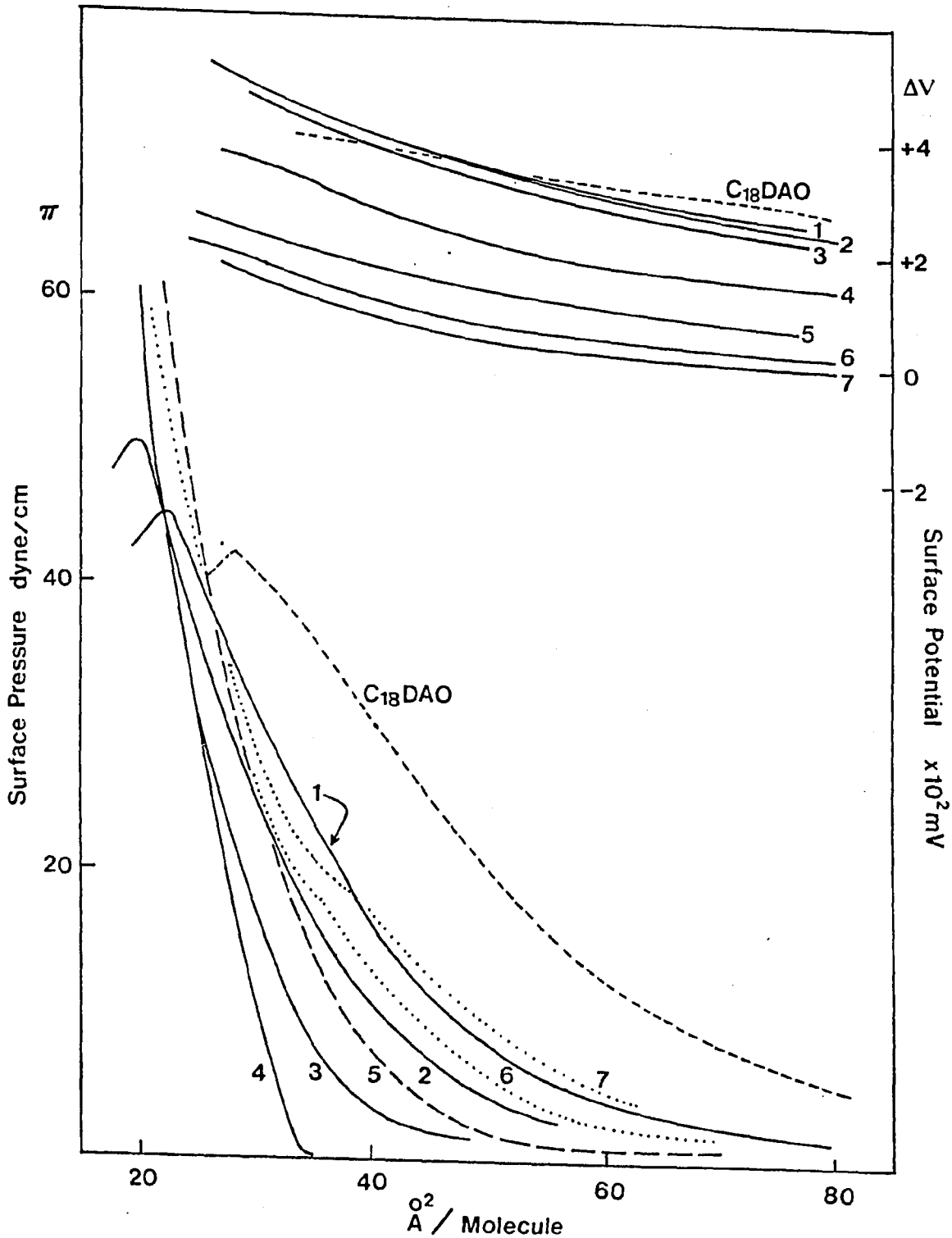

terms of the C_{18}DAO/SODS molar ratio, the 4:1 and 3:1 mixed films have higher collapse pressures than the C_{18}DAO film, but lower than that of the SODS film. The 2:1 and 1:1 mixtures form solid films, and the isotherms become identical at high pressure and small area, but the equimolar mixture shows the most condensed film for large areas. Mixed films containing excess SODS show the highest collapse pressures, suggesting these films are quite stable. Surface potentials of the mixed films generally fall between the values of those of the pure component films. However, for small areas mixtures containing excess amine oxide show an even higher potentials than the pure C_{18}DAO film, probably due to closer packing of the molecules.

Mixed monolayers on the pH 5.5 subsolution (Fig.5.4) show pronounced condensation, indicating very strong interaction among the components; which include both the cationic and nonionic forms of amine oxide, as well as the long chain sulfate. The most condensed curve is observed for the 2:1 amine oxide/SODS mixture, closely followed by the equimolar mixture, and at high pressures the two isotherms become identical. Unlike the case at high pH subsolution, no phase transition was detected in the present case. Surface potentials of the mixed films fall between those of the amine oxide and SODS at constant area. However, the 4:1 and 3:1 films have surface potential values that are slightly higher than the pure amine oxide film at small area.

At the lowest pH value of the subsolution investigated, viz., pH 2.2, the amine oxide molecules are protonated, therefore large interactions are expected with an anionic substance, such as the long chain sulfate. Such an interaction is reflected in the monolayer behaviour of the mixed film, as shown in Fig.5.5. The mixed films are all more condensed than the pure component films, with the equimolar mixture exhibiting the most condensed curve. Phase transitions are still detected in some cases when the SODS content is in excess, but with

lower transition pressures than the SODS single component film, and the transition pressure increases with increasing amount of the anionic constituent. A well defined film collapse is observed only when the amine oxide is in large excess (4:1 and 3:1). All others become incompressible at high pressures. The surface potentials are similar to those discussed previously.

C_{18}DAO/SDS

Mixtures of C_{18}DAO/SDS were spread on subsolutions of pH 10.9 (NaOH) and pH 5.5 (HCl), and 0.01M NaCl. Since SDS is highly soluble in water and hence has a high desorption rate, compressions were made at a faster speed. The resulting curves were fitted such that the vertical portion of each curve corresponds to 20 $\mathring{a}^2$/molecule, which approximates the limiting value of an alkyl chain, if the original curve show a value smaller than that. Figs.5.6 and 5.7 show the fitted isotherms for pH 5.5 and pH 10.9, respectively. At low pH, it appears that the addition of SDS causes contraction of the film, and that transition in film type is evident for all mixtures. It also appears that the relative degree of film contraction increases with increasing amount of SDS in the mixed film. However, with excess SDS in the mixture, the apparent increase is probably caused by the desorption of SDS. At high pH, the mixed isotherms are similar to those obtained at low pH, except that the transition in film type is evident only when the amount of SDS is equal to or greater than the amount of amine oxide. There seems to be a more systematic increase in film contraction with increasing amount of SDS in the mixed film. Interaction between the two components is definite, since SDS alone did not reveal a reasonable compression pattern under the present experimental conditions.

5.4. DISCUSSION

Figure 5.6 π-A isotherms of mixed films of C_{18}DAO and sodium dodecyl sulfate (SDS) on pH 5.5 (HCl), 0.01M NaCl subsolution at 25 °C. Each curve is fitted such that the high pressure region corresponds to 20Å^2 if the experimental value preceded this number. C_{18}DAO/SDS ratio: 1-4:1, 2-3:1, 3-2:1, 4-1:1, 5-1:2, 6-1:3, 7-1:4.

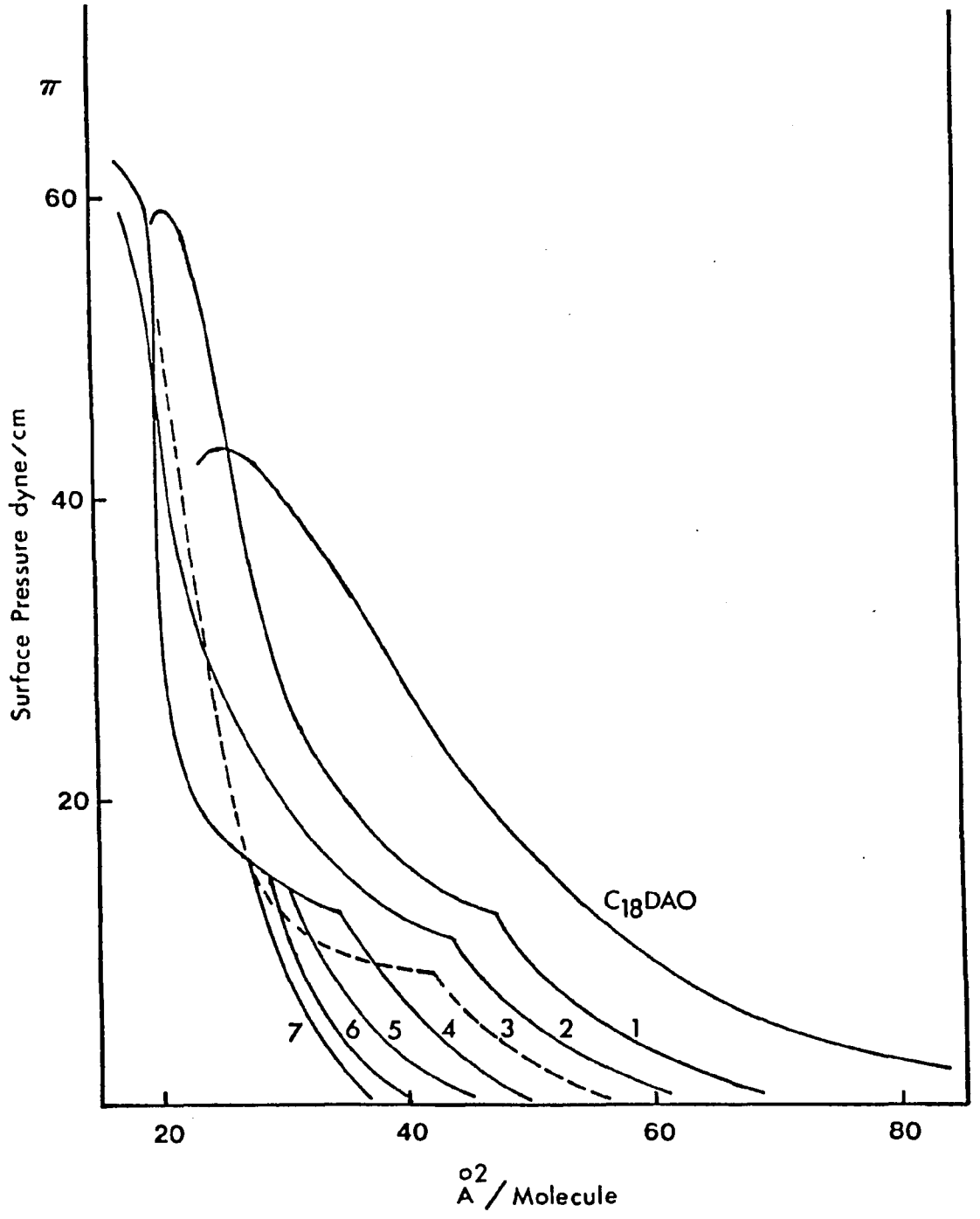

Figure 5.7 π-A isotherms of mixed films of C_{18}DAO and SDS on pH 10.9 (NaOH), 0.01M NaCl subsolution at 25°C. Each curve is fitted such that the high pressure region corresponds to 20Å^2 if the experimental value precedes this number. C_{18}DAO/SDS ratio: 1-4:1, 2-3:1, 3-2:1, 4-1:1, 5-1:2, 6-1:3, 7-1:4.

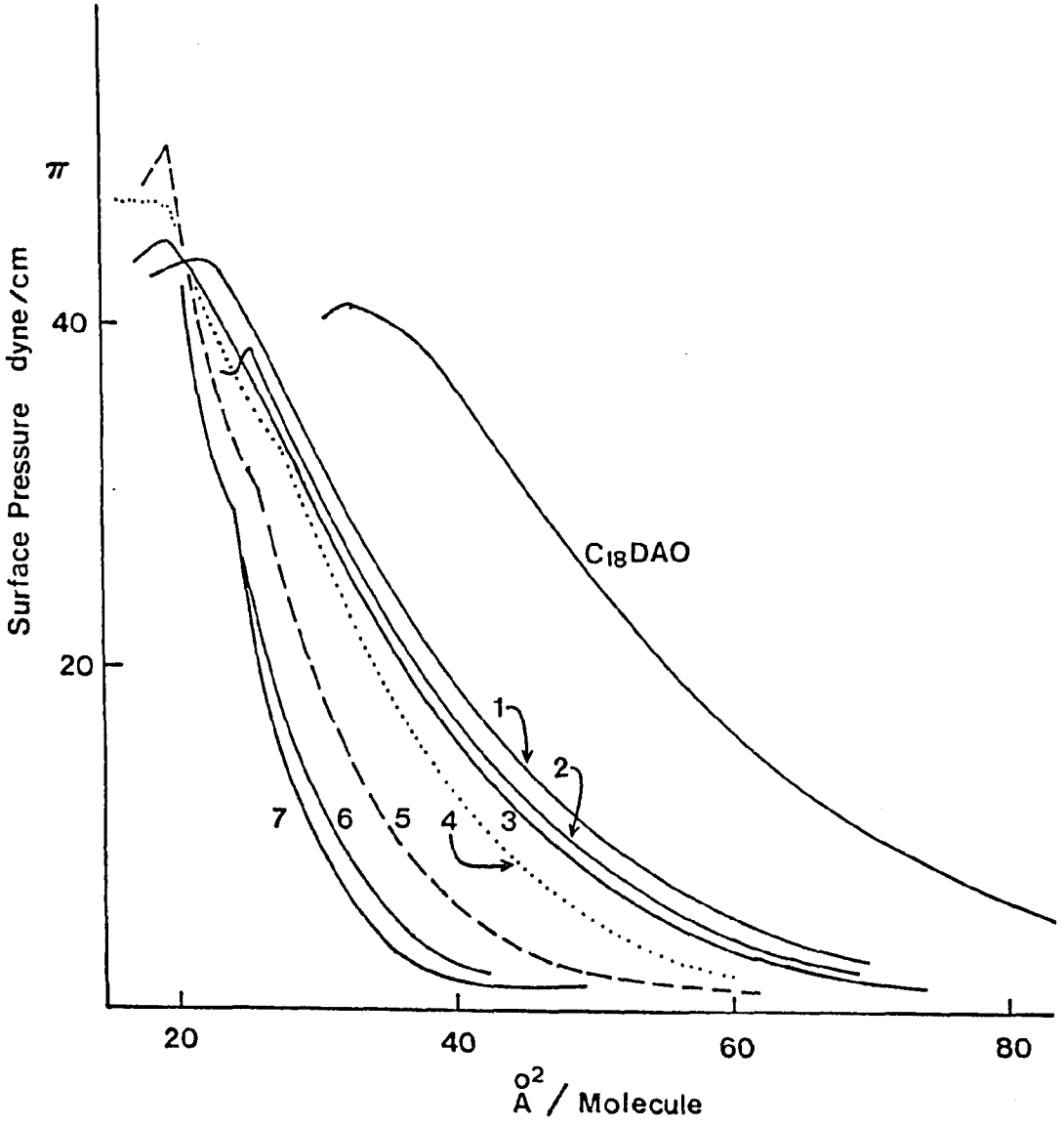

5.4.1. C_{18}DAO Films

The unusual feature of alkyldimethylamine oxide monolayers is that the ionised form yields a less expanded film than the nonionised species, contrary to the expectation that the presence of charged head groups should result in a more expanded film, due to electrical repulsion among the charges. This particular characteristic of amine oxide films has been attributed (1) to the ability of the hydroxy group in ionised amine oxide to hydrogen bond, this leads to a reduction in repulsive forces among the head groups, giving rise to the condensing effect upon ionisation. At an intermediate pH, viz., pH 5.5, the appearance of cationic species can cause the condensing effect by associating with the nonionic species, since the ionisable proton is capable of hydrogen bonding to the neighbouring oxygen thereby decreases the average distance between adjacent head groups effectively. In the bulk solution, this effect manifests itself in an increase in the viscosity if the solution concentration is sufficiently high. From the acid-base titration studies of the C_{12} and C_{14} homologs (Chapter 2), it was reported that the appearance of cationic species leads to a substantial increase in the solution viscosity, reaching a maximum value at half ionisation. This change in viscosity was explained in terms of reduction of repulsion, and the formation of elongated micelles.

The surface potential of the nonionised species is relatively high for a nonionic surfactant. This indicate that there is a strong dipole in the head group, which is the primary cause of expansion of the film. Mixtures of cationic and nonionic species have yet an even higher surface potential values, this may due to, at least in part, the closer packing of the molecular assembly in the film, consequent of the diminishing repulsion in the head group region.

It has been shown in Chapter 2 that the cationic form of amine oxide is more soluble in water; it has a higher CMC value than the nonionised amine

oxide. More importantly, a C-13 nmr study of this class of compound (Chapter 3) indicated that the degree of penetration of water molecules into the micellar core increases with increasing cationic character of the micelle (up to three carbons of a fully ionised micelle), resulting in an upfield chemical shift of carbon atoms near the head group region with increasing degree of protonation of the micelle surface. The condensing effect on the monolayer upon ionisation can therefore be considered as a consequence of the increased solvation; the molecules penetrate into the bulk aqueous substrate. At an intermediate substrate pH, the protonated molecules are more soluble, and are therefore more embedded in the subsolution, while the nonionised fraction remains higher in the surface in order to minimise paraffin-water interfacial area. Under these conditions, the monolayer can assume the least expanded configuration, because of possible "staggering" of the surfactant molecules, and this spatial arrangement is best seen at half ionisation. Further acidification of the aqueous substrate increases the fraction of molecules ionised, but the condensing effect due to increased solvation is offset by an increased electrical repulsion between neighbouring charged head groups, resulting in a slight expansion of the monolayer. This interpretation is most consistent with both the C-13 nmr and the monolayer results.

5.4.2. SODS Films

For an ionised monolayer, a relatively large surface potential is expected, negative in sign for a long chain sulfate monolayer. However, the present results show that the surface potential is small, indicating that the surface is probably not completely ionised, or that the counter ions, although dissociated, are within a very close vicinity to the plane of the negatively charged interface, as was suggested by the electromotive force determination of the apparent binding of counterions (Na^+ ions) on the sodium dodecyl sulfate micelle surface (6),

and on sodium tetradecyl sulfate micelle surface from the an electrochemical study (8).

The expansion of the film with increasing acidity of the substrate may caused by the competition of counterions at the interface. The swamping amount of H^+ ions in a low pH subsolution competes with Na^+ ions at the negatively charged interface. Such competition has been shown to exist between H^+ ions and K^+ ions at the negatively charged micelle-solution interface (9). Studies on the counterion effects in sodium docosyl sulfate monolayers (5, 10) have shown that the film expansion follows the sequence $Li^+ > Na^+ > K^+$. It follows that H^+ should give rise to the most expanded film.

5.4.3. Mixed Films

Isotherm data from two-component monolayers are frequently represented by plotting the mean molecular area as a function of film composition at constant surface pressure. A linear relationship is usually obtained when the two components are immiscible or when they form an ideal two-dimensional solution. For miscible components, deviations from ideality result in a non-linearity in the plot. Positive deviations indicate an increase in the area occupied by either one or both components, probably due to a more repulsive interaction in nature, whereas negative deviations are indicative of condensation. Figs.5.8-5.10 represent such plots for the systems C_{18}DAO/SODS studied on pH 10.9, 5.5, and 2.2 subsolutions, respectively. Clearly these two components interact favourably so as to produce condensation of relatively large magnitude. At least two factors are involved in the process: 1) chain length compatibility and 2) head group interaction. The former is responsible for the hydrophobic interaction between the chains: compatible chains results in maximum cohesive interactions between the alkyl groups while incompatible chains have a disruptive effect on the packing of molecules in the monolayer. Shibata *et al* (11)

Figure 5.8 Mean molecular area vs. composition plots for C_{18}DAO/SODS mixed films spread on 0.01M NaCl, pH 10.9 (NaOH) subsolution at 25°C.

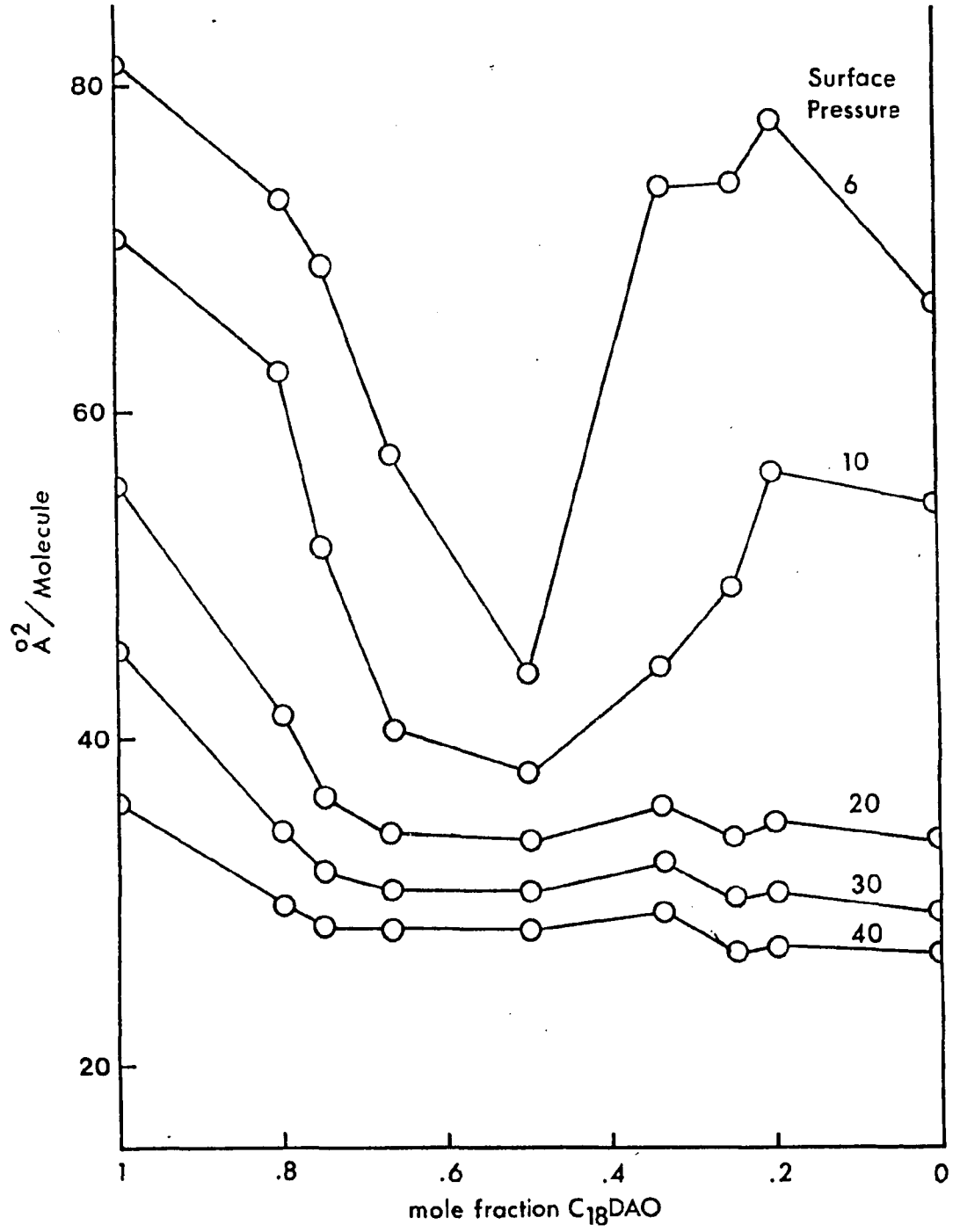

Figure 5.9 Mean molecular area vs. composition plots for C_{18}DAO/SODS mixed films spread on 0.01M NaCl, pH 5.5 (HCl) subsolution at 25°C.

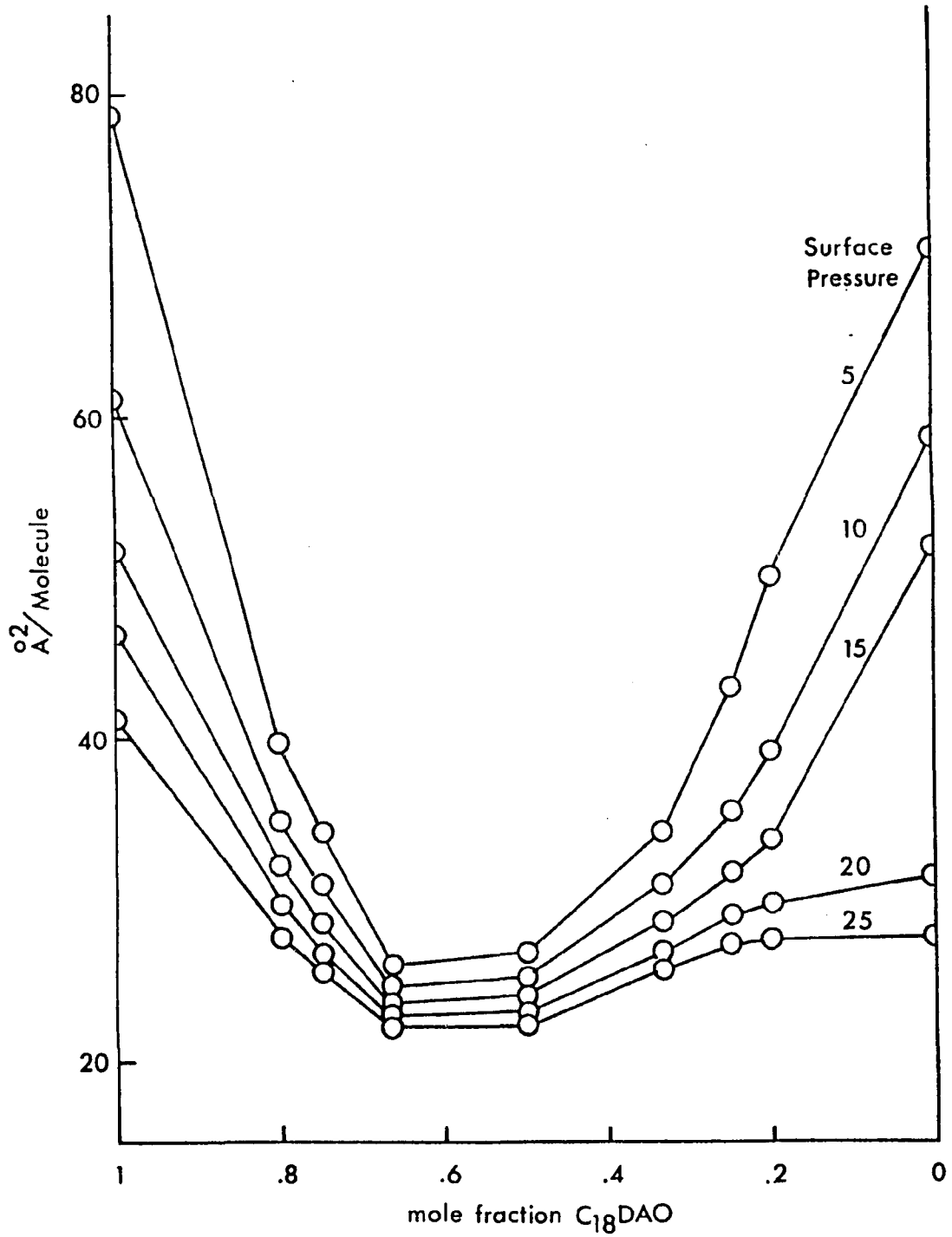

Figure 5.10 Mean molecular area vs. composition plots for C_{18}DAO/SODS mixed films spread on 0.01M NaCl, pH 2.2 (HCl) subsolution at 25°C.

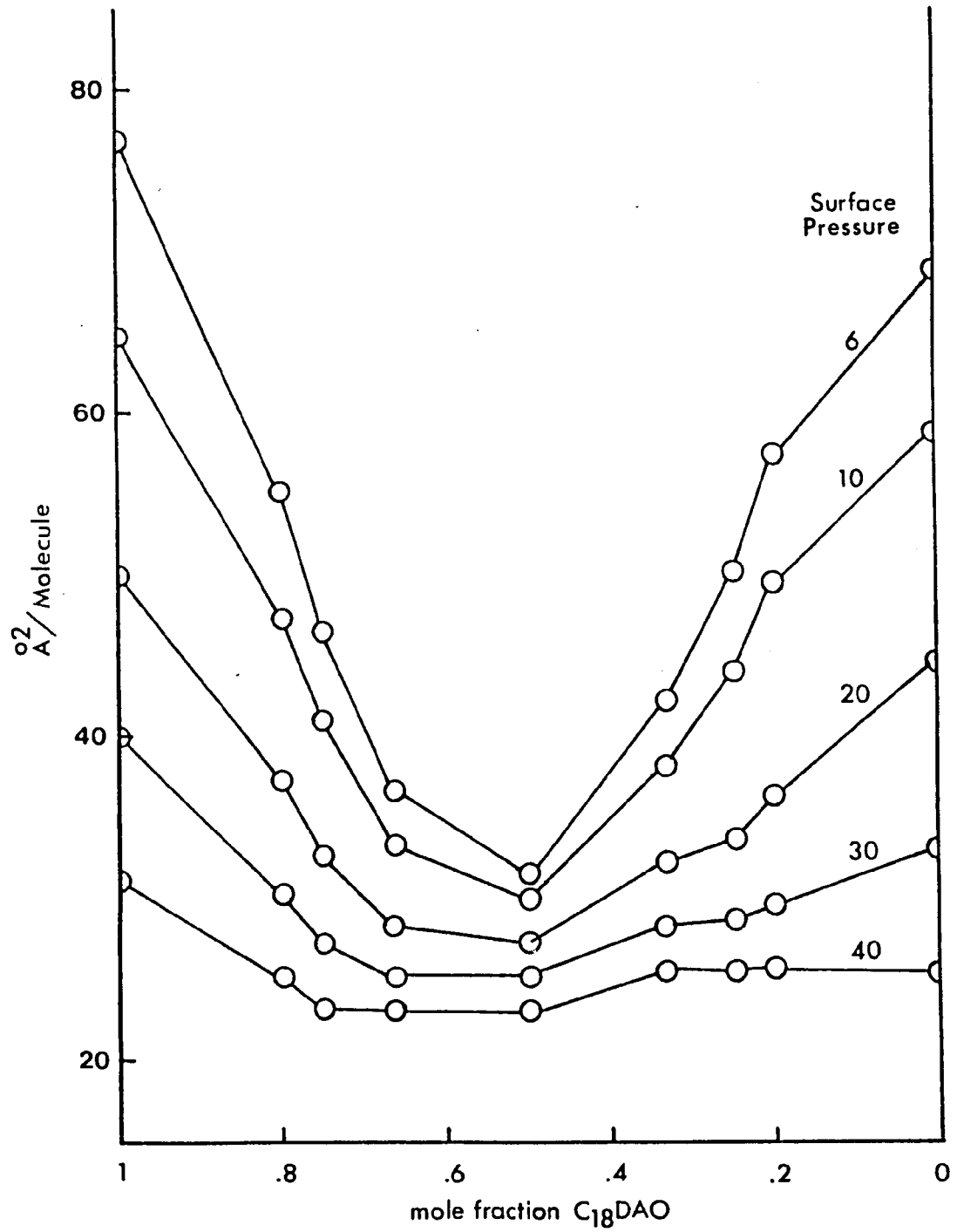

have shown that the most pronounced condensing effect is usually observed when the two components have equal chain length, for a fixed total number of carbon atoms. This compatibility is important in determining the properties of mixed micellar solutions, which has been shown in Chapter 4, and in the formation of microemulsion systems (12-14).

The second factor, namely the head group interaction, can also influence the surface properties of mixed surfactant solutions markedly. In particular, anionic/cationic surfactant mixtures exhibit the largest effect (15,16). In nonionic/anionic surfactant mixtures, a synergistic effect can still take place to a significant extent, as revealed in Fig.5.8 (pH 10.9, nonionic amine oxide with anionic long chain sulfate), since insertion of nonionic surfactant molecules into an ionic surfactant molecular assembly minimises electrostatic repulsion (17).

As mentioned in Chapter 4, except in a very acidic medium in which the the amine oxide molecules are protonated by the excess protons already present in the bulk solution, it is also possible that the strong interactions between these two species is a reflexion of an induced acid-base equilibrium shift of the amine oxide in the aqueous medium, brought about by the addition of the long chain sulfate. As is known from the Gouy-Chapman theory (18, 19), a diffuse layer of counter cations builds up and anion depletion is established near a negatively charged surface. One additional consequence of this negative surface potential is the accumulation of protons at the surface and hence the surface pH is lower than the bulk value. The presence of a long chain sulfate in an amine oxide molecular assembly can therefore significantly modify the acid-base equilibrium state of amine oxide; production of the protonated species is enhanced. This interpretation is confirmed by the solution behaviour of C_{18}DAO/SDS mixtures. Solutions of these two components have been shown to be turbid and birefringent, and the addition of SDS to C_{18}DAO results in the

production of filament-like structures and an increase in the bulk pH value. This suggests the formation of a new species between protonated C_{18}DAO and SDS, which is also responsible for the surface tension lowering (Chapter 4). The increase in bulk pH value is then a consequence of the consumption of hydrogen ions in the production of the cationic amine oxide, and the protonated amine oxide and the long chain sulfate precipitate out stoichiometrically.

Mixtures of compatible chain systems, viz., C_{12}DAO/SDS and C_{14}DAO/SDS, lead to the formation of mixed micelles and are also accompanied by an increase in the pH of the solution. However, the increase in pH in these two cases may not be caused by the protonation process. Protonation in its usual sense implies an actual bond formation. If the amine oxide molecules are protonated, then an ion-ion interaction with the sulfate will be reflected in the bulk by the formation of an insoluble 1:1 double long chain salt; the absence of precipitation would then be indicative of the absence of any substantial ion-ion interaction. In the cases of C_{12}DAO/SDS and C_{14}DAO/SDS mixtures, since no precipitation occurs for all mixing ratios investigated, the observed increase in bulk pH is probably caused by the adsorption of H_3O^+ ions on the micelle surface, rather than actual protonation of amine oxide molecules. Only when there are sufficient protons available, such as with the addition of an acid, will protonation of the amine oxide and the formation of the double chain complex take place. This alternative interpretation of the increased pH value has been considered previously. Therefore it is proposed that there are two different mechanisms, both of which are needed in order to explain the interactions between alkyldimethylamine oxide and alkyl sulfate satisfactorily. When the alkyl chains match in length, paraffin-paraffin interaction is maximised, the formation of mixed micelle is favoured and is accompanied by the adsorption of hydronium ions on the surface. When the alkyl chains do not

match, head group interaction predominates, and protonation of amine oxide is favoured, resulting in the formation of a 1:1 insoluble complex.

Goddard and Kung (1) have investigated the mixed monolayer properties of docosyldimethylamine oxide and nonadecyl benzene sulfonate under conditions identical to this study. The mean molecular area versus composition plots show small positive deviations from ideality, and the π-A curves of the mixed films are of similar shape. This is probably caused by the presence of the benzene ring in the chain; this bulky group has a negative steric effect on the packing of the alkyl chains. Nevertheless, favourable interactions can still be expected. Kolp *et al* (2) investigated the solution behaviour of the shorter chain homologs, dodecyldimethylamine oxide and dodecyl benzene sulfonate in dilute solutions. They found that the protonated amine oxide molecules and the long chain sulfonate precipitate metathetically. Removal of the bulky group optimises the packing of the chains, and can produce synergistic effects. Another study (20) has confirmed that mixtures of dodecyldimethylamine oxide and sodium dodecane sulfonate show a pronounced surface tension lowering upon mixing, and that precipitation occurs only in dilute solutions. Hence the expected but not detected interaction between C_{22} amine oxide and nonadecyl benzene sulfonate is therefore also a steric effect caused by the presence of bulky group in the mixed molecular assembly.

5.5. REFERENCES

1. Goddard, E. D., and Kung, H. C., *J. Colloid Interface Sci.* **43**, 511 (1973).

2. Kolp, D. G., Laughlin, R. G., Krause, F. P., and Zimmerer, R. E., *J. Phys. Chem.* 67, 51 (1963).

3. Christodoulou, A. P., and Rosano, H. L., in "*Molecular Association in Biological and Related Systems*", ACS Advan. Chem. Ser. 84, 210 (1968).

4. Corkill, J. M., Goodman, J. F., Harrold, S. P., and Tate, J. R., *Trans. Faraday Soc.* 63, 247 (1967).

5. Hendrix, Y., and Mari, D., *J. Colloid Interface Sci.* 78, 74 (1980).

6. Feistein, M. E., and Rosano, H. L., *J. Colloid Interface Sci.* 24, 73 (1967).

7. Mingins, J., and Pethica, B. A., *Trans. Faraday Soc.* 59, 1892 (1963).

8. Hall, D. G., and Price, T. J., *J. Chem. Soc. Faraday Trans. I* 80, 1193 (1984).

9. Rosano, H. L., Chrisdotoulou, A. P., and Feistein, M. E., *J. Colloid Interface Sci.* 29, 335 (1969).

10. Goddard, E. D., Kao, O., and Kung, H. C., *J. Colloid Interface Sci.* 27, 616 (1968).

11. Shibata, O., Kaneshina, S., and Nakamura, M., *J. Colloid Interface Sci.* 77, 182 (1980).

12. Tadros, T. F., in "*Structure/Performance Relationships in Surfactants*", ACS Symposium Series **253**, 153 (1984).

13. Stilbs, P., Rapacki, K., and Lindman, B., *J. Colloid Interface Sci.* 95, 583 (1983).

14. Birdi, K. S., *Colloid Polymer Sci.* 260, 628 (1982).

15. Hua, X. Y., and Rosen, M. J., *J. Colloid Interface Sci.* 90. 212 (1982).

16. Lucassen-Reynders, E. H., Lucassen, J., and Giles, D., *J. Colloid Interface Sci.* 81, 150 (1982).

17. Moi, Y., Nishikido, N., Saito, M., and Matuura, R., *J. Colloid Interface Sci.* 52, 356 (1975).

18. Verwey, E. J. W., and Overbeek, J. Th. G., "*Theory of the Stability of Lyotropic Colloids*", Elsevier, Amsterdam (1948).

19. Davis, J. T., and Rideal, E. K., "*Interfacial Phenomena*", Academic Press, New York (1961).

20. Rosen, M. J., Friedman, D., and Gross, M., *J. Phys. Chem.* **11**, 3219 (1964).

CHAPTER 6

SOLUBILISATION AND MICROEMULSION THE DUPLEX FILM MODEL

6.1. INTRODUCTION

One phenomenon closely related to the micelle solubilisation process is the formation of the so-called *microemulsions*. The term was first introduced by Hoar and Schulman (1) to describe the transparent or transluscent systems which form *spontaneously* when oil and water (brine) are mixed with a relatively large amount of surfactant and a cosurfactant (usually a medium chain alcohol). Typically, microemulsions consist of dispersions of very small drops with radii of the order of 50-500 å of either oil-in-water (O/W) or water-in-oil (W/O). Microemulsions differ from ordinary emulsions (macroemulsions) in two main aspects, namely their thermodynamic stability and the lack of turbidity. However, the former point is still under discussion (2), and there does not exist a universally accepted definition of a microemulsion (3).

Schulman (4) postulated that the surfactant and cosurfactant can produce a mixed adsorbed film that could result in a transitory negative interfacial tension between oil and water, leading to a decrease in interfacial free energy which favours spontaneous microemulsification. This model (known as the duplex film) has been criticised and subsequently refined to include other effects on system free energy which become significant for small values of interfacial tension, such as the increase in entropy caused by dispersion of a phase into small drops.

Rehbinder (5) recognised that the interfacial tension need not to be negative for spontaneous microemulsification, as long as the tension is low enough such that the free energy decrease caused by the entropy of dispersion outweights the increase in interfacial free energy from dispersion. This idea has been extended by others (6-8). Ruckenstein (9) also showed that the adsorption of surfactant at the surface of a drop is another factor which favours dispersion. An increase in interfacial area is accompanied by a decrease in free energy of an adsorbed surfactant molecule compared to that of a molecularly dispersed state in the bulk phase. More recently, Rosano and Lyons (10) have shown that the adsorption of cosurfactant molecules at the drop surface also reduces the system free energy. Miller and Neogi (11) have developed a thermodynamic model for dilute microemulsion systems which includes the combined effects of bending and dispersion. The duplex film model is used for the interface. Their model yields interesting predictions of microemulsion behaviour, but some of the parameters used to characterise bending effects are not readily related to known properties of the surfactant (12).

Rosano *et al* (13) have investigated microemulsions prepared from alkyldimethylamine oxide/sodium alkyl sulfate/oil/brine (5% NaCl) mixtures without added alcohol as cosurfactant. This particular choice of surfactant mixture has been shown, in Chapters 4 and 5, to possess the potential to produce microemulsions, since these two surfactants interact strongly so as to lower the surface tension of water even further, a necessary (but insufficient) criterion for spontaneous dispersion, as discussed above. This chapter describes the study made on the amine oxide/alkyl sulfate microemulsion systems using the duplex film method which permits a direct study of the oil-monolayer interaction.

6.2. EXPERIMENTAL

6.2.1. Chemicals

Octadecyldimethylamine oxide (C_{18}DAO) was a commercial sample from Onyx Chemical Company, Jersey City, N.J. (25% active). After evaporating the solvent the crude product was recrystallised several times from ethyl acetate. The final product was dried and stored *in vacuo* over P_2O_5. Sodium octadecyl sulfate (SODS) was a sample prepared in this laboratory previously, and was recrystallised from ethanol before use. Reagent grade oils, n-dodecane (nC_{12}), n-tetradecane (nC_{14}) and n-hexadecane (nC_{16}) were purchased from Aldrich Chemical Company, Milwaukee, WI., and were used as received.

6.2.2. Solution Preparation

The spreading solutions were prepared as follows: C_{18}DAO was dissolved in 45/5, the SODS in 25/25, benzene/methanol mixture, and the concentration of these solutions was 1.157×10^{-3}M. For mixed monolayers, amine oxide/sulfate mixtures were made from the stock solutions prior to spreading. Since it was reported that a 1:1 mole ratio produces the lowest surface tension (Chapter 4) as well as the most condensed film (Chapter 5), mixed monolayers at this ratio was chosen for the present investigation. The hydrocarbon spreading solutions were prepared by diluting ~0.25 mL of the oil to 25 mL in volumetric flasks with benzene. The surfactant and the hydrocarbon solutions were spread separately with Agla microsyringes to produce the duplex film. The amount of oil spread was calculated to correspond to a duplex film thickness of ~200-400 å, typical of the radius of an O/W microemulsion droplet. A 0.01M NaOH, 5% NaCl solution was used as the substrate. Compression of the film was started after 3 min. of deposition to allow solvent evaporation. The experimental apparatus employed has been described in

Chapter 5 and elsewhere (2,14).

6.3. RESULTS

6.3.1. C_{18}DAO Systems

Figure 6.1 shows the surface pressure-area (π-A) isotherms of C_{18}DAO (curve 1) and its duplex films (curve 2 with nC_{12}, curve 3 with nC_{16}), spread on 0.01N NaOH, 5% NaCl subsolution. Since the substrate is highly alkaline, all the amine oxide molecules are essentially nonionised (Chapter 2). The expanded nature of the monolayer, discussed in Chapter 5, was attributed to the presence of a strong dipole in the head group, evident by its positive surface potential which is relatively high for a nonionic surfactant.

Addition of nC_{12} causes a slight expansion of the film (curve 2), and the collapse region of the duplex films, for all practical purposes, is about the same as that of the pure C_{18}DAO monolayer. The magnitude of expansion caused by the addition of nC_{14} (not shown) is very close to that of the nC_{12} oil. The nC_{16} duplex (curve 3) on the other hand, shows a greater expansion as well as higher collapse pressure, suggesting this film is probably more stable. Monolayers are usually more expanded at the oil/water interface than at the air/water interface (15,16), due to the penetration of oil molecules into the film, and the relative magnitude of expansion can be related to the compatibility of the oil and surfactant chain length.

6.3.2. SODS Systems

The π-A isotherms of the SODS systems are shown in Fig.6.2. Except for the nC_{14} duplex, phase transition which is characteristic of SODS (Chapter 5) is detected in all cases. It is seen also that the relative magnitude of expansion increases with increasing oil chain length; the nC_{16} which is more compatible to the SODS gives rise to the most expanded film. This observation again

Figure 6.1 Surface pressure-area (π-A) isotherms of $C_{18}DAO$ monolayer (curve 1) and duplex films (curve 2 with nC_{12}, curve 3 with nC_{16}), spread on 0.01M NaOH, 5% NaCl subsolution at 25 °C.

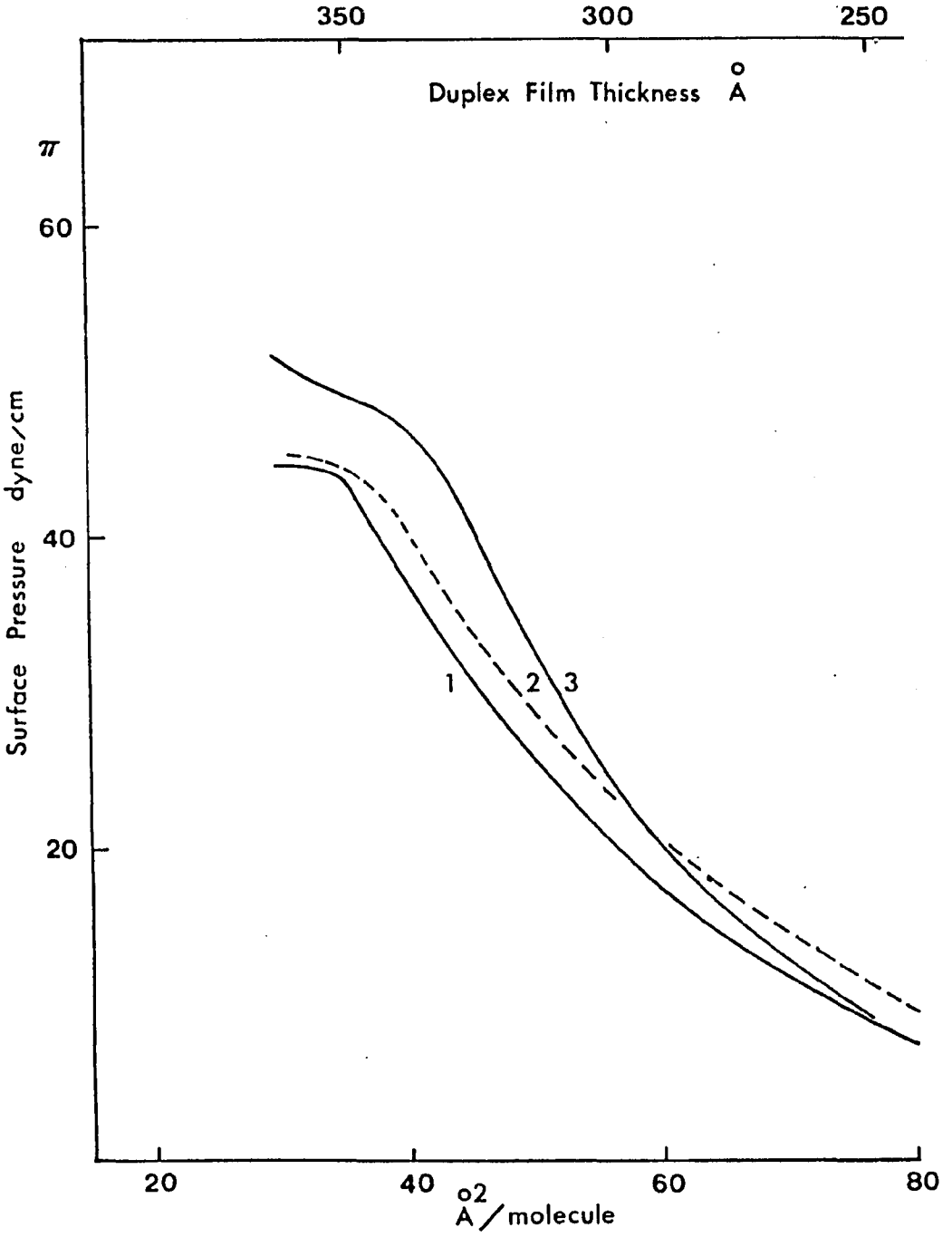

Figure 6.2 Surface pressure-area (π-A) isotherms of SODS monolayer (curve 1), and duplex films (curve 2 with nC_{12}, curve 3 with nC_{14}, curve 4 with nC_{16}), spread on 0.01M NaOH, 5% NaCl sub-solution at 25 °C.

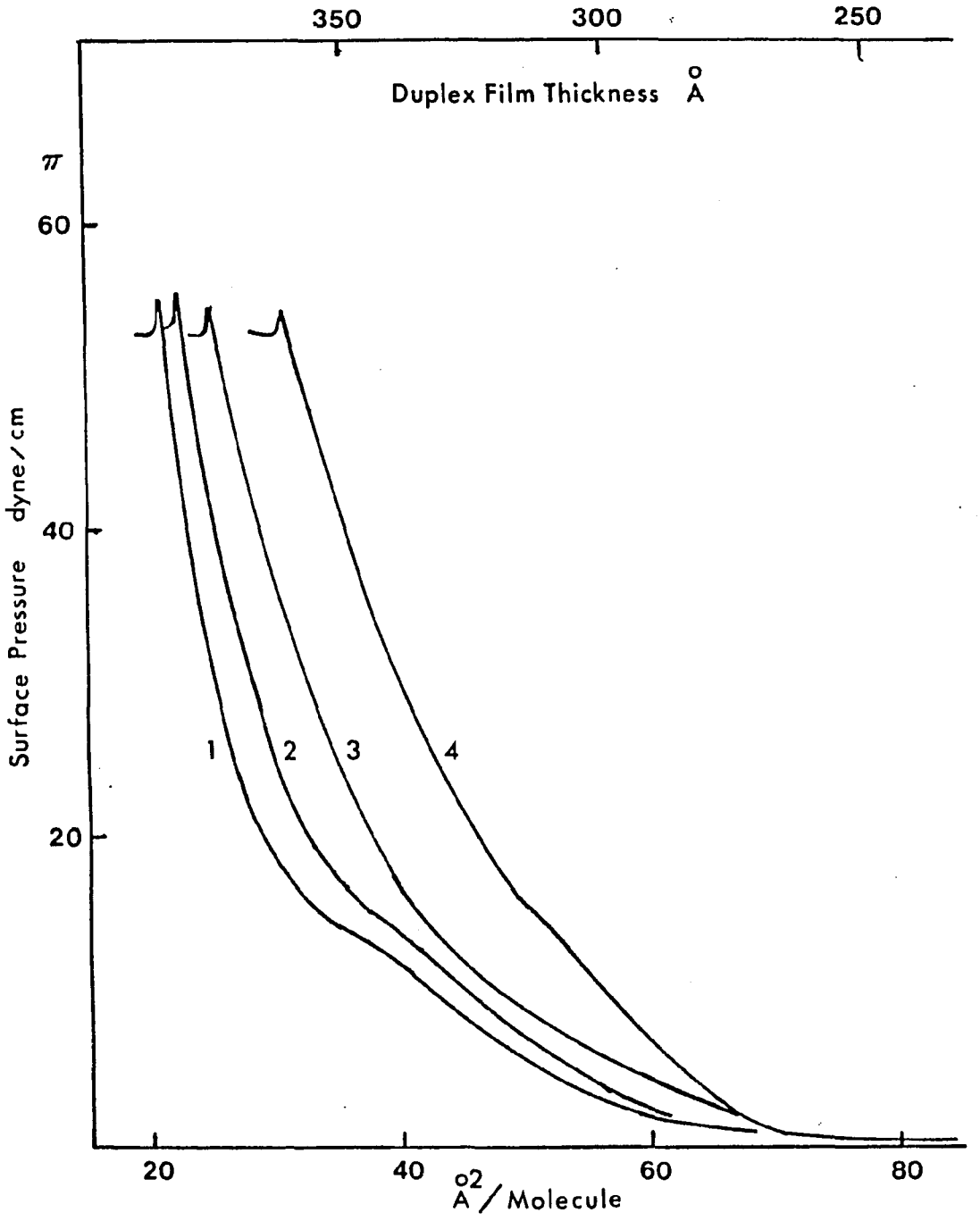

illustrates the importance of chain compatibility effect, a concept already discussed in Chapter 4, as well as by many other investigators. For example, Shah and Shiao (17) studied the average area per molecule in mixed monolayers of alkyl alcohols. They found that minimum area/molecule is obtained when both components possess the same chain length, and interpreted the results in terms of the thermal motion of surfactant molecules in the monolayer. The collapse pressures of these films do not vary from each other significantly. The near constancy in the collapse pressures suggests that these films have about the same stability.

6.3.3. C_{18}DAO/SODS Mixed Systems

The isotherms for these systems are shown in Fig.6.3. The mixed monolayer shows a much higher collapse pressure than either of the pure film, indicating an enhanced stability upon mixing, caused by the strong interaction between the two surfactant species. Addition of nC_{12} does not alter the film features to any significant extent, since the oil molecules are unable to penetrate into the monolayer, due to the large difference in the chain length, therefore they are "squeezed" out of the film on compression (2). The nC_{14} duplex shows expansion on compression, and become incompressible at high pressure; it increases the stability of the film. Optimum penetration of oil molecules into the film is observed with nC_{16}, but this reduces the stability of the film, as evident by the slight lowering of callapse pressure.

6.4. DISCUSSION

6.4.1. The Duplex Film Model

It was originally postulated by Schulman (4) that microemulsification occurs when the surfactant and cosurfactant, in the right ratio, produce a mixed adsorbed film that would reduce the interfacial tension (γ_i) between the oil and

Figure 6.3 Surface pressure-area (π-A) isotherms of 1:1 C_{18}DAO/SODS mixed monolayer (curve 1) and duplex films (curve 2 with nC_{12}, curve 3 with nC_{14}, curve 4 with nC_{16}), spread on 0.01M NaOH, 5% NaCl subsolution at 25 °C.

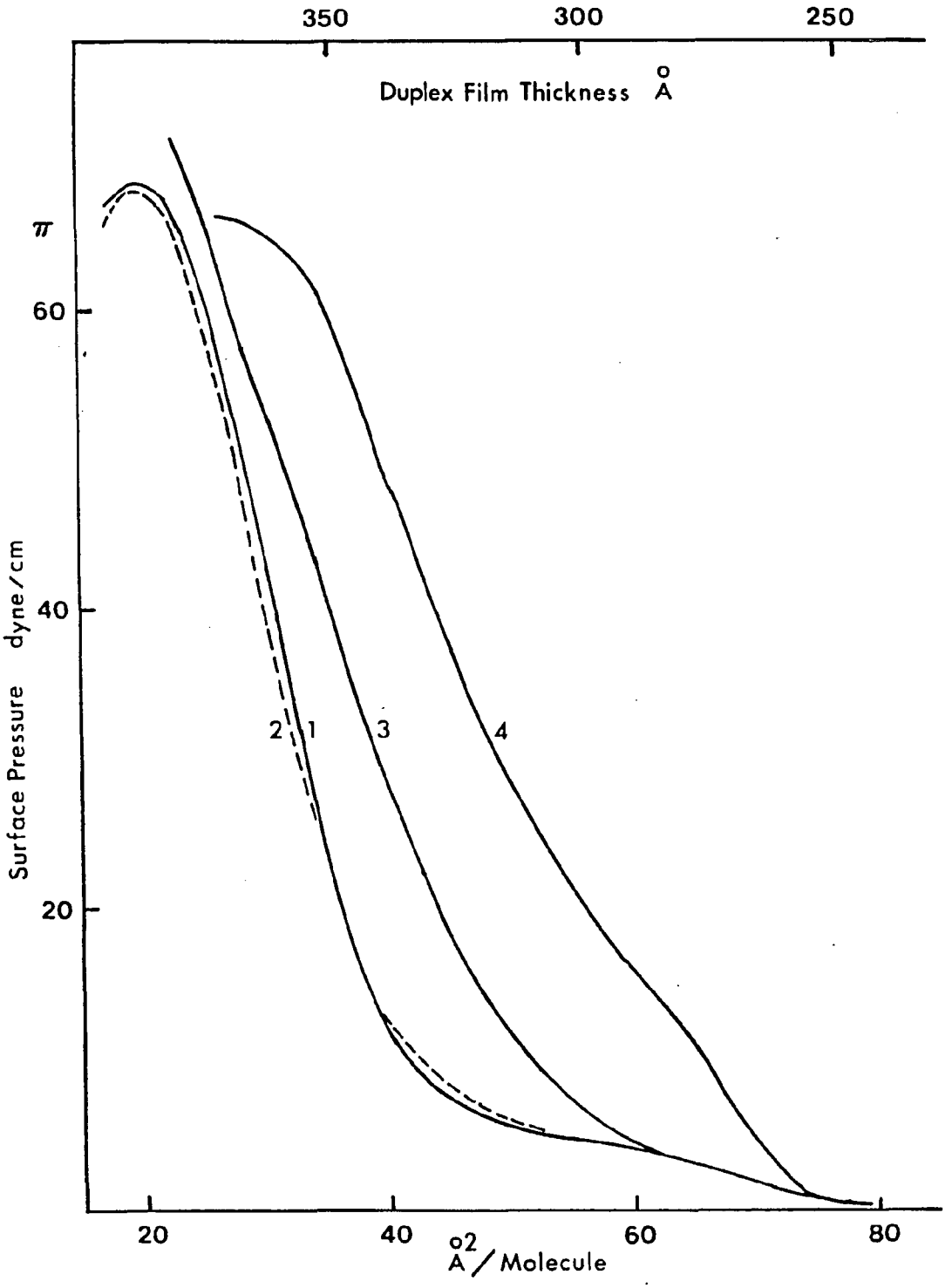

water to below zero. There would then be a free energy $-\gamma_i dA$ available for dispersion, where A is the interfacial area. The interfacial tension in the presence of the mixed film is given by

$$\gamma_i = \gamma_{o/w} - \pi_i \qquad [6.1]$$

where $\gamma_{o/w}$ is the O/W interfacial tension without the film present and π_i is the spreading pressure of the film. If the oil molecules penetrate the monolayer, the film pressure π_i increases. If π_i exceeds $\gamma_{o/w}$, γ_i becomes negative, and at equilibrium γ_i attains the value of zero. If the concept of zero interfacial tension is accepted, stabilisation of microemulsion is implied (18). In the case of a duplex film,

$$\gamma_i = \gamma_{a/w} - \gamma_{o/a} - \pi_D \; (= \gamma_{o/w} - \pi_i) \qquad [6.2]$$

where $\gamma_{a/w}$ is the air/water surface tension, $\gamma_{o/a}$ is the oil/air interfacial tension, and π_D is the measured spreading pressure of the film.

According to Rosano *et al* (2, 19) an insoluble liquid monolayer of a surfactant species at its collapse pressure (π_c) can be considered as a duplex film one molecule thick and that $\pi_c = \pi_D$. In the present cases, $\gamma_{a/w} \simeq 72$ dyne/cm and $\gamma_{o/a} \simeq 29$ dyne/cm, or $\pi_D \simeq 43$ dyne/cm when $\gamma_i = 0$. Therefore if the experimental π_D value is greater than 43 dyne/cm, negative interfacial tension is attained, resulting in a spontaneous dispersion. Refering to Figs. 6.1, 6.2 and 6.3, it is seen that all the duplex films show collapse pressures that are greater than the critical value (it should be noted that these experimental values are not the equilibrium values), suggesting all are capable of forming microemulsions which is clearly not the case. Microemulsification has been shown to be a highly selective process; only with the right combination of surfactants and oil would such a process take place (2,13).

However, according to Eq.6.2 a change in the interfacial tension between oil and water is necessarily accompanied by a change in the collapse pressure of the film due to the presence of oil molecules (difference between the duplex and the monolayer), since both $\Delta\gamma_{a/w}$ and $\Delta\gamma_{o/a}$ are zero, viz.,

$$\Delta\gamma_i = -\Delta\pi_D \qquad [6.3]$$

If the collapse pressure of the duplex is greater than that of the monolayer, interfacial tension reduction is achieved ($\Delta\gamma_i$ = negative). Eq.6.3 therefore represents another restriction in the duplex film theory for spontaneous dispersion. Of the systems investigated, most are thereby ruled out as possible candidates capable of forming microemulsions, except the C_{18}DAO/nC_{16} and C_{18}DAO/SODS/nC_{14} systems. The former seems to be unlikely; from experience, microemulsions usually do not form with only a single surfactant, with no added cosurfactant. The second system is more likely to form microemulsions, since the combination of C_{18}DAO and SODS resembles amphiphiles with double chains, which are known to form microemulsions without other additives (20, 21).

6.4.2. Amine Oxide/Alkyl Sulfate/Oil/Brine Microemulsion

Rosano *et al* (13) have made a systematic study of the formation of microemulsions using alkyl sodium sulfate (with alkyl chain containing 12 to 16 carbons) as the surfactant, octane through hexadecane as the oil, and aqueous solutions of alkyldimethykamine oxide (dodecyl through hexadecyl) as the cosurfactant. The cosurfactant was added by titration. Although no attempt was made to form microemulsions with the octadecyl homologs, the surfactants used in the present study, a parallel can still be drawn between the two studies. It was reported that out of the forty-five combinations, only sixteen resulted in the formation of microemulsion, demonstrating the highly

specific nature of the process. It is interesting to note that these systems always go through a highly viscous phase during titration prior to the occurrence of microemulsification. The viscous state signifies the formation of mixed micelles, which was discussed in Chapter 4, and dispersion of oil follows, corresponding to the onset solubilisation of oil molecules into the interior of the mixed micelle.

In a subsequent investigaton using the vapour pressure technique, Cavallo and Rosano (22) demonstrated that microemulsification is a concerted, structure-forming process; in the microemulsion region the solution exhibits a vapour pressure which is much less than that of the system without the oil. Using the present duplex film results and assuming the droplets are spherical, Cavallo and Rosano were able to calculate the molecular weight and the radius of the drop, and reasonable values are obtained.

6.5. EPILOGUE

It is clearly demonstrated in this thesis that microemulsification is very closely related to, if not the same as, the phenomenon of micelle solubilisation. In order to gain an insight into the facinating field of microemulsion and emulsion teghnology in general, one must rely on a good understanding of the (comparatively speaking) simpler micellar systems. This can only be achieved by starting with a detailed study of the surfactant solution by itself; this is the characterisation stage. Only from here is it possible to increase the complexity of the system by introducing additives but yet be able to explain the observations, leading to a prediction of the future, such as the phase behaviours of other systems, as well. Indeed, a number of research groups (23-25) have gone back to the fundamental study of micellar solutions, coincidentally, in a concerted manner, with the aim that it can lead to a better understanding of the physical chemistry of microemulsion systems.

6.6. REFERENCES

1. Hoar, T. P., and Schulman, J. H., *Nature (London)* 152, 102 (1943).

2. Rosano, H. L., Lan, T., Weiss, A., Whittam, J. H., and Gerbacia, W. E. F., *J. Phy. Chem.* 85, 468 (1981).

3. Friberg, S. E., *Colloid and Surfaces* 4, 201 (1982).

4. Schulman, J. H., and Montagne, J. B., *Ann. New York Acad. Sci.* 92, 366 (1961).

5. Rebinder, P. A., *Proc. 2nd Inter. Congr. on Surface Activity (London)* 1,476 (1957).

6. Ruckenstein, E., and Chi, J. C., *J. Chem. Soc. Faraday Trans. II* 71, 1690 (1975).

7. Ruckenstein, E., in "*Micellisation, Solubilisation and Microemulsion*", Plenum, New York II, 755 (1976).

7. Reiss, H., *J. Colloid Interface Sci.* 53, 61 (1975).

8. Ruckenstein, E., *Chem. Phys. Lett.* 57, 517 (1978).

10 Rosano, H. L., and Lyons, G. B., *J. Phy. Chem.* 89, 363 (1985).

11. Miller, C. A., and Neogi, P., *AICheE J.* 26, 212 (1980).

12. Mukherjee, S., Miller, C. A., and Ford, T. Jr., *J. Colloid Interface Sci.* 91, 223 (1983).

13. Rosano, H. L., Cavallo, J. L., and Lyons, G. B., manuscript in preparation.

14. Christodoulou, A. P., and Rosano, H. L., in "*Molecular Association in Biological and Related Systems*", ACS Advan. Chem. Ser. 84, 210 (1968).

15. Davies, J. T., *Proc. Roy. Soc. Series A (London)* 208, 224 (1951).

16. Mingins, J., Owens, N. F., Taylor, J. A. G., Brooks, J. H., and Pethica, B. A., in "*Monolayers*", Goddard, E. D. Ed., ACS Advan. Chem. Ser. 144, 14 (1975).

17. Shah, D. O., and Shiao, S. Y., in Ref. 16, p.153.

18. Gerbacia, W., and Rosano, H. L., *J. Colloid Interface Sci.* 44, 242 (1973).

19. Rosano, H. L., Schiff, H., and Schulman, J. H., *J. Phy. Chem.* 66, 1928 (1962).

20. Zulauf, M., and Eicke, H. F., *J. Phy. Chem.* 83, 480 (1979).

21. Angel, L. R., Evans, D. F., and Ninham, B. W., *J. Phy. Chem.* 87, 538 (1983).

22. Cavallo, J. L., and Rosano, H. L., manuscript in preparation.

23. Barakat, Y., Fortney, L. N., Schechter, R. S., Wade, W. H., Yiv, S. H., and Graciaa, A., *J. Colloid Interface Sci.* 92, 561 (1983).

24. Mitchell, D. J., Tiddy, G. J. T., Waring, L., Bostock, T., and McDonald, M., *J. Chem. Soc. Faraday Trans. I* 79, 975 (1983).

25. Zana, R., Yiv, S., Strazielle, C., and Lianos, P., *J. Colloid Interface Sci.* 80, 208 (1981).

APPENDIX A

CHAIN-CHAIN INTERACTION ENERGY

When one surfactant molecule leaves the aqueous solution and enters the micelle, it liberates an energy ω_0. Here the paraffinic part is considered since the polar head group remains in contact with water. The total energy liberated in this manner, in the formation of half micelle of N molecules, is not exactly $N\omega_0$, because in the model employed here, the peripheral molecules remain partially wetted by water. Let us call α the fraction of a peripheral molecule that is in contact with water. The energy liberated by such a molecule is then $\omega_0(1 - \alpha)$.

Let us calculate the number n of peripheral molecules. If l is the distance between two peripheral molecules in a hexagonal array, the perimeter of a circle passing by the first row of molecule is:

$$2\pi \left(R - \frac{l\sqrt{3}}{4}\right) nl \qquad [A1]$$

where R is the radius of the micelle.

If σ is the area occupied by one molecule:

$$\sigma = \frac{\sqrt{3}}{2} l^2 \qquad [A2]$$

and that the total surface area of the half micelle is:

$$N\sigma = \pi R^2 \qquad [A3]$$

therefore we obtain:

$$n = (2\pi\sqrt{3})^{\frac{1}{2}}\sqrt{N} - \frac{\pi\sqrt{3}}{2} = 3.3\sqrt{N} - 2.7 \qquad [A4]$$

The energy liberated due to chain interaction in the half micelle is then:

$$W_0 = [N - \alpha(3.3\sqrt{N} - 2.7)]\omega_0 \qquad [A5]$$

or, substitution of Eq.[A4] into Eq.[A5]:

$$W_0 = [N - \alpha(3.3\sqrt{N} - 2.7)]\omega_0 \qquad [A6]$$

Hence addition of one molecule to the aggregate will liberate an energy given by:

$$\frac{dW_0}{dN} = (1 - \frac{1.65\alpha}{\sqrt{N}})\omega_0 \qquad [A7]$$

APPENDIX B

HEAD GROUP INTERACTION ENERGY

In the case of a half micelle, let us calculate the energy $dW_e/dN = W_e$ to be supplied to a molecule in order to overcome the eletrostatic force when the molecule enters the structure. It is assumed that the electrostatic moment of a molecule does not decrease when it is placed in a depolarising field. Bringing together from infinity to a distance l two identical and parallel dipoles with moments m, it is then necessary to supply an energy of m^2/Kl^3 (K = dielectric constant of the medium).

We now refer to Fig.B1. In order to bring a dipole to position 0 which is on the periphery, energy has to be supplied. This energy is separated into two parts: the first part W_{e1} deals with dipoles already present within the distance ρ_0. In view of the short distances which are involved, it is reasonable to do the calculation dipole by dipole. The second part W_{e2} is calculated by method of continuous analysis dealing with dipoles with distance from 0 larger than ρ_0.

We consider W_{e2} first. In an area $rd\theta\,dr$, we have $rd\theta\,d\rho/\sigma$ dipoles where σ is the area occupied by one dipole. The energy W_{e2} needed to place one dipole in 0 is therefore:

$$W_{e2} = \int_{\phi}^{\pi-\phi}\int_{\rho_0}^{\rho} \frac{m^2 r d\theta\, dr}{Kr^3\sigma} \qquad [B1]$$

The solution of the double integral is:

$$W_{e2} = \frac{m^2}{\rho_0 K\sigma}(\pi-2\phi) + \frac{m^2}{RK\rho}\ln\tan\frac{\phi}{2} \qquad [B2]$$

Figure B.1 Schematic representation of half micelle for the calculation of head group interaction energy.

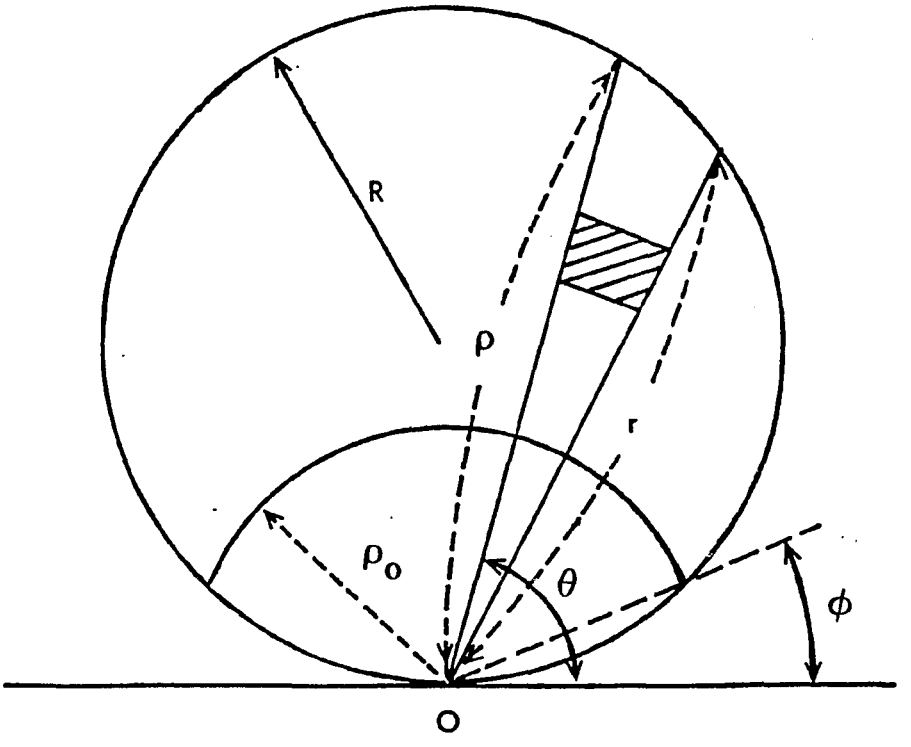

and that ρ_0 and ϕ are related by:

$$\rho_0 = 2R \sin\phi \qquad [B3]$$

If there are N dipoles in the circle with radius R, then from Eq.[A3] and Eq.[B2]:

$$W_{e2} = \frac{\beta}{down\ 10\sqrt{N}} \left(\frac{\pi - 2\phi}{2\sin\phi} + \ln\tan\frac{\phi}{2}\right) \qquad [B4]$$

with

$$\beta = \frac{m^2\sqrt{\pi}}{K\sigma^{\frac{3}{4}}} \qquad [B5]$$

Consider now the area S limited by the circle of radius R and the circle of radius ρ_0. This area contains N_0 molecules, therefore:

$$S = N_0\sigma \qquad [B6]$$

Let us evaluate ϕ as a function of N_0 and N. The exact expression of S is:

$$S = R^2[\pi - \sin 2\phi - (\pi - 2\phi)\cos 2] \qquad [B7]$$

ϕ is generally quite small, therefore we may use the series expansion to the ϕ^4 term:

$$S = 2R^2\phi^2\left[\pi - \frac{4}{3}\phi - \frac{\pi\phi^2}{3} + \ldots\ldots\right] \qquad [B8]$$

and from Eqs.[A3] and [B5]:

$$\phi^2\left[\pi - \frac{4}{3}\phi - \frac{\pi}{3}\phi^2 + \ldots\ldots\right] = \frac{\pi}{2}\frac{N_0}{N} \qquad [B9]$$

solving for ϕ:

$$\phi = \frac{1}{\sqrt{2}}\left(\frac{N_0}{N}\right)^{\frac{1}{2}}\left[1+\frac{\sqrt{2}}{3\phi}\left(\frac{N_0}{N}\right)^{\frac{1}{2}} + \frac{20+3\pi^2}{36\pi^2}\frac{N_0}{N}\right] \qquad \text{[B10]}$$

The expression for W_{e2} is therefore:

$$W_{e2} = \frac{\beta}{\sqrt{N_0}}\left[\frac{\pi}{\sqrt{2}}+\frac{1}{2}\left(\frac{N_0}{N}\right)^{\frac{1}{2}}\ln\frac{lnN_0}{N} - \right.$$

$$\left.\left(\frac{4}{3}+\frac{3}{2}ln\,2\right)\left(\frac{N_0}{N}\right)^{\frac{1}{2}} + \frac{1}{3\pi\sqrt{2}}\frac{N_0}{N}\right] \qquad \text{[B11]}$$

The choice of N_0 depends on the packing of the molecules, and it is reasonable to chose a number between 4 and 10. For example, if N_0= 8 (close-pack), it is necessary to consider the seven closest neighbours located on the same side of a straight line passing the reference molecule, so we have three molecules at distance l, three molecules at distance $3^{1/2}l$ and one at $2l$. The energy W_{el} is given by:

$$W_{el} = \frac{m^2}{Kl^3}\left(3+\frac{1}{\sqrt{3}}+\frac{1}{8}\right) \qquad \text{[B12]}$$

taking into account Eqs. A2 and B5 we obtain:

$$W_{el} = \beta\frac{3^{\frac{3}{4}}}{2\sqrt{2\pi}}\left(3+\frac{1}{\sqrt{3}}+\frac{1}{8}\right) \qquad \text{[B13]}$$

The head group interaction energy is therefore:

$$W_e = \beta\left[\frac{\pi}{4}+\frac{3^{\frac{3}{4}}}{2\sqrt{2\pi}}\left(3+\frac{1}{\sqrt{3}}+\frac{1}{8}\right) - \frac{lnN}{2\sqrt{N}}EQ\,[B\,14] - \frac{4}{2\sqrt{N}} + \frac{2}{2\pi N}\right]$$

APPENDIX C

ENERGY OF FORMATION OF CYLINDRICAL MICELLES

Basic Hydrostatics

From the equation of motion in cylindrical coordinates we have:

$$0 = -\frac{1}{r}\frac{d}{dr}(rP_N) + \frac{P_T}{r} \qquad [C1]$$

where r is the distance from the center of a circle outward, P_T is the stress tensor in the Θ direction (Θ being the angle of a wedge inscribed in a circle), and P_N the stress tensor in the r direction.

Equation [C1] can be written as:

$$0 = -\frac{1}{r}\left(P_N + r\frac{dP_N}{dr}\right) + \frac{P_T}{r}$$

or,

$$\frac{dP_N}{dr} = \frac{P_T - P_N}{r} \qquad [C2]$$

which describe the condition of local mechanical equilibrium. Let P_b be the isotropic stress tensor in the bulk:

$$\frac{d[\,r(P_N - P_b)\,]}{dr} = P_T - P_b \qquad [C3]$$

and

$$\frac{d[\,r^2(P_N - P_b)\,]}{dr} = r(P_N + P_T - 2P_b) \qquad [C4]$$

$$\frac{d[\,r^3(P_N - P_b)\,]}{dr} = r^2(2P_N + P_T - 3P_b) \qquad [C5]$$

Intergration of Eqs.[C3], [C4] and [C5] leads to:

$$r\,(P_N - P_b)\Big|_{r_\alpha}^{r_\beta} = \int_{r_\alpha}^{r_\beta} (P_T - P_b)\,dr \qquad [C6]$$

$$r^2(P_N - P_b)\Big|_{r_\alpha}^{r_\beta} = \int_{r_\alpha}^{r_\beta} r\,(P_N + P_T - 2P_b)\,dr \qquad [C7]$$

$$r^3(P_N - P_b)\Big|_{r_\alpha}^{r_\beta} = \int_{r_\alpha}^{r_\beta} r^2(2P_N + P_T - 3P_b)\,dr \qquad [C8]$$

where α and β are the inner and outter phases, respectively.

If $(P_N - P_b) \rightarrow 0$ as $r \rightarrow 0$, Eqs. C6-C8 resulted in the following:

$$0 = \int_0^{\alpha} (P_T - P_b)\,dr \qquad [C9]$$

$$0 = \int_0^{\infty} rP_N\,dr + \int_0^{\infty} rP_T\,dr - 2\int_0^{\infty} rP_b\,dr$$

rearrangement leads to

$$\int_0^{\infty} r\,(P_T - P_b)\,dr = \int_0^{\infty} r\,(P_b - P_N)\,dr \qquad [C10]$$

and

$$0 = 2\int_0^{\infty} r^2P_N\,dr + \int_0^{\infty} r^2P_T\,dr - 3\int_0^{\infty} r^2P_b\,dr$$

$$= 3\int_0^\infty r^2 P_N dr + \int_0^\infty r^2 P_T dr - 3\int_0^\infty r^2 P_b dr - \int_0^\infty r^2 P_N dr$$

or

$$\int_0^\infty r^2 (P_N - P_T) dr = 3\int_0^\infty r^2 (P_N - P_b) dr \qquad [C11]$$

Let P_0 be the value of P_N when r=0, intergration of Eq.[C2] gives:

$$P_0 - P_b = -\int_0^\infty \frac{P_T - P_N}{r} dr \qquad [C12]$$

Thermodynamic Relationships

Consider the system treated previously is confined in a cylinder with radius L such that L contains the non-uniform interfacial region. Using a wedge portion with angle Θ and and length Z. Let N_i denotes the amount of surfactant molecules therein. At equilibrium the state of this portion is determined by the variables L, T, N_i, Z and Θ. At constant T:

$$dF = dW + \sum \mu_i dN_i \qquad [C13]$$

where F is the Helmholtz free energy and dW is any mechanical work done on the system brought about by any infinitesimal change in Z and Θ by an amount of dZ dΘ in order to increase the surface area of this wedge portion. This work can be divided into two components: work needs to be done in expanding Θ, and to elongate Z, dW_1 and dW_2, respectively, such that

$$dW_1 = -\Theta dZ \int_0^L r P_T dr \qquad [C14]$$

and

$$dW_2 = -Zd\,\Theta\int_0^L rP_T'dr \qquad [C15]$$

At constant μ_i, Eq.[C13] can be written as

$$d(F - \sum\mu_i N_i) = dW = dW_1 + dW_2 \qquad [C16]$$

and at constant T, L and Z, Eq.[C16] becomes

$$d(F - \sum\mu_i N_i) = -\Theta dZ\int_0^L rP_T\,dr - Zd\,\Theta\int_0^L rP_T'dr \qquad [C17]$$

For a cylindrical system, F - $\Sigma\ \mu_i N_i$ is a homogeneous equation of Θ and Z of the second order, hence

$$F - \sum\mu_i N_i = -\frac{1}{2}[\Theta Z\int_0^L rP_T\,dr + Z\,\Theta\int_0^L P_T'dr]$$

$$= -\frac{1}{2}\Theta Z\int_0^L r(P_T + P_T')dr \qquad [C18]$$

Alternatively, direct intergration of either Eq.[C14] or [C15] will result in an equivalent expression to Eq.[C18] as well:

$$F - \sum\mu_i N_i = -\Theta Z\int_0^L rP_T\,dr$$

and

$$F - \sum\mu_i N_i = -Z\,\Theta\int_0^L rP_T'dr$$

therefore

$$\int_0^L rP_T\,dr = \int_0^L rP_T'dr \qquad [C18\text{-a}]$$

Defining E as

$$E = F + P_b V - \sum \mu_i N_i \qquad [C19]$$

where $V = \Theta Z L^2/2$. Eq.[19] can be written as

$$E = F + P_b \pi Z L^2 - \sum \mu_i N_i \qquad [20]$$

if Θ is in radians. Since $d(P_b Z L^2/2) = P_b \Theta Z L \, dL$, from Eq.[C18]:

$$E = -\frac{1}{2}\Theta Z \int_0^L r (P_T + P_T^{'}) dr + \Theta Z \int_0^L r P_b \, dr$$

$$= -\frac{1}{2}[\Theta Z \int_0^L r (P_T + P_T^{'} - 2P_b) dr] \qquad [C21]$$

and from Eq.[C18-a]

$$E = -\Theta Z \int_0^L r (P_T - P_b) dr \qquad [C21\text{-a}]$$

If L is chosen such that $P_T = P_b$, the upper limit in Eq.[C21] may be replaced by $r = \infty$.

For the complete system of a cylinder and its surroundings $\Theta = 2\pi$, $V = \pi L^2 Z$, $dV = 2\pi r Z \, dr$, and

$$F - \sum \mu_i N_i = -\int_V (P_T + P_T^{'}) dV \qquad [C22]$$

$$E_c = -\int_V (P_T + P_T^{'} - 2P_b) dV \qquad [C23]$$

or

$$E_c = -2\int_V (P_T - P_b) dV \qquad [C23\text{-a}]$$

where E_c is the value of E for the complete cylinder.

The Free Energy of Formation

We now introduce the concepts of surface tension and the surface of tension. Consider a hypothetical system consisting of a cylindrical region of radius R and length Z, with uniform pressure P_0 separating from its surroundings at pressure P_b by a membrane of zero thickness with tension σ. We now match the forces and moments in this hypothetical situation with the real system. We take a vertical plane through the center of each system and consider a segment on that plane of length δZ. The forces and moments acting on one side of this segment in both cases are therefore equal,

$$dZ\int_0^\infty P_T\,dr = \delta Z\int_0^R P_0 dr + \delta Z\int_r^\infty P_b\,dr - \delta Z\,\sigma \qquad [C24]$$

and

$$dZ\int_0^\infty rP_T\,dr = \delta Z\int_0^R rP_0 dr + \delta Z\int_R^\infty rP_b\,dr - \delta Zr\,\sigma \qquad [C25]$$

where Eq.[C24] describes the force balance and Eq.[C25] describes the moment balance.

Rearrangement of Eq.[C24] leads to

$$\delta Z\int_0^\infty (P_T - P_b)dr = \delta Z\int_0^R P_0 dr - \delta Z\int_R^\infty P_b\,dr - \delta Z\,\sigma$$

$$= -\delta Z\,\sigma + (P_0 - P_b)\delta ZR \qquad [C26]$$

however, according to Eq.[C9], the l.h.s. of this expression is zero, therefore:

$$(P_0 - P_b) = \frac{\sigma}{R} \qquad \text{[C27]}$$

Rearrangement of Eq.[C25] leads to

$$\delta Z \int_0^{\infty} r\,(P_T - P_b)\,dr = \delta Z \int_0^{R} r\,(P_0 - P_b)\,dr - \delta Z r\,\sigma$$

$$= \delta Z\,(P_0 - P_b)\frac{R^2}{2} - \delta Z R\,\sigma \qquad \text{[C28]}$$

Substituting Eq.[C27] into Eq.[C28] gives

$$\delta Z\,\sigma R = -2\delta Z \int_0^{\infty} r\,(P_T - P_b)\,dr \qquad \text{[C29]}$$

and when compared with Eqs.[C21-a] and [C23-a] yields

$$E_c = 2\pi Z R\,\sigma \qquad \text{[C30]}$$

Equation [C30] represents the expression of the free energy of formation of a cylindrical micelle.

Hall and Mitchell (*J. Chem. Soc. Faraday Trans.II* 79, 185 (1983)) have used this model to derive an expression for the free energy associated with the formation of a spherical droplet. Their equation is identical to the one derived by Sørensen (*Chem. Eng. Commun.* **20**, 93 (1983)), based on classical, thermodynamic nucleation theory modified to take into account a variable surface tension in the formation of a critical droplet. Therefore, this (mechanical-thermodynamical) approach seems to be a valid alternative.